Adenosine Triphosphate Binding Cassette Subfamily C Member 1 (ABCC1) Modulates Amyloid Precursor Protein (APP) Processing: A Potential Therapeutic Target for the Treatment of Alzheimer's Disease

by

Wayne Jepsen

A Dissertation Presented in Partial Fulfillment
of the Requirements for the Degree
Doctor of Philosophy

Approved March 2021 by the
Graduate Supervisory Committee:

Matthew Huentelman, Co-Chair
Kenro Kusumi, Co-Chair
Kendall Jensen
Jason Newbern

ARIZONA STATE UNIVERSITY

May 2021

ABSTRACT

Alzheimer's disease (AD) is the world's leading cause of dementia and is the sixth leading cause of death in the United States. While AD has been studied for over a century, little progress has been made in terms of treating or preventing disease progression; therefore, new therapeutic drug targets must be identified. Current clinical trials focus on inhibiting Beta-Secretase 1 (BACE1), the major enzyme involved in the formation of the amyloid beta (Abeta) peptide fragments that aggregate to form insoluble plaques in the brains of AD patients. However, many of these clinical trials have been halted due to neurological effects or organ damage with no substantial cognitive improvements. Because the current leading theory of AD is that the buildup of amyloid plaques leads to metabolic changes that result in the intraneuronal accumulation of hyperphosphorylated Microtubule Associated Protein Tau (TAU, encoded by the MAPT gene), which causes cell death resulting in brain atrophy and dementia (known as the Amyloid Cascade Hypothesis), identifying drug targets that modulate Amyloid Precursor Protein (APP) processing – without directly inhibiting BACE1 – may prove to be a viable treatment. In this work, the role of the Adenosine triphosphate Binding Cassette subfamily C member 1 (ABCC1) was studied in the context of AD. Rare mutations in ABCC1 were identified in a familial case of late-onset AD and in a sporadic case of early-onset AD, and previous laboratories have demonstrated that Abeta is a substrate for ABCC1-mediated export. Although the final experiments reveal no significant difference between the mutant and reference alleles, the data demonstrate that overexpression of ABCC1 modulates APP processing, resulting in decreased Abeta formation and increased alpha-secretase cleavage of the APP molecule, likely via transcriptional modulation of genes that are capable of altering APP metabolism. Therefore, pharmacological interventions that increase either ABCC1 expression or activity may be capable of halting, reversing, or preventing disease progression. Many cancer drug development pipelines have been employed to identify compounds that decrease ABCC1 expression or activity, and it is likely that compounds have been identified that have the opposite effect. These drugs should be studied in the context of Alzheimer's disease.

DEDICATION

To my parents, Dean and Angela, for loving and supporting me in so many ways along this journey.

To my sister, Tina, and brother-in-law, Curtis, for making my first internship a possibility.

To my sister, Jeanette, and brother-in-law, Marcus, for helping to keep me sane.

To my extended family for loving and supporting me.

To Sherwood for letting me live in your house all of these years.

To all of my friends: Bangarang!

And especially to all those touched by Alzheimer's disease, this work is for you.

ACKNOWLEDGMENTS

I would like to thank the Arizona Alzheimer's Consortium and the Principal Investigator, Eric Reiman, as well as the Salt River Project Grant Program for financial support of this work.

I would also like to thank Catherine and David from the Jackson Laboratory for all of the incredible work they did for us from generating our mouse model to running the cognitive battery and shipping mouse tissue to us.

I would like to thank all of the doctors and clinicians who have had a hand in making this work possible: Dr. Thomas Beach and Dr. Geidy Serrano from the Banner Sun Health Research Institute and Dr. Richard Caselli from the Mayo Clinic.

In the Huentelman lab, past and current, I would like to thank everyone that has taught me anything, helped me in any way, inspired me, or has just made me laugh. Adrienne, Amanda, Anna, Annie, Ashley, Candace, Chris, Francis, Ignazio, Isabelle, Josh, Marcus, Matt, and Ryan, thanks for all the good times. And a special thank you to Val for making all of our lives easier.

I would also like to thank the members of the Center for Rare Childhood disorders who have had an impact on me and my career choices: Keri, Sampath, Szabi, and Vinodh, thank you for all of the incredible work you do and have allowed me to do.

A special thank you to my mentor, Dr. Matthew Huentelman, for taking me on as an intern and allowing me to fulfill my goals within your lab. Thank you for always pushing me to do better and be better. Thank you for showing me what is important and how to stand by my science. And, of course, thank you for all of the fun times!

And thank you to all of my other committee members, Dr. Kenro Kusumi, Dr. Kendall Jensen, and Dr. Jason Newbern (and thank you to Dr. Miles Orchinik). Thank you for supporting me throughout this process and showing me what good mentorship and good science looks like.

TABLE OF CONTENTS

Page

LIST OF TABLES v

LIST OF FIGURES vi

LIST OF SYMBOLS / NOMENCLATURE vii

CHAPTER

1 INTRODUCTION 1

2 GENETICS OF FAMILIAL LOAD AND SPORADIC EOAD 10

Introduction 10

Materials and Methods 13

Results 14

Discussion 17

3 IN VITRO ANALYSIS OF ABCC1 VARIANTS 20

Introduction 20

Materials and Methods 24

Results 29

Discussion 41

4 EFFECTS OF ABCC1 MUTATION IN THE 5XFAD ALZHEIMER'S DISEASE MOUSE MODEL 69

Introduction 69

Materials and Methods 71

Results 75

Discussion 79

5 DISCUSSION 93

REFERENCES 105

APPENDIX

A GENES OF INTEREST TABLE FROM RNA SEQUENCING 120

B WIRB APPROVAL LETTER FOR THE USE OF HUMAN SUBJECTS 130

LIST OF TABLES

Table Page

1. ANOVA Table from the First APP Metabolite Experiment 30
2. ANOVA Table from the Second APP Metabolite Experiment 31
3. ANOVA Table from the Third APP Metabolite Experiment 37
4. ANOVA Table from the Fourth APP Metabolite Experiment 39
5. ANOVA Table from the Percent Alternate Arm Return of the Y-maze 76
6. RNA-seq Results Comparing *Abcc1* Genotypes in NTG and 5xFAD Mice 88

LIST OF FIGURES

Figure		Page
1.	Diagram of the Missing Genetics of Alzheimer's Disease	12
2.	Genetic Workflow of the Late-Onset Alzheimer's Disease Family	15
3.	Genetic Workflow of the Early-Onset Alzheimer's Disease Family	17
4.	Results from the First and Second APP Metabolite Experiments	42
5.	Ratio of Abeta to sAPPalpha from the First and Second APP Metabolite Experiments	44
6.	Flow Cytometry Utilizing Fluorescent Abeta1-42 and Thiethylperazine	47
7.	Normalized Counts for *TIMP3* and *CD38* from the First RNA-seq Experiment	49
8.	MSD Results from the Third APP Metabolite Experiment	55
9.	Ratio of sAPPalpha to sAPPbeta From the Third APP Metabolite Experiment	57
10.	MSD Results from the Fourth APP Metabolite Experiment	59
11.	Ratio of sAPPalpha to sAPPbeta from the Fourth APP Metabolite Experiment	61
12.	Results from the Second RNA-seq Experiment	63
13.	Results from the Third RNA-seq Experiment	65
14.	Taq-Man Results for *TIMP3* and *CD38* Relative Expression in ReNcell VM Cells	67
15.	Spontaneous Alternation Averages Across Genotypes in the Y-maze	80
16.	Total Arm Entries and Percent Alternate Arm Return Across Genotypes in the Y-maze	81
17.	Percent Freezing Post Fourth Foot Shock from the Fear Acquisition Experiment	84
18.	Mean Total Freezing Across Genotypes in the Fear Memory Experiment	85
19.	MSD Results of the Mouse Brain APP Metabolite Experiment	87
20.	Gene-Set Enrichment Analysis Comparing *Abcc1*(WT) 5xFAD and NTG Mice	89
21.	Gene-Set Enrichment Analysis Comparing *Abcc1*(Y1186C) 5xFAD and NTG Mice	91

LIST OF SYMBOLS / NOMENCLATURE

Symbol	Name
5xFAD	Alzheimer's disease mouse model carrying five familial Alzheimer's disease mutations in its transgenes
A930017K11Rik	RIKEN cDNA A930017K11 gene (mouse)
ABCA7	Adenosine triphosphate-binding cassette family A member 7
Abeta	Amyloid beta
Abeta1-40	Amyloid beta polypeptide amino acids 1 through 40
Abeta1-42	Amyloid beta polypeptide amino acids 1 through 42
ABI3	Abelson-interactor gene family member 3
ACE2	Angiotensin-converting enzyme 2
AChEI	Acetylcholinesterase inhibitor
ACTB	Beta actin
AD	Alzheimer's disease
ADAD	Autosomal dominant Alzheimer's disease
ADAM10	A disintegrin and metalloprotease domain 10
ADAM17	A disintegrin and metalloprotease domain 17
ADP	Adenosine diphosphate
AICD	Amyloid precursor protein intracellular domain
ANOVA	Analysis of variance
APLN	Apelin
APOE	Apolipoprotein E
APP	Amyloid Precursor Protein
APP/PS1	Amyloid Precursor Protein/Presenilin 1, an Alzheimer's disease mouse model
ATP	Adenosine triphosphate
AZD3293	Alternate name for lanabecestat
BACE1	Beta-secretase 1
BAM	Binary alignment map
BAN2401	Alternate name for lecanemab
BE(2)-m17	Name of a commercially available human neuroblastoma cell line
BIIB037	Alternate name for aducanumab
BMP6	Bone morphogenetic protein 6
C4BPB	Complement component 4 binding protein beta
C57BL/6J	C57 black six mice from the Jackson Laboratory

Symbol	Name
CADD PHRED	Combined annotation dependent depletion scored on a PHRED-scale
cas9	CRISPR associated protein 9
CCK	Cholecystokinin
CD2AP	Cluster of differentiation 2 associated protein
CD33	Cluster of differentiation 33
CD34	Cluster of differentiation 34
CD38	Cluster of differentiation 38 (human)
Cd38	Cluster of differentiation 38 (mouse)
CD3D	Cluster of differentiation 3 antigen, delta subunit
CFI	Complement factor 1
CHO	Chinese hamster ovary, a cell line
CNP520	Alternate name for umibecestat
COX1	Cyclooxygenase 1
CR1	Complement receptor 1
CRISPR	Clustered regularly interspaced short palindromic repeat
CSF	Cerebralspinal fluid
CTNNA3	Catenin alpha 3
CYP19A1	Cytochrome P450 family 19 subfamily A member 1
CYP1A2	Cytochrome P450 family 1 subfamily A member 2
DCC	Deleted in colorectal carcinoma netrin 1 receptor
DEGs	Differentially expressed genes
DMSO	Dimethyl sulfoxide
DNA	Deoxyribonucleic acid
DPP4	Dipeptidyl peptidase 4
E2609	Alternate name for elenbecestat
ECL	Electrochemiluminescence
EF1alpha	Human elongation factor 1 alpha
ELISA	Enzyme-linked immunosorbent assay
EMEM	Eagle’s minimal essential media
EOAD	Early-onset Alzheimer’s disease
ERBB4	Erb-B2 receptor tyrosine kinase 4
FAD	Familial Alzheimer’s disease
FAS	Fas cell surface death receptor
FASTQ	A genetic sequence file format with quality scores

Symbol	Name
FBS	Fetal bovine serum
FDA	United States Food and Drug Administration
FGFR3	Fibroblast growth factor receptor 3
FOXC1	Forkhead box C1
GC	GC vitamin D binding protein
GHRH	Growth hormone releasing hormone
GLI3	Glioma-associated oncogene family zinc finger 3
GOIs	Genes of interest
GRCh37	Genome Reference Consortium human genome build 37
GRIK1	Glutamate ionotropic receptor kainate type subunit 1
GSEA	Gene-set enrichment analysis
GWAS	Genome-wide association study
HCN1	Hyperpolarization activated cyclic nucleotide gated potassium channel 1
HDC	Histidine decarboxylase
HET_5xFAD	5xFAD mouse heterozygous for the Abcc1(Y1186C) mutation
HET_NTG	C57BL/6J mouse heterozygous for the Abcc1(Y1186C) mutation
HIV	Human immunodeficiency virus
HLA-DRB1	Human leukocyte antigen DR beta 1
HNF1B	Hepatic nuclear factor homeobox 1-beta
INPP5D	Inositol Polyphosphate-5-Phosphatase D
JNJ-54861911	Alternate name for atabecestat
K2 EDTA	Dipotassium ethylenediaminetetraacedic acid
KCNIP4	Potassium channel interacting protein 4
KCNMB2	Potassium Calcium-Activated Channel Subfamily M Regulatory Beta Subunit 2
Krt6a	Keratin 6A (mouse)
LOAD	Late-onset Alzheimer’s disease
log2FC	Log base two fold-change
LY2062430	Alternate name for solanezumab
MAF	Minor allele frequency
MAFA	Musculoaponeurotic fibrosarcoma oncogene homolog A
MAPT	Microtubule-associated protein TAU
MBP	Myelin basic protein
MC	Motor cortex

Symbol	Name
MEGF10	Multiple epidermal growth factor-like domains protein 10
MK-8931	Alternate name for verubecestat
MRP1	Multiple drug resistance protein 1
MSD	Meso Scale Discovery, a electrochemilluminescence assay platform
MSD	Membrane spanning domain
MUSK	Muscle associated receptor tyrosine kinase
NAV3	Neuron navigator 3
NBD	Nucleotide binding domain
NEUROD1	Neuronal differentiation 1
NKX6-1	NK6 homeobox 1
NMDA	N-Methyl-d-aspartate
NOX5	Nicotinamide adenine dinucleotide phosphate oxidase 5
OTX2	Orthodenticle Homeobox 2
p3	Amyloid beta polypeptide amino acids 17-40 or 17-42
PAM site	Protospacer adjacent motif
PBS	Phosphate-buffered saline
pCMV(CAT)T7-SB100	Commercially available vector encoding the transposase SB100X, which is used with the Sleeping Beauty transposon system
PCR	Polymerase chain reaction
Pen Strep	Penicillin and streptomycin
PFC	Prefrontal cortex
PICALM	Phosphatidylinositol binding clathrin assembly protein
PLA2G4A	Phospholipase A2 group 4A
PLCG2	Phospholipase C gamma 2
PLD3	Phospholipase D family member 3
PLXNA4	Plexin A4
pSBbi-Hyg	Sleeping Beauty transposon vector with bidirectional promoter and hygromycin resistance gene
pSBbi-Pur	Sleeping Beauty transposon vector with bidirectional promoter and puromycin resistance gene
PSEN1	Presenilin 1
PSEN2	Presenilin 2
PTGER4	Prostaglandin E receptor 4
PTGS1	Prostaglandin-endoperoxide synthase 1

Symbol	Name
qRT-PCR	Quantitative reverse transcriptase polymerase chain reaction
ReNcell VM	Commercially available human neuroprogenitor cell line derived from the ventral mesencephalon
RG1450	
RIPA buffer	Radioimmunoprecipitation assay buffer
RNA	Ribonucleic acid
RNA-seq	Ribinucleic acid sequencing
RO4909832	Alternate name of gantenerumab
RQ	Relative quantification
sAPPalpha	Soluble amyloid precursor protein alpha
sAPPbeta	Soluble amyloid precursor protein beta
SDM	Site-directed mutagenesis
SEMA3A	Semaphorin 3A
SEZ6	Seizure related 6 homolog
SfiI	Restriction endonuclease derived from *Streptomyces fimbriatus*
sgRNA	Single guide ribonucleic acid
SLC24A4	Solute carrier family 24 member 4
SNCAIP	Synuclein alpha interacting protein
SORCS2	Sortilin related VPS10 domain containing receptor 2
SORCS3	Sortilin related VPS10 domain containing receptor 3
SSTR1	Somatostatin receptor 1
TAU	Product of *MAPT* gene (human)
Tau	Product of Mapt gene (mouse)
TGFB3	Transforming growth factor beta 3
TNFRSF1B	Tumor necrosis factor receptor superfamily member 1B
TNFSF10	Tumor necrosis factor superfamily member 10
TREM2	Triggering receptor expressed on myeloid cells 2
Tukey HSD	Tukey honestly significantly different post-hoc statistical test
UTR	Untranslated region
WNT4	Wingless-type MMTV integration site family, member 4
WT	Wild-type
WT_5xFAD	5xFAD mouse homozygous for Abcc1(WT)
WT_NTG	C57BL/6J mouse homozygous for Abcc1(WT)

Symbol	Name
Xist	X inactive specific transcript (mouse)
ε2	Epsilon 2 allele of the *APOE* gene
ε3	Epsilon 3 allele of the *APOE* gene
ε4	Epsilon 4 allele of the *APOE* gene

CHAPTER 1

INTRODUCTION

Alzheimer's disease (AD) is the leading cause of dementia in the world and is the sixth leading cause of death in the United States with a projected societal cost of nearly $1.1 trillion per year by the year 2050 ("2020 Alzheimer's disease facts and figures," 2020). First described in 1901 by German psychologist Alois Alzheimer, he noted severe memory loss and behavioral issues in his patient, Auguste Deter, a condition he referred to as "presenile dementia" (Cipriani, Dolciotti, Picchi, & Bonuccelli, 2011). Upon Deter's death, Alzheimer used a number of neuropathological staining methods and identified extracellular amyloid plaques and intraneuronal tau tangles in her brain, which became the pathological hallmarks of the disease eventually called Alzheimer's disease (Cipriani et al., 2011). After nearly 120 years of research, the reason for the formation of these pathological hallmarks remains elusive; In fact, it is still debated whether the accumulation of amyloid plaques and aggregation of hyperphosphorylated TAU result in – or are consequences of – the disease (Selkoe & Hardy, 2016). That is, does the excessive accumulation of these proteins cause the metabolic changes that result in neuronal cell death, brain atrophy, and dementia, or do such metabolic changes occur and result in the aggregation of these proteins?

Much is known about how these pathologies form within the brain, though little is known about why they occur. The Amyloid Precursor Protein (APP, encoded by the *APP* gene) is a single-pass transmembrane protein expressed ubiquitously throughout the body, and is expressed mostly by neurons within the brain (O'Brien & Wong, 2011). The function of the protein and its various metabolites are poorly understood, but it is known that differential cleavage of the protein can result in numerous peptides that have very different roles within the brain. The two major cleavage pathways of the APP molecule are known as the alpha- and beta-secretase pathways. Cleavage of the APP molecule by an alpha-secretase results in the production of soluble APP alpha (sAPPalpha), a peptide that is associated with increased cognitive function and neuroplasticity (Jimenez et al., 2011; V. T. Y. Tan et al., 2018; Taylor et al., 2008). Subsequent cleavage by the gamma-secretase complex results in the production of two

additional peptides: p3 and APP intracellular domain (AICD) (Kowalska, 2004). The role of p3 is not well understood, though it has been shown to form fibrillary aggregates, and treatment of cells with p3 can result in signaling cascades associated with inflammation (Szczepanik, Rampe, & Ringheim, 2001). AICD, when formed via the alpha-secretase pathway, is generally understood to be degraded within the cytoplasm (Edbauer, Willem, Lammich, Steiner, & Haass, 2002; Grimm et al., 2015).

If, however, APP is first cleaved by a beta-secretase, soluble APP beta (sAPPbeta) is released into the extracellular space, and subsequent cleavage by the gamma-secretase complex produces Abeta and AICD (O'Brien & Wong, 2011). The resulting Abeta fragments are those that are capable of aggregating via their hydrophobic domains to produce the insoluble amyloid plaques that are one of the major hallmarks of AD. AICD produced via this pathway is known to be able to translocate to the nucleus where is can have an effect on gene expression resulting in a range of consequences from re-entry into the cell cycle to cell death (Bukhari et al., 2017). The role of the beta-secretase pathway is poorly understood within the context of the healthy human brain, though theories exist that it serves as an antimicrobial molecule capable of sequestering bacteria, fungi, and viruses from the brain tissue (Gosztyla, Brothers, & Robinson, 2018), or that they can act as antioxidative molecules to prevent reactive oxygen species from damaging brain tissue (Zou, Gong, Yanagisawa, & Michikawa, 2002). Regardless of why Abeta is formed, its aggregation into amyloid plaques is generally understood to occur years before the onset of AD symptoms, and generally occurs before the formation of intraneuronal hyperphosphorylated-TAU tangles (Selkoe & Hardy, 2016).

The *MAPT* (Microtubule-Associated Protein Tau) gene encodes the protein TAU, which serves as a microtubule-stabilizing protein within the healthy brain (Kadavath et al., 2015). Microtubules are generally dynamic structures that can dissociate and reassemble depending on the immediate environment surrounding the protein monomers that form the larger structure (Horio, Murata, & Murata, 2014). Within neurons, microtubules are a critical component of the cytoskeleton that allows for the formation of axons and dendritic spines, as well as proper axonal function, as they serve as physical routes for motor proteins to deliver endosomes containing

signaling molecules either towards or away from the axon (Fourriere, Jimenez, Perez, & Boncompain, 2020). Proteins such as TAU stabilize these microtubules to prevent their disassembly and maintain axonal function (Kadavath et al., 2015). Within the context of Alzheimer's disease, the TAU protein within neurons is often subject to hyperphosphorylation, causing the proteins to aggregate into TAU tangles which interfere with neuronal function and ultimately result in neuronal cell death (Šimić et al., 2016). The specific molecular mechanisms that result in the formation of this pathological hallmark will not be discussed in great detail, as APP and its metabolites are the main focus of this work.

Beyond just the neuropathological hallmarks of the disease, AD is a severe, degenerative neurological disorder. The disease is characterized by loss of short-term memory, declining cognition, and eventually loss of long-term memory and identity; but even beyond this, AD results in such severe neurological issues that bodily functions cease to function normally until the patient is completely incapable of caring for themselves or interacting with the world around them (Hughes, Berg, Danziger, Coben, & Martin, 1982). This severe decline of neurological function generally leads to secondary complications that result in the patient's death. These include improperly swallowing of foods or liquids resulting in pneumonia, bedsores and blood clots from lack of movement, undiagnosed sepsis, malnutrition, dehydration, and injuries from falls (Arcand, 2015). In this sense, AD does not kill a patient, but will result in complications that cause death. It is a terminal illness, though the time of death may be decades after diagnosis; however, the prognosis is always the same: a severe decline in cognition and memory until death.

Alzheimer's disease, though devastating to the patients, also has severe public health and economic impacts, and is often a financial and emotional hardship on the families of those patients who generally serve as direct caregivers. In terms of public health, the rates of AD-related deaths have been consistently increasing over the past two decades, while deaths from other conditions with some of the highest mortality rates, such as heart disease, stroke, and HIV, have been steadily decreasing ("2020 Alzheimer's disease facts and figures," 2020). Without a proper treatment to prevent, slow, or halt progression of the disease, these rates are expected to increase dramatically in the next three decades as the largest generation in the United States, the

“baby boomers” continue to age. This leads to severe economic impacts in terms of Medicare costs, as these patients will require transportation, doctor visits, diagnostic tests, medications, and care-giving whether at home or in a care facility (“2020 Alzheimer’s disease facts and figures,” 2020).

Many patients with AD do live with their families and are cared for by their relatives (Koca, Taşkapilioğlu, & Bakar, 2017). This can be because of the desire of the family to keep their loved one close to them, or that the family does not have the financial ability to support other care options. This leads to an extreme toll on the relatives as AD patients will require nearly around-the-clock care towards the end of their life to receive help with necessary daily activities such as bathing and feeding. Beyond that, caregivers must also maintain an AD patient’s physical safety in a number of ways: ensuring that household appliances are not hazardous, preventing the patient from wandering out of the house and getting injured or lost, or physically moving them to prevent blood clots and bedsores once the patient is bed-ridden. Caregivers must also manage the patient’s finances by receiving their income such as retirement or social security payments, as well as maintain their property or services such as paying their mortgage, health insurance, electricity, or phone bills (Koca et al., 2017). Taking on this enormous responsibility in itself is no small task, but the emotional strain is compounded by the fact that the caretaking relative is watching their loved one lose their memory and their sense of self. For many, they feel as though they have lost their loved one years before their death.

Although age is the single greatest risk factor for AD, the elderly are not the only ones susceptible to the disease. Alzheimer’s disease is currently divided into two major categories: early-onset AD (EOAD) and late-onset AD (LOAD), in which the age-of-onset is before or after the age of 65, respectively. Within each of these distinctions are two subcategories: familial Alzheimer’s disease – in which a family history of AD is apparent, and there appears to be a heritable component to the disease – and sporadic Alzheimer’s disease – with no previous family history of AD (Bekris, Yu, Bird, & Tsuang, 2010).

In EOAD, familial AD is generally understood to be autosomal dominant Alzheimer’s disease (ADAD), and is characterized by dominant mutations in the *APP*, *PSEN1*, or *PSEN2*

genes, though this accounts for less than one percent of all AD cases (Mendez, 2017). Several causal mutations have been identified in each gene, but all are known to increase the amount of Abeta produced from the cleavage of the APP molecule. Individuals carrying such mutations do have variable ages of onset for AD, but for some, symptoms can become apparent in as early as the fourth decade of life. Because these autosomal dominant mutations all cause increased Abeta production, which seems to be the primary cause of ADAD, these mutations have formed the basis of the Amyloid Cascade Hypothesis, which states that the increased aggregation of Abeta, which is not balanced by proper clearance of the peptides, results in metabolic changes within the brain that leads to the formation of hyperphosphorylated tau tangles within neurons, which results in neuronal cell death – the ultimate cause of memory loss, cognitive decline, and decreased brain function (Selkoe & Hardy, 2016). This hypothesis is also supported by the fact that many individuals with Down syndrome, also known as trisomy 21, tend to develop Alzheimer's disease early in life (Hartley et al., 2015). This is believed to be because the *APP* gene is located on chromosome 21, and the 50% increase in *APP* expression compared to the general population results in an increased production of Abeta.

In LOAD, familial AD is more of a sporadic type than ADAD, though some genetic variants clearly influence the likelihood of disease development. The biggest genetic component to familial LOAD is the influence of the *APOE* genotype on disease risk (Bekris et al., 2010). Apolipoprotein E (APOE) is a protein involved with cholesterol metabolism and homeostasis (Mahley, 2016). The three main *APOE* alleles are known as ε2, ε3, and ε4. *APOE* ε3 is the most common *APOE* allele in the human population, and because of this, it is concluded that this allele confers a zero percent increase in an individual's chances of developing AD. However, those who are heterozygous for the ε4 allele are more likely to develop LOAD, and ε4 homozygotes are five times more likely to develop LOAD than ε4 heterozygotes (Neu et al., 2017). Conversely, the ε2 allele seems to have a protective effect in which individuals who are homozygous for the ε2 allele are even less likely to develop LOAD than ε2 heterozygotes (Talbot et al., 1994).

The second greatest known genetic risk factor for LOAD is just a single mutation in the *TREM2* gene (p.Arg47His) (Abduljaleel et al., 2014). *TREM2* encodes the Triggering Receptor

Expressed on Myeloid cells 2 (TREM2), and is highly expressed by microglial cells, the resident immune cells of the brain (Zheng et al., 2018). Carriers of the TREM2(Arg47His) mutation are known to have at least three times the risk of developing LOAD than the general population (Abduljaleel et al., 2014). Why this mutation causes an increase in the risk for LOAD is not entirely understood, though it is postulated that either TREM2 is not cleaved properly, which leads to improper signaling, or that the mutated receptor impairs the ability of microglia to clear amyloid plaques from the brain. It may also be that this mutation increases the inflammatory response when there is an insult to the brain, such as the aggregation of amyloid plaques (Zheng et al., 2018).

Many other genes have been implicated in Alzheimer's disease through the use of Genome-Wide Association Studies (GWAS), which allows for the association of common genetic variants with the prevalence of AD within a given cohort. Via these studies, genes such as *CR1*, *PICALM*, and *ADAM10* have been shown to influence the onset or progression of the disease (Bellenguez, Grenier-Boley, & Lambert, 2020), though the penetrance of these alleles is incomplete; that is, carrying any number of these alleles does not guarantee that one will develop AD, though the chances of developing the disease increases when more of these alleles are carried by an individual. Though GWAS has illuminated many of the molecular mechanisms that seem to drive the progression of AD, the identification of specific genes involved has not provided viable drug targets for the treatment or prevention of Alzheimer's disease.

While the genetics of familial ADAD and sporadic LOAD are understood more than ever before, the prevalence of sporadic EOAD and familial LOAD alludes to unknown genetic risk factors that cannot be identified by studies like GWAS. This is because GWAS only examines common genetic variants, and sporadic EOAD or familial LOAD may be due to rare genetic variants not commonly seen in the general public. The basis of this work is the hypothesis that the identification of rare, protein-coding variants in AD-associated genes, identified by GWAS or other means, will elucidate the missing genetic components that cause these distinct forms of AD, and that these unknown genetics may finally reveal a valid drug target for the treatment or prevention of Alzheimer's disease.

While there are currently FDA-approved medications for the treatment of AD, they do very little in terms of treating the disease. These drugs are divided into two classes. For mild to moderate AD, acetylcholinesterase inhibitors (AChEI) are used to increase the levels and duration of acetylcholine in the central nervous system (CNS), one of the major excitatory neurotransmitters associated with cognition, learning, and memory. These drugs include donepezil, galantamine, and rivastigmine (Sharma, 2019). For moderate to severe AD, or for patients who have contraindications to AChEIs, a *N*-methyl-d-aspartate (NMDA) receptor antagonist is used to decrease neuronal excitotoxicity, a hypothesized driver for neuronal cell death in AD (Rogawski & Wenk, 2006). The only drug currently approved in this class is memantine. Both classes of drugs can provide short-term improvements in memory and cognition in some patients, yet no single case has been documented in which the progression of AD has been halted or reversed ("2020 Alzheimer's disease facts and figures," 2020); therefore, a new class of drugs is required to treat this disease.

Clinical trials are underway for an entirely new class of drugs which block the function of the protein BACE1, the major beta-secretase enzyme that cleaves APP to produce Abeta, the peptide that aggregates into the insoluble amyloid plaques that are one of the two major pathological hallmarks of the disease (Das & Yan, 2019). If successful, these drugs would confirm the amyloid cascade hypothesis, which states that the accumulation of Abeta within the brain causes the metabolic changes that result in the intraneuronal aggregation of hyperphosphorylated tau, which results in neuronal cell death (Selkoe & Hardy, 2016). However, while these drug trials are still underway, many have been halted early due to unforeseen cognitive or motor issues, lack of improved cognition, or liver damage in a high proportion of participants (Das & Yan, 2019). The reasons for these side effects might be many: Off-target effects of the BACE1 inhibitors, unknown role of BACE1 in the brain, unknown role of BACE1 in other tissue types, or unknown role of Abeta within the healthy brain. As previously stated, many of these clinical trials are still ongoing, and even if they all fail in the end, it is likely that future drug development will continue to focus on reducing amyloid plaque deposition in the brain, though direct inhibition of BACE1 may be the incorrect mechanism to achieve this goal.

Therefore, when alternative ways of altering APP metabolism are discovered, these pathways should be investigated and targeted with small molecules as potential future treatments for AD.

In this work, we investigated the genetics of a familial case of late-onset Alzheimer's disease in which six of the ten siblings were diagnosed with AD after the age of 65. Of most interest was a mutation that co-segregated with AD in the gene *ABCC1* (p.Tyr1189Cys), also known as *MRP1*, a gene that encodes the Adenosine triphosphate Binding Cassette protein C member 1 (ABCC1). ABCC1 is an organic anion transporter whose most common substrates are glutathione, reduced glutathione, glutathione conjugates, sphingosine-1-phosphate, and leukotriene C4, but ABCC1 has also been shown to export Abeta from the cerebral spinal fluid to the periphery blood. Furthermore, mutation of the tyrosine 1189 residue has been shown to alter substrate specificity of the transporter. We hypothesized that the Tyr1189Cys mutation would reduce or ablate ABCC1-mediated export of Abeta, which would increase cerebral Abeta levels, and could be the causal mutation afflicting the family with AD. We later discovered a second *ABCC1* mutation (p.Arg1342Gly) in single patient with a sporadic case of EOAD, which was also investigated using the platform created to study the familial mutation, following the same hypothesis.

Though the final experiments revealed no significant difference between either of the mutant alleles compared to the reference allele, because of the platform we utilized, we gained novel insights about the consequences of increasing *ABCC1* expression on APP metabolism. That is, increased *ABCC1* expression reduces extracellular Abeta levels, and skews APP processing towards the alpha- versus beta-secretase pathways. If ABCC1 protein levels or ABCC1 activity can be increased, it may be possible to not only decrease cerebral Abeta levels, but also to significantly reduce the amount of Abeta being produced. This may serve as a viable treatment for AD by removing the potentially disease-causing Abeta that already resides in the brain, as well as preventing further buildup of the plaques by limiting creation of these peptides.

As previously stated, *ABCC1* is also known as *MRP1* (Multidrug Resistance Protein 1), because it was first discovered in cancer cells where it is known for its ability to confer chemoresistance by exporting chemotherapeutics from the cytoplasm of the cell to the

extracellular space (Cole, 2014). *MRP1* was later called *ABCC1* when it was discovered that this protein is a relative of the larger class of Adenosine triphosphate Binding Cassette (ABC) proteins. Because of its ability to allow cancer cells resistance to chemotherapies, many drug development pipelines have already been used to identify small molecules that are capable of either inhibiting the transporter action of ABCC1 or of decreasing ABCC1's expression (Cihalova, Ceckova, Kucera, Klimes, & Staud, 2015; Cihalova, Staud, & Ceckova, 2015; Csandl, Conseil, & Cole, 2016; Gana et al., 2019; Gao et al., 2020; Jiang et al., 2016; Kumar & Jaitak, 2019; Ranjbar et al., 2019; Sampson, Peterson, Tan, & Iram, 2019; Schafer, Kohler, Lohe, Wiese, & Hiersemann, 2017; Schmitt, Stefan, & Wiese, 2016; Silbermann et al., 2020; Silbermann, Stefan, Elshawadfy, Namasivayam, & Wiese, 2019; Sorf et al., 2019; K. Stefan, Schmitt, & Wiese, 2017; K. W. Tan, Sampson, Osa-Andrews, & Iram, 2018; Whitt et al., 2016; Wong et al., 2018). Logically, when thousands to hundreds of thousands of small molecules are investigated for this specific purpose, it is highly likely that compounds have been identified that do the opposite of what these pipelines intended: small molecules that increase ABCC1-mediated export, or that increase ABCC1 expression. The results of this work call upon the principle investigators of such pipelines to publicly identify these compounds so that they can be studied in the context of Alzheimer's disease.

CHAPTER 2

GENETICS OF FAMILIAL LOAD AND SPORADIC EOAD

INTRODUCTION

The current genetic landscape of Alzheimer's disease (AD) is cloudy, as only a small number of mutations in just three genes are known to cause autosomal dominant AD (ADAD), the familial form of early-onset Alzheimer's disease; that is, individuals who carry just one copy of these mutant alleles have an approximately 100% chance of developing AD. These mutations occur in the genes *APP*, *PSEN1*, and *PSEN2*, and each of them increases beta-secretase mediated cleavage of the APP molecule, therefore increasing Abeta levels (Lanoiselée et al., 2017). However, ADAD only accounts for less than one percent of all AD cases (Bateman et al., 2011). Individuals with trisomy 21, also known as Down syndrome, who carry a third copy of chromosome 21, also have an extremely high risk of developing AD, likely because the *APP* gene is found on chromosome 21. Presumably, this additional dosage of the APP protein results in increased cerebral Abeta levels which leads to amyloid plaque deposition (Bateman et al., 2011). Because of these genetic factors and their molecular consequences that clearly drive the progression of AD, the amyloid cascade hypothesis of Alzheimer's disease has been proposed which states that the aggregation of Abeta into amyloid plaques results in metabolic changes within the brain that lead to TAU hyperphosphorylation, which causes TAU to aggregate within neurons, leading to neuronal cell death (Selkoe & Hardy, 2016).

However, these ADAD mutations or copy number variants of the APP gene are not the only genetic variants known to influence disease progression, but they are the only genetic variants known to directly cause AD. Through the use of genome-wide association studies (GWAS), many other genes have been implicated in influencing AD progression or in increasing susceptibility to the disease. These include genes generally involved with the immune response and inflammation (*CR1*, *CD33*, *TREM2*, etc.), endocytosis (*PICALM*, *CD2AP*, *SLC24A4*, etc.), or lipid metabolism (*APOE*, *PLD3*, *ABCA7*, etc.) (Karch & Goate, 2015). Though specific variants within these genes are associated with the development of AD, no individual carrying these variants is guaranteed to develop the disease. In this sense, GWAS has not served the purpose

of identifying causal variants of AD, but has helped to illuminate the molecular mechanisms and physiological processes that drive disease progression.

Of the genes associated with AD discovered via GWAS, two are the greatest contributors to calculated disease risk: *APOE* and *TREM2* (Wolfe, Fitz, Nam, Lefterov, & Koldamova, 2019). *APOE* encodes the Apolipoprotein E, which plays an important role in lipid transport within the central nervous system. The three most common *APOE* alleles are known as ε2, ε3, and ε4. The ε3 allele is the most common allele in the human population, and is considered to be neutral when calculating the risk of developing AD; that is, ε3 homozygotes are considered to be at no greater risk of developing AD compared to the general population. The ε4 allele confers a greater risk of developing AD, with ε4 heterozygotes having an increased risk of developing AD, while ε4 homozygotes are believed to have 15 times greater risk of developing the disease (Saddiki et al., 2020). The ε4 allele is also associated with earlier onset of the disease in a dose-dependent manner (C. C. Liu, Kanekiyo, Xu, & Bu, 2013). This risk is different between males and females, as females are more likely to develop AD (Scheyer et al., 2018). It is currently believed that the ε2 allele, which is rare compared to ε3 and ε4, may confer a protective effect when it comes to the risk of developing AD (Z. Li, Shue, Zhao, Shinohara, & Bu, 2020). It is necessary to point out that carrying one or two *APOE* ε4 alleles does not guarantee the development of AD, as individuals have been identified that are homozygous for *APOE* ε4 who never develop AD, as well as individuals who carry no ε4 alleles who develop the disease.

TREM2 codes for the Triggering Receptor Expressed on Myeloid cell 2, where it is expressed by microglia in the central nervous system (Wolfe et al., 2019). The *TREM2* allele that has been identified as conferring increased risk of AD is that which encodes the Arg47His mutation. Individuals carrying this mutation are currently believed to be at four times greater risk of developing AD than the general population, though the exact mechanism by which the risk is increased is unknown (Wolfe et al., 2019). Again, as with the *APOE* alleles, carrying one or more copies of the *TREM2* Arg47His polymorphic allele does no guarantee that a patient will develop AD.

While these genetic risk factors are becoming clearer for Autosomal Dominant Alzheimer's disease (ADAD), also known as Familial Alzheimer's disease (FAD), as well as sporadic Late-Onset Alzheimer's disease (LOAD), not much is understood about the genetic components contributing to the onset of sporadic Early-Onset Alzheimer's disease (EOAD) or familial LOAD. In this study, we seek to identify genetic risk factors associated with these two less-understood groups, and the hypothesis is visualized in Figure 1.

Figure 1

Diagram of the Missing Genetics of Alzheimer's Disease

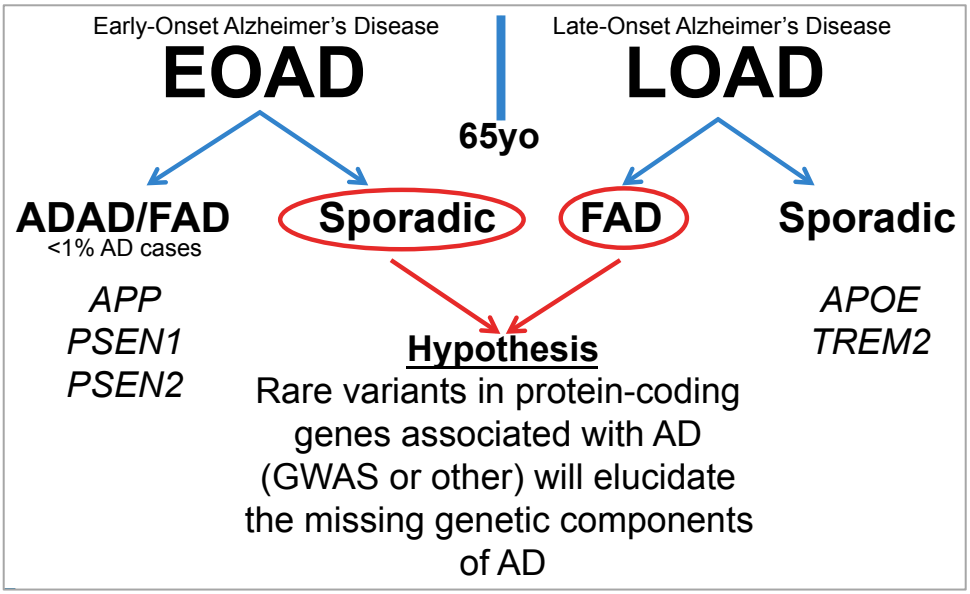

Note. Alzheimer's disease is currently separated into two major categories: early-onset AD (EOAD) and late-onset AD (LOAD), which is defined as disease onset before or after the age of 65, respectively. The genetics of familial EOAD and sporadic LOAD are better understood than sporadic EOAD or familial LOAD. The purpose of this work is to elucidate the missing genetic components of AD by studying these less investigated cases.

For our study, we enrolled the living members of a family in which six out of ten siblings developed Alzheimer's disease after the age of 65, who do not carry any of the known ADAD mutations, and identified a mutation in *ABCC1* (p.Tyr1189Cys) carried only by the affected

individuals. In a separate cohort of EOAD individuals, we identified a second rare *ABCC1* (p.Arg1342Gly) polymorphism carried by a patient who developed Alzheimer's disease before the age of 65. As previous studies have shown that ABCC1 is capable of exporting Abeta from the cytoplasm of the endothelial cells comprising the blood-brain barrier to the peripheral blood (Krohn et al., 2011), and thus plays a role in clearance of Abeta from the brain, we decided to study these mutations. We hypothesized that both of these mutations would alter ABCC1 protein function in a manner that decreases its ability to export Abeta, and thus may increase cerebral Abeta levels, significantly increasing the chances of amyloid plaque deposition and AD onset.

MATERIALS AND METHODS

For the family in our study, informed consent was given in accordance with the Western International Review Board (WIRB) protocol #20120789, and all research was performed in accordance with relevant guidelines and regulations. Saliva was collected using the Oragene OGD-500 saliva collection kit (DNA Genotek Inc., Ottawa, Canada) and DNA was extracted using the prepIT L2P DNA purification kit (DNA Genotek Inc.) according to the manufacturer's instructions. DNA was resuspended in EB Buffer (Qiagen, Hilden, Germany) and quantified using the Quant-iT PicoGreen dsDNA Assay Kit (ThermoFisher Scientific, Waltham, MA, USA). DNA library preparation was performed using the TruSeq Exome Kit and sequenced on the HiSeq2500 (Illumina, San Diego, CA, USA). Sequencing depth was 100X. Reads were aligned to the human reference genome GRCh37 using the Burrows-Wheeler Aligner (H. Li & Durbin, 2010), and variant calling was conducted using the Genome Analysis Toolkit (McKenna et al., 2010). Variant analysis was achieved using VarSeq (Golden Helix, Bozeman, MT, USA). Sanger sequencing was conducted by DNAlab (Arizona State University, Tempe, AZ, USA) to confirm the identified variants.

For the EOAD patient in our study, blood was collected using the BD Vacutainer Venous Blood Collection Tube with K2 EDTA (BD Biosciences, San Jose, CA, USA), and DNA was extracted and purified using the DNeasy Blood and Tissue Kit (Qiagen) and resuspended in EB buffer (Qiagen). Purified DNA was quantified using the Quant-iT PicoGreen dsDNA Assay Kit

(ThermoFisher Scientific) and was sequenced by Novogene Co. Ltd. (Beijing, China). Reads were aligned to human reference genome GRCh37 using the Burrows-Wheeler Aligner (H. Li & Durbin, 2010), and variants were called using the Genome Analysis Toolkit (McKenna et al., 2010). Variant analysis was accomplished using VarSeq (Golden Helix).

RESULTS

For our LOAD family, WES analysis resulted in 347,774 total variants identified. Variants were filtered according to the following parameters: GATK variant "PASS" (pass/fail quality control for individual base reads) = 307,973 remaining; sequencing depth ≥ 5 reads = 248,824; GATK quality (a confidence rating based upon the quality of the flanking reads) ≥ 300 = 223,232; GATK genotype quality (a quality score for each base weighted by the quality of that sample's overall sequencing quality) ≥ 20 = 213,005; minor allele frequency (MAF) (NHLBI ESP6500SI-V2-SSA137) ≤ 0.02 (or no data) = 165,330; sequence ontology (removed 3'-UTR, 5'-UTR, intronic, and intergenic variants) = 4,104; not carried by unaffected = 315; inherited by all affected = 54, gnomAD 12 allele count ≤ 50 = 10. Only one gene on this list was known to influence AD pathology, ABCC1. This genomic filtering approach is visualized in Figure 2.

Figure 2

Genetic Workflow of the Late-Onset Alzheimer's Disease Family

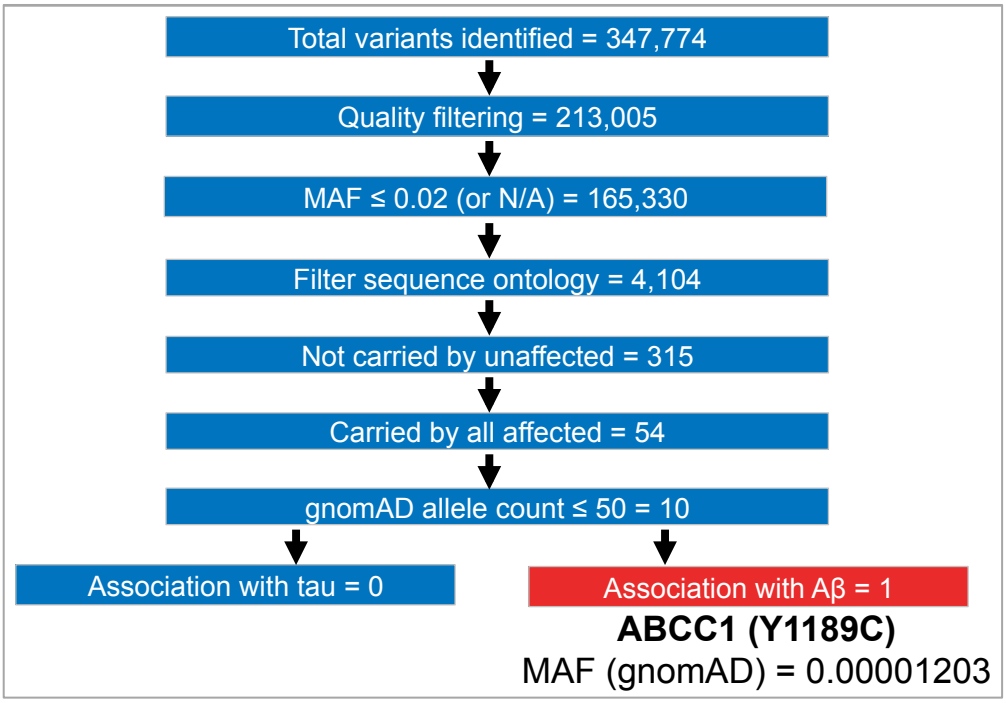

Note. Genomic workflow for the LOAD family featuring a filtering approach specifically designed to identify rare, protein-coding variants in our AD patients. The outline approach also specifically identifies why, out of nearly 350,000 identified variants, we chose to investigate the *ABCC1* (p.Tyr1189Cys) mutation.

For the EOAD patient, 1,932,256 total variants were identified from the raw sequencing data. After filtering for sequencing quality, 788,624 variants remain, and filtering out ambiguous zygosity leaves 357,374 total variants. We then filter the variants against public databases to identify only those variants that are carried by less than or equal to two percent of the general population, which leaves 317,992 variants. We then utilize the CADD PHRED scores of each of these variants to identify variants that occur in highly conserved regions of the genome (CADD greater than or equal to 20), which can be indicative of necessary genetic elements, and this leaves 16,074 variants. We also filter the variants for their sequence ontology, which removes 5' and 3' variants that do

not create novel start or stop codons, and this leaves 936 variants. We then filter the variants against our in-house list of genes to exclude because they are either highly variable genes, or are genes not expressed within the central nervous system (such as genes encoding mucin proteins), which leaves 828 variants. We further filter this list to look for rare variants by excluding variants that have an allele count that is greater than or equal to 200 in the public database gnomAD (Karczewski et al., 2020), which leaves just 210 variants of interest. The genes in which these final variants occur are then filtered against a list populated with the number of PubMed results for that gene and a second or third term. For example, if the hypothetical *GENE* was searched for in PubMed with the term Alzheimer (PubMed search = *GENE* Alzheimer), and more than 2 results appeared in PubMed, *GENE* would not be excluded from our list. In this case, 41 genes are associated with AD, 44 genes are associated with amyloid, and 38 genes are associated with TAU. From this final list of genes, *ABCC1* (p.Arg1342Gly) was selected for further analysis for multiple reasons: 1. It is very rare, as it is only seen a frequency of 0.0000107 in the general population, 2. The high CADD score of 26.7 means this nucleotide is highly conserved, and 3. We already had a pipeline in place for the analysis of *ABCC1* variants and their effects on APP metabolism. A visualization of this genomic workflow can be seen in Figure 3.

Figure 3

Genomic Workflow of the Early-Onset Alzheimer's Disease Patient

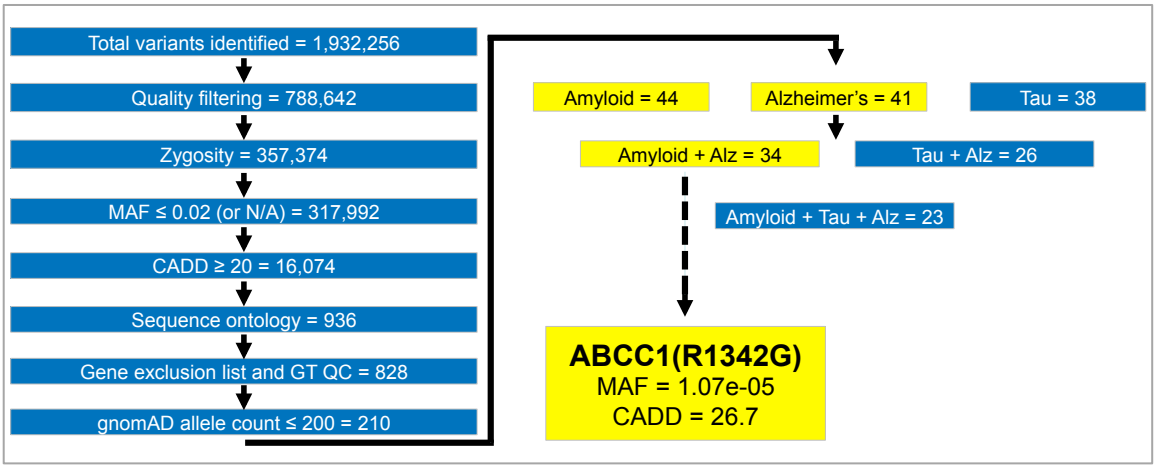

Note. Genomic workflow for the EOAD patient featuring a filtering approach designed to identify rare, protein-coding variants that may influence AD progression. ABCC1(Arg1342Gly) was chosen for further analysis because we were already studying, and had a pipeline in place, to answer this question.

DISCUSSION

ABCC1 encodes the Adenosine triphosphate Binding-Cassette protein family C member 1 (ABCC1 protein), an organic anion transporter that exports anionic molecules from the cytoplasm to the extracellular space (Cole, 2014). The protein is a 17-pass transmembrane protein with three major membrane-spanning domains (MSDs). All adenosine triphosphate binding cassette proteins contain two MSDs, known as MSD1 and MSD2; however, ABCC1 has a third MSD, known as MSD0, whose function is currently unknown (Cole, 2014).

The current model for ABCC1 protein function is that it allows cytoplasmic anions to bind to its binding pocket, which causes a conformational change within the protein that allows for ATP to bind to one of its nucleotide-binding domains (NBDs) (Linton & Higgins, 2007). Binding of ATP to NBD1 causes the second NBD (NBD2) to also bind to the ATP molecule, which causes another conformational change that opens the extracellular portion of the protein, while closing off the intracellular portion. Bound anions then freely diffuse to the extracellular space, and the two

NBDs work together to catalyze the dephosphorylation of ATP to ADP via hydrolysis, and the energy released from this reaction causes the ABCC1 molecule to return to its resting state. This process of using ATP hydrolysis to reset the protein is known as the “ATP switch” mechanism (Linton & Higgins, 2007).

The major canonical substrates of ABCC1 are glutathione, reduced glutathione, leukotriene C4, and sphingosine-1-phosphate (Cole, 2014). However, a large amount of literature exists on the ABCC1 protein (also known as MRP1, or Multidrug Resistance Protein 1), because it was discovered that the protein is capable of exporting chemo therapeutics, used in cancer treatment, from the cytoplasm to the extracellular space, thus providing drug resistance to cancer cells that express large amounts of the protein (Munoz, Henderson, Haber, & Norris, 2007).

Our variant analysis of the LOAD family identified ABCC1(Tyr1189Cys) as the mutation of highest interest in this familial case of late-onset Alzheimer’s disease. ABCC1, an organic anion transporter with a wide variety of substrates, has been identified as important for the export of Abeta from the endothelial cells of the blood brain barrier to the circulation in mouse models (Krohn et al., 2015, 2011). Furthermore, tyrosine 1189 of ABCC1 is one of two adjacent, highly-conserved tyrosine residues that are known to confer substrate specificity or affect overall function of the protein (Conseil, Deeley, & Cole, 2005; Deeley, Westlake, & Cole, 2006). In gnomAD, the world’s largest public database of combined whole exome and whole genomes of individuals over age 18, only 3 males carry the Y1189C mutation, with a resulting allele frequency of 1.22E-05, and no other germline mutation at either tyrosine has been documented (Karczewski et al., 2020). This not only highlights the rarity of our variant of interest, but also may reflect the importance of these tyrosine residues for proper ABCC1 function.

The variant analysis of our EOAD patient revealed many genes of interest in terms of their association to Alzheimer’s disease, but we chose to study ABCC1(Arg1342Gly) because we already had both an interest in rare *ABCC1* variants, as well as we already had a pipeline in place to study the effects of *ABCC1* mutations on APP processing and metabolism. In gnomAD, the MAF of this exact mutation is 1.07E-05, where only 3 individuals are heterozygous for this mutation, and no one is homozygous (Karczewski et al., 2020). There are 2 other documented

substitutions at this residue document in gnomAD, ABCC1(Arg1342Trp) with a MAF of 1.78E-05 (3 heterozygotes, and 1 homozygote), and ABCC1(Arg1342Gln) with a MAF of 3.19E-05 carried by 1 heterozygote (Karczewski et al., 2020). The mutation resides in the cytoplasmic topological domain just 8 amino acids downstream of the nucleoprotein-binding domain, required for ATP binding which the protein hydrolyzes to reset the protein to its resting state via the hypothesized “ATP switch” mechanism (Linton & Higgins, 2007). Because of the rarity of mutations at this residue, as well as its proximity to residues absolutely required for proper protein function, we hypothesized that this mutation would also inhibit the transport of Abeta from the cytoplasm to the extracellular space by altering the tertiary structure of the protein within this domain, which may reduce ATP hydrolysis, and thus inhibit the protein from resetting to its resting configuration required for substrate binding.

CHAPTER 3

IN VITRO ANALYSIS OF ABCC1 VARIANTS

INTRODUCTION

While *ABCC1* has been indirectly linked to Alzheimer's disease via mouse models (Krohn et al., 2015, 2011), no study has directly linked *ABCC1* to AD in humans. Furthermore, no study has linked any germline *ABCC1* polymorphism to any human disease. Though we hypothesize that both of our identified mutations are having a biological effect within our patients, we cannot assume that the Tyr1189Cys or Arg1342Gly mutations in *ABCC1* are the causal mutation in our LOAD family, or our EOAD patient, respectively. We cannot assume that they have any influence whatsoever on the onset or progression of disease, or that they alter the function of the protein in a manner that prevents it from exporting Abeta from the cytoplasm of cells to the extracellular space. In order to explore these possibilities, we generated and utilized an *in vitro* cellular model to look for changes in the concentrations of extracellular APP metabolites that may be due to either of these mutations, and controlled the experiment to see if any effect can be found by simply overexpressing the human reference *ABCC1* allele.

Our laboratory had previous data demonstrating that the BE(2)-m17 human neuroblastoma cell line expresses the *APP* gene, and that the cells also endogenously express all of the molecular machinery required to generate at least Abeta1-40 and Abeta1-42, making it a valid model for understanding the consequences of gene overexpression and the resulting consequences on APP metabolism. This is why we chose to use these cells in our study.

We utilized the Sleeping Beauty Transposon system, a two-vector-based transposable system that allows us to integrate our desired DNA sequences into a nearly random location within the genome of our target cells (Kowarz, Löscher, & Marschalek, 2015), to generate our control and experimental cell lines. First, a cell line was generated to overexpress a codon-optimized *APP* gene, whose product is the human reference APP protein, which allowed us to ensure that all APP metabolites would be at sufficiently detectable levels in our quantitative immunoassays. This cell line was then used to create the empty-vector control cell line, which provides the exogenous genetic material found in the experimental cell lines, but without

encoding the *ABCC1* gene, as well as the experimental cell lines which overexpress the codon-optimized *ABCC1* genes. The products of the codon-optimized *ABCC1* genes are either human reference ABCC1 protein, the ABCC1(Tyr1189Cys) protein, or the ABCC1(Arg1342Gly) mutant proteins. This allowed us to culture the cells and measure the extracellular levels of APP metabolites.

The first set of APP metabolite experiments did not examine the Arg1342Gly *ABCC1* mutation, and yielded results that seemed to contradict previous literature. Briefly, mean extracellular Abeta levels were lower in *ABCC1*-overexpressing cells compared to the empty vector control which was surprising because ABCC1 has been shown to export Abeta from the cytoplasm to the extracellular space (Krohn et al., 2011), not from the extracellular space to the cytoplasm. We therefore concluded that either our model was not working properly, perhaps that the ABCC1 protein was being inserted backwards into the plasma membrane, or that increased expression of *ABCC1* was altering APP metabolism, a novel insight not identified in any previous literature.

We tested this hypothesis by treating the cells with fluorescent Abeta, then used flow cytometry to quantify the percentage of fluorescent cells in each population. If our model is working properly, we expected to see a lower percentage of fluorescent cells in the *ABCC1*-overexpressing cells, as the fluorescent Abeta that enters the cells by any mechanism would expectedly be exported by ABCC1. We also treated the cells with thiethylperazine, a small molecule that has been shown to increase ABCC1-mediated export activity (Krohn et al., 2011), to ensure that the percentage of fluorescent cells is lowest for *ABCC1*-overexpressing cells treated with thiethylperazine compared to any other group. This is exactly what we observed, and this result was confirmed with a second fluorescent Abeta conjugated to an alternate fluorophore, both with and without thiethylperazine. Therefore, we concluded that our model was working appropriately, and that *ABCC1* overexpression was altering APP metabolism by some unknown mechanism.

In pursuit of that mechanism, we sequenced the transcriptome of the cell lines, and identified two genes whose differential expression due to *ABCC1* overexpression could be

involved in the altered cleavage of APP, based on previous literature. The increased *ABCC1* expression significantly reduced the expression of *TIMP3* which encodes the Tissue Inhibitor of Metalloproteinases 3, a protein that is capable of irreversibly inhibiting alpha-secretases (Hyang-Sook Hoe et al., 2007). *ABCC1* overexpression also decreased the expression of *CD38*, encoding the Cluster of Differentiation 38. Previous studies have shown that knockout of *CD38* reduces APP processing by limiting beta- and gamma-secretase activity (Blacher et al., 2015). The differential expression of both of these genes may be the reason why APP metabolism is altered in our cell model, though the mechanism by which these genes are differentially expressed is unknown.

We then confirmed our first APP metabolite experiments with an alternative platform (Meso Scale Discovery, MSD) utilizing our cryopreserved cells from the first set of experiments. We also examined the consequences of the Arg1342Gly *ABCC1* mutation with the MSD, and generated this cell line in parallel to newly created empty-vector and non-mutated *ABCC1* cells. This allowed us to confirm our first findings with those same cells, as well as to ensure that the results we observed were not due to location-specific integration of our vectors within the genome of the cells. This set of experiments confirmed that *ABCC1* overexpression alters APP processing by increasing the ration of alpha- over beta-secretase mediated cleavage of the APP molecule. These sets of experiments also demonstrated that neither of the *ABCC1* mutations we studied result in statistically significant differences in extracellular APP metabolite concentrations compared to the reference, and thus are likely not significantly contributing to the phenotype observed in our LOAD family, or our EOAD patient.

We also performed RNA-sequencing of the cryopreserved cell lines and the newly generated cell lines to confirm that *TIMP3* and *CD38* were differentially expressed. Indeed, *TIMP3* expression was reduced in every experiment. *CD38*, on the other hand, was trending towards significance in the newly generated cell lines, but did not reach the threshold of statistical significance.

To confirm that the differential expression of *TIMP3* and *CD38* due to *ABCC1* overexpression was not specific to the BE(2)-m17 human neuroblastoma cell line, we transfected

a second cell line, the ReNcell VM human neuroprogenitor cell line, with the empty vector and the non-mutant *ABCC1*-overexpressing vector and used qRT-PCR to specifically look for changes in *TIMP3* and *CD38* expression. We confirmed that *TIMP3* and *CD38* downregulation due to *ABCC1* overexpression was not limited to the BE(2)-m17 cells, but was also significantly different in the ReNcell VM cell line. Therefore, we can conclude that increasing *ABCC1* expression can alter the expression of these two genes in a manner that can skew APP processing away from the beta-secretase, amyloidogenic pathway, and towards the neuroprotective, alpha-secretase pathway.

This allows us to conclude that increased expression of *ABCC1* results in decreased Abeta production and increased alpha-secretase-mediated cleavage of the APP molecule. Taken together with previous literature that shows that ABCC1 is capable of exporting Abeta from the cytoplasm of endothelial cell lining the blood-brain barrier to the peripheral blood (Krohn et al., 2011), *ABCC1* may be a valuable drug target for the treatment of Alzheimer's disease. That is, if expression of *ABCC1*, or export activity of ABCC1, is increased, we may be able to indirectly reduce the production of Abeta, as well as increase clearance of proteins from the brain. This bimodal influence of *ABCC1* on amyloid deposition could essentially allow for a single molecule to achieve what the two main types of current AD clinical trials are trying to achieve: decrease Abeta production, or increased Abeta clearance. Many cancer drug development pipelines have already been utilized to find molecules that decrease *ABCC1* expression or that impair ABCC1 export, as the ABCC1 protein can confer chemoresistance to cancer cells by exporting chemotherapeutics from the cytoplasm to the extracellular space (Munoz et al., 2007). Logically, compounds have already been identified that do the opposite of what these pipelines intended: either increasing *ABCC1* expression, or increasing ABCC1-mediated export. These compounds should be studied in the context of Alzheimer's disease because of their potential to bimodally prevent the onset, or attenuate the progression, of the disease.

MATERIALS AND METHODS

Expression Vector Generation.

Codon-optimized *APP* was synthesized and cloned into the Sleeping Beauty transposon vector pSBbi-Hyg (A gift from Eric Kowarz, Addgene plasmid #60524) at the SfiI sites in the proper orientation (downstream of the EF1alpha promoter) by GenScript (Piscataway, NJ, USA). The resulting plasmid is hereafter referred to as pSBbi-Hyg-APP. Codon-optimized *ABCC1* (human reference amino acid sequence, hereafter referred to as ABCC1(WT)) was synthesized and cloned the same way into Sleeping Beauty transposon vector pSBbi-Pur (A gift from Eric Kowarz, Addgene plasmid #60523) by GenScript, and the resulting plasmid is hereafter referred to as pSBbi-Pur-ABCC1(WT). *ABCC1* (p.Tyr1189Cys), hereafter referred to as ABCC1(Y1189C) was obtained via site-directed mutagenesis (SDM) and cloned into the pSBbi-Pur vector by GenScript, and the resulting plasmid is hereafter referred to as pSBbi-Pur-ABCC1(Y1189C). All vectors received from GenScript were accompanied by quality control documents and full sequencing of the final plasmids. *ABCC1* (p.Arg1342Gly), hereafter referred to as ABCC1(R1342G), was obtained via SDM performed in-house using the overlapping primer method (H. Liu & Naismith, 2008).

For the SDM, the primers were used 5'-GGGACTGTTTGGAATCAACG-3' and 5'-CGTTGATTCCAAACAGTCCC-3' and pSBbi-Pur-ABCC1(WT) served as the template DNA. Polymerase chain reaction (PCR) was performed using the Phusion High-Fidelity DNA Polymerase according to the manufacturer's instructions. Cycling occurred as follows in the DNA Tetrad 2 Thermal Cycler (Bio-Rad Laboratories, Hercules, CA, USA): 98 °C for 30 sec, 12 cycles of 98 °C for 10 sec, 48 °C for 30 sec, 72 °C for 5 min and 25 sec, then a final extension at 72 °C for 10 min. The reaction was then transformed into NEB 5-alpha Competent *E. coli* cells (New England Biolabs, Ipswich, MA, USA), and plated on LB Broth Base (Invitrogen, Carlsbad, CA, USA) and Agar (Fisher Scientific) plates supplemented with 100ug/mL ampicillin (MilliporeSigma, Burlington, MA, USA). Resulting colonies were screened by inoculating 3.0mL overnight cultures of LB Broth Base (Invitrogen) in DI water supplemented with 100ug/mL ampicillin (MilliporeSigma), and plasmids were extracted from cultures using the QIAprep Spin Miniprep Kit

(Qiagen). The desired mutation was confirmed via Sanger sequencing at DNAlab (Arizona State University). Remaining plasmid DNA from the confirmed clone was subject to SfiI (New England Biolabs) digest, according to the manufacturer's instructions, and was run on a 0.8% UltraPure Agarose gel (ThermoFisher Scientific). The *ABCC1*-encoding fragment was manually excised and purified using the NucleoSpin Gel and PCR Clean-up Mini Kit (Macherey-Nagel, Düren, Germany). Purified DNA fragment was then subcloned into freshly SfiI- (New England Biolabs) digested, gel-purified, and 5' and 3' dephosphorylated (Antarctic Phosphatase, New England Biolabs) pSBbi-Pur plasmid using T4 DNA Ligase (New England Biolabs), according to the manufacturer's instructions. Ligation reaction was transformed into NEB 5-alpha Competent *E. coli* cells (New England Biolabs) and plated on the same plates as previously described. Resulting colonies were screened as previously described. The remaining culture of the confirmed clone was then used to inoculate two 50mL overnight cultures of the same media previously described. Final experimental plasmids were purified from these cultures using the Plasmid Midi Kit (Qiagen), according to the manufacturer's instructions.

Cell Line Generation.

BE(2)-m17 human neuroblastoma cells (ATCC, Manassas, VA, USA) were cotransfected with pSBbi-Hyg-APP and pCMV(CAT)T7-SB100 (A gift of Zsuzsanna Izsvak, Addgene plasmid #34879) via electroporation using the Amaxa Nucleofector II Device (Lonza Group AG, Basel, Switzerland) with the Cell Line Nucleofector Kit V (Lonza Group AG) using setting X-001. Cells were grown in equal parts EMEM (ATCC) and Ham's F-12 Nutrient Mix (ThermoFisher Scientific) supplemented with 10% FBS (Gibco, ThermoFisher Scientific) and Pen Strep (Gibco, ThermoFisher Scientific), and selected for with 1.0mg/mL Hygromycin B (Invitrogen). This cell line was used to create the control cell line and the three experimental cell lines.

The BE(2)-m17 control cell line was generated by cotransfecting the pSBbi-Hyg-APP BE(2)-m17 cells with pSBbi-Pur and pCMV(CAT)T7-SB100 using the same transfection technique previously described. Cells were selected for in media previously described supplemented with 10ug/mL Puromycin Dihydrochloride (Gibco). This control line will be referred

to as APP-Puro in the remainder of the text. The three experimental cell lines were generated by cotransfecting pSBbi-Hyg-APP BE(2)-m17 cells with either pSBbi-Pur-ABCC1(WT), pSBbi-Pur-ABCC1(Y1189C), or pSBbi-Pur-ABCC1(R1342G) with pCMV(CAT)T7-SB100 using the same transfection technique previously described. These cell lines will be referred to as APP-ABCC1(WT), APP-ABCC1(Y1189C), and APP-ABCC1(R1342G), respectively, for the remainder of the text. Cells were cultured and selected for in media previously described supplemented with 10ug/mL Puromycin Dihydrochloride (Gibco). Following successful selection, all cell lines were grown and maintained in the media previously described supplemented with 200ug/mL Hygromycin B (Gibco) and 2.0ug/mL Puromycin Dihydrochloride (Gibco).

ReNcell VM (MilliporeSigma) experimental cell lines were generated by cotransfecting pSBbi-Pur or pSBbi-Pur-ABCC1(WT) with pCMV(CAT)T7-SB100 using the Amaxa Nucleofector II Device (Lonza Group AG) with Cell Line Nucleofector Kit V (Lonza Group AG) and setting X-001. These cell lines will be referred to as ReNcell VM-Puro and ReNCell VM-ABCC1(WT) for the remainder of the text. Cells were cultured in ReNcell Media (MilliporeSigma) supplemented with Pen-Strep (Gibco, ThermoFisher Scientific), and selected for with 10ug/mL Puromycin Dihydrochloride (Gibco). Cells were maintained in this media, but with just 2.0ug/mL puromycin. Expression of APP and ABCC1 were confirmed by Western blot for all cell lines generated.

APP Metabolite Experimental Setup.

APP metabolite experiments were performed in batches, plated and harvested weekly, and samples stored until three weeks of experiments could be assayed together, with only one *ABCC1* mutation being examined at time. Weekly, 1.4e07 BE(2)-m17 control cells (pSBbi-Hyg-APP + pSBbi-Pur), ABCC1(WT) cells (pSBbi-Hyg-APP + pSBbi-Pur-ABCC1(WT)), and ABCC1(Y1189C) (pSBbi-Hyg-APP + pSBbi-Pur-ABCC1(Y1189C)) or ABCC1(R1342G) (pSBbi-Hyg-APP + pSBbi-Pur-ABCC1(R1342G)) were plated in a well of a untreated six-well plate with 3.0mL previously described BE(2)-m17 media, but without selection antibiotics. Media was changed for each well each of the next two days to 1.0mL media, then 0.75mL media, respectively. On the fourth day, supernatant was harvested, supplemented with 1.0mM 4-(2-

Aminoethyl)benzenesulfonyl fluoride hydrochloride (AEBSF, MilliporeSigma) in DMSO, and clarified at 10,000xg for 10 minutes at room temperature. Clarified supernatant was transferred to a new tube and stored at -80 °C until assayed. Performed in parallel with the supernatant harvesting, cells within the plate were lysed for either RNA extraction for RNA sequencing (RNA-seq) using the Quick-RNA Miniprep Plus Kit (Zymo Research, Irvine, CA, USA) or protein purification using RIPA Buffer (ThermoFisher Scientific), and each was used in accordance with the manufacturer's protocol. Purified RNA or protein was stored at -80 °C until assayed.

Extracellular APP metabolites were measured using enzyme-linked immunosorbent assays (ELISAs) or electrochemilluminescence (ECL) assays. For the ELISAs, Abeta1-40 was measured using the Amyloid beta 40 Human ELISA Kit (Invitrogen), Abeta1-42 was measured using either the Amyoid beta 42 Human ELISA Kit (Invitrogen) or the Amyloid beta 42 Human ELISA Kit, Ultrasensitive (Invitrogen), and sAPPalpha was measured using the Human Soluble Amyloid Precursor Protein alpha (sAPPalpha) ELISA Kit (MyBioSource, San Diego, CA, USA). All ELISAs were run according to the manufacturer's protocol with 50-fold dilutions of samples for the sAPPalpha ELISA and 4-fold dilutions for the other ELISAs. All ELISA plates were read on the Cytation 3 Multi-Mode Reader (Biotek, Winooski, VT, USA) and data was analyzed using a four-parameter logistic regression. All data points are the mean of technical quadruplicates. Statistical analyses performed were ANOVA and Tukey's Honest Significantly Different Test.

For the ECL assays, Abeta1-40 and Abeta1-42 were measured simultaneously using the Abeta Peptide Panel 1 (6E10) Multiplex Kit (Meso Scale Discovery, Rockville, MD, USA), and sAPPalpha and sAPPbeta were measured simultaneously using the sAPPalpha/sAPPbeta Kit (Meso Scale Discovery). All samples were diluted 5-fold for each assay. Plates were read on the MESO QuickPlex SQ 120 (Meso Scale Discovery), and raw data was analyzed using a four-parameter logistic regression. All data points represent the means of technical quadruplicates.

Flow Cytometry Experiments.

Cell lines were incubated with media supplemented with 200nM human Beta-Amyloid (1-42) HiLyte Fluor 555 (AnaSpec, Fremont, CA, USA) or 200nM human Beta-Amyloid (1-42) HiLyte

Fluor 488 (AnaSpec), with or without thiethylperazine (MilliporeSigma) for approximately 18 hours. Cells were then washed twice with phosphate buffered saline (PBS), trypsinized, and spun-down. Pelleted cells were washed once with ice cold PBS, then resuspended in 1% FBS in ice cold PBS, and kept on ice until assayed. Sorting occurred on the FACSCanto II (BD Biosciences) or the Sony SH100S (Sony Biotechnologies Inc.), and initially gated using untreated cells. Values are reported as the percentage of fluorescent cells.

RNA-seq Experiments.

The first RNA-seq experiment utilized the TruSeq RNA Library Prep Kit v2 on the NextSeq500 (Illumina), and results mapped to 37,703 unique Ensembl IDs. The mean total reads per sample was 58.0±15.1 million. The next two RNA-seq experiments utilized the SMARTer Stranded Total RNA-Seq Kit v2 – Pico Input Mammalian (Takara Bio Inc., Kusatsu, Shiga, JP), and were sequenced on the NovaSeq 6000 (Illumina). Results mapped to 54,723 and 55,109 unique Ensembl IDs, respectively. The mean total reads per sample was 73.2±14.6 and 50.6±7.6 million reads, respectively. FASTQs were generated with bcl2fastq v2.18 (Illumina). Reads were aligned with STAR v2.7.3a (Dobin et al., 2013) to generate BAM files, and differential expression analysis was accomplished using featureCounts from Subread package v2.0.0 (Y. Liao, Smyth, & Shi, 2014) and DeSeq2 v1.26.0 (Y. Liao et al., 2014). Gene Set Enrichment Analysis (GSEA) was performed using the ReactomePA package (Yu & He, 2016) in R.

Quantitative Reverse Transcription Polymerase Chain Reaction.

Reverse transcription (RT) and no-RT reactions were achieved using SuperScript IV VILO Master Mix (Thermo Fisher Scientific) using 750ng of RNA in a 20uL reaction. qPCR was performed using 1uL of the RT or no-RT reactions and TaqMan Fast Advanced Master Mix (Applied Biosystems) multiplexed with primer/probe set for ACTB (Hs01060665_g1, VIC-MGB) and either TIMP3 (Hs00165949_m1, FAM-MGB) or CD38 (Hs00120071_m1, FAM-MGB). Reactions were run on the QuantStudio 6 Flex Real-Time PCR System (Applied Biosciences), according to the manufacturer's protocol. Samples were measured in quadruplicate an quantified

using the RQ = 2^(-(delta delta CT)) method (Livak and Schmittgen, 2001), and values reported as means of those technical replicates. Statistical analysis for qRT-PCR was Student's two-tailed T-test.

RESULTS

First APP Metabolite Experiments.

To determine if ABCC1 or the mutant ABCC1(Y1189C) alters the extracellular metabolic profile of APP derivatives, we measured Abeta1-40, Abeta1-42, and sAPPalpha supernatant concentrations by ELISA, using transfected BE(2)-m17 human neuroblastoma cells.

In the first experiment measuring extracellular Abeta1-40, supernatant from APP-Puro cells had a mean of 1650.96 pg/mL, while APP-ABCC1(WT) had a mean of 1089.28 pg/mL, and APP-ABCC1(Y1189C) had a mean of 1248.79 pg/mL of Abeta1-40. There was a significant difference between the groups [ANOVA; F(2,6)=71.39, p=6.56E-05]. Post-hoc analysis utilizing the Tukey HSD test revealed that the means were significantly different between the APP-Puro and APP-ABCC1(WT) supernatants [TukeyHSD; p=6.10E-05], the APP-Puro and APP-ABCC1(Y1189C) supernatants [TukeyHSD; p=4.10E-04], and the APP-ABCC1(WT) and APP-ABCC1(Y1189C) supernatants [TukeyHSD; p=0.038].

When measuring Abeta1-42 concentrations in the supernatants, APP-Puro cells had a mean of 190.90 pg/mL, APP-ABCC1(WT) cells had a mean of 128.18 pg/mL, and APP-ABCC1(Y1189C) cells had a mean of 153.70 pg/mL, with a significant difference between the groups [ANOVA; F(2,6)=11.63, p=8.62E-03]. Post-hoc analysis utilizing the Tukey HSD test revealed that the means were significantly different between the APP-Puro cell line and the APP-ABCC1(WT) cell line [TukeyHSD; p=7.20E-03], but not between any of the other comparisons.

We also measured sAPPalpha, and examined the ratios of the sum of Abeta1-40 and Abeta1-42 over sAPPalpha, to look for skewing of APP metabolism from the beta- to alpha-secretase pathway. The APP-Puro cell line had a ratio of 1.56, while the APP-ABCC1(WT) and APP-ABCC1(Y1189C) had ratios of 1.02 and 1.24, respectively. There was a significant difference between the mean ratios of the three groups [ANOVA; F(2,6)=18.55, p=2.70E-03].

Post-hoc analysis utilizing the Tukey HSD test revealed that the means were significantly different between the APP-Puro and APP-ABCC1(WT) cell lines [TukeyHSD; p=2.20E-03], as well as between the APP-Puro and APP-ABCC1(Y1189C) cell lines [TukeyHSD; p=0.026]. There was no significant difference between the mean ratios of the APP-ABCC1(WT) and APP-ABCC1(Y1189C) cell lines. The summary of the ANOVA data for this set of experiments can be found in Table 1. Box plots of these data, as well as Tukey HSD p-values, can be found in Figure 4.

Table 1

ANOVA Table from the First APP Metabolite Experiment

First APP Metabolite Experiment
APP-Pur, APP-ABCC1(WT), APP-ABCC1(Y1189C)

Analyte		ANOVA Tables				
Abeta1-40		**DF**	**Sum Sq**	**Mean Sq**	**F value**	**Pr (>F)**
	Var	2	502676	251338	71.39	6.56E-05
	Res	6	21124	3521		
Abeta1-42		**DF**	**Sum Sq**	**Mean Sq**	**F value**	**Pr (>F)**
	Var	2	5968	2984.2	11.63	8.62E-03
	Res	6	1540	256.6		
sAPPa/Abeta		**DF**	**Sum Sq**	**Mean Sq**	**F value**	**Pr (>F)**
	Var	2	0.4415	0.2208	18.55	2.70E-03
	Res	6	0.0714	0.0119		

The second APP metabolite experiment yielded similar statistical results. For Abeta1-40, the mean supernatant concentration from the APP-Puro cell line was 2478.28 pg/mL, while the means for the APP-ABCC1(WT) and APP-ABCC1(Y1189C) cell lines were 1658.41 pg/mL and 1813.71 pg/mL, respectively. There was a significant difference between the means of the groups [ANOVA; F(2,6)=14.38, p=2.70E-03]. The post-hoc analysis utilizing the Tukey HSD test revealed that the means between the APP-Puro and APP-ABCC1(WT) cell lines were significantly different [TukeyHSD; p=5.60E-03], as well as the means between the APP-Puro and APP-ABCC1(Y1189C) cell lines [TukeyHSD; p=0.015]. There was no significant difference between the means of the APP-ABCC1(WT) and APP-ABCC1(Y1189C) cell lines.

For Abeta1-42, the mean supernatant concentration from the APP-Puro cell lines was 130.25 pg/mL, while the means were 73.07 pg/mL and 91.22 pg/mL for the APP-ABCC1(WT) and APP-ABCC1(Y1189C) cell lines, respectively. There was a significant difference between the groups [ANOVA; F(2,6)=7.018, p=0.027]. Post-hoc analysis utilizing the Tukey HSD test revealed a significant difference between the means of the APP-Puro and APP-ABCC1(WT) cell lines. No significant difference was identified between any of the other groups.

For the ratio of the sum of Abeta1-40 and Abeta1-42 over sAPPalpha, the mean ratio for the APP-Puro cell line was 2.12, while the mean ratios for APP-ABCC1(WT) and APP-ABCC1(Y1189C) were 1.46 and 1.86, respectively. No significant difference in the mean ratios was found between any of the groups [ANOVA; F(2,6)=3.325, p=0.107]. The summary of the ANOVA data can be found in Table 2, and box plots with accompanying p-values can be found in Figure 5.

Table 2

ANOVA Table from the Second APP Metabolite Experiment

Second APP Metabolite Experiment APP-Pur, APP-ABCC1(WT), APP-ABCC1(Y1189C)						
Analyte			**ANOVA Tables**			
Abeta1-40		**DF**	**Sum Sq**	**Mean Sq**	**F value**	**Pr (>F)**
	Var	2	1137957	568979	14.38	5.15E-03
	Res	6	237477	39580		
Abeta1-42		**DF**	**Sum Sq**	**Mean Sq**	**F value**	**Pr (>F)**
	Var	2	5122	2560.9	7.018	2.69E-02
	Res	6	2190	364.9		
sAPPa/Abeta		**DF**	**Sum Sq**	**Mean Sq**	**F value**	**Pr (>F)**
	Var	2	0.6646	0.3323	3.325	1.07E-01
	Res	6	0.5996	0.0999		

These results were surprising because, as previously stated, ABCC1 has been shown to export Abeta from the cytoplasm to the extracellular space (Krohn et al., 2011), and if Abeta is, in

fact, a substrate for ABCC1, we would expect to see higher extracellular concentrations of Abeta species.

Abeta Export Assay.

To test whether ABCC1 exports Abeta, both cell lines were incubated with 200nM fluorescent Abeta1-42 (Beta-Amyloid (1-42), HiLyte Fluor 555-labeled, Human, AnaSpec, Fremont, CA, USA) for 18 hours, and then cells were subject to flow cytometry (FACSCanto II, BD Biosciences, Franklin Lakes, NJ) to quantify the percentage of fluorescent cells. 79.7% of the APP-Puro cells were fluorescent, while only 68.4% of APP-ABCC1(WT) cells and 70.3% of APP-ABCC1(Y1189C) cells displayed intracellular fluorescence. Furthermore, when incubated with fluorescent Abeta1-42 and 25uM thiethylperazine (MilliporeSigma, Burlington, MA, USA), a small molecule previously shown to increase ABCC1-mediated transport of Abeta, we observed that 60.9% of the APP-Puro cells were fluorescent, while just 42.4% of APP-ABCC1(WT) cells and 39.0% of APP-ABCC19Y1189C) cells were fluorescent. Because we were not attempting to prove anything new about ABCC1-mediated export of Abeta, but rather ensuring that our model was working in a manner that aligned with previous literature, this experiment was not repeated for the purpose of statistical analysis.

However, this experiment was repeated using a second fluorescent peptide (Beta-Amyloid (1-42), HiLyte Fluor 488-labeled, Human, AnaSpec) and just the APP-Puro and APP-ABCC1(WT) cell lines to ensure that the results we observed were not due to potential issues that arise when handling fluorescent peptides (for example, aggregation, degradation, photo bleaching, etc). Like with the previous experiment, cells were treated with the fluorescent Abeta1-42 at a 200nM concentration, with or without 25uM thiethylperazine, and subject to flow cytometry (Sony SH800S, Sony Biotechnology Inc., San Jose, CA, USA). In this second experiment, we observed that 94.4% of empty vector control cells were fluorescent, while only 84.3% of ABCC1-overexpressing cells were fluorescent. When incubated with thiethylperazine, 91.8% of empty vector control cells were fluorescent, while 70.6% of ABCC1-overexpressing cells were fluorescent (see Figure 6). This confirms that our model is working as expected because it agrees

with previous reports: that ABCC1 does export Abeta, and that thiethylperazine increases ABCC1 transport activity.

First transcriptomic analysis.

Because we demonstrated that ABCC1 does export Abeta from the cytoplasm to the extracellular space, we hypothesized that ABCC1 may alter transcript levels of proteins capable of altering APP metabolism. To this end, we conducted RNA-sequencing of the cell lines and focused our analysis on the differences between the APP-ABCC1(WT) cell line versus the APP-Puro cell line, as this is where the greatest difference in APP metabolite values was observed during the first round of APP metabolite experiments. When comparing just these two cell lines, analysis revealed 2470 differentially expressed genes (DEGs) with adjusted p-values less than or equal to 0.001, of which 2192 were protein coding. We hypothesized that because of the drastic reduction in extracellular Abeta, if a single gene were responsible for the altered APP processing, that it would have a log base two fold change (log2FC) with an absolute value greater than or equal to 1.5, which left 268 genes of interest (GOIs). Each gene was manually researched for their association to Alzheimer's disease and amyloid pathology. This left 55 GOIs, 10 of which have known roles in APP/Abeta metabolism or transport – but whose expression levels are altered in the opposite direction one would expect for the observed ELISA results – and two with expression levels that may account for the lower levels of extracellular Abeta. All GOIs are discussed in Appendix A with a focus on this experiment, and in the context of the proceeding two RNA-seq experiments discussed later.

The genes whose expression levels may account for the reduced extracellular Abeta levels are *CD38* and *TIMP3*, with differential expression visualized in Figure 7. *CD38* encodes the Cluster of Differentiation 38, an enzyme that synthesizes and hydrolyzes cyclic adenosine 5'-diphosphate-ribose, a molecule that regulates intracellular calcium signaling (Chini, Chini, Kato, Takasawa, & Okamoto, 2002). It has been shown that *Cd38* knockout AD mouse models have attenuated cognitive deficits, decreased cerebral amyloid burden, and that primary neurons cultured from those mice secrete significantly less Abeta species (Blacher et al., 2015). The

authors found that knockout of *Cd38* alters beta- and gamma-secretase activity, effectively reducing both (Blacher et al., 2015). This aligns with the observations made in our experiment, that when *CD38* expression is reduced with a log2FC of -2.98 in the APP-ABCC1(WT) cell line (N=6, n=3, p=7.21E-09, padj=1.78E-07), extracellular Abeta levels are also reduced. This reduction in *CD38* expression is also observed in the APP-ABCC1(Y1189C) cell line, where it had a log2FC of -2.11 (N=6, n=3, p=4.35E-06, padj=1.11E-04), but there is no statistically significant difference in *CD38* expression when comparing the APP-ABCC1(WT) and APP-ABCC1(Y1189C) cell lines. Therefore, the reduction of *CD38* expression may contribute to the altered APP processing, though the mechanism by which ABCC1 alters *CD38* expression is not known.

TIMP3, our second candidate gene, encodes the Tissue Inhibitor of Metalloproteinases 3, a protein that can irreversibly inhibit APP-cleaving alpha-secretases like ADAM10 and ADAM17 (Hyang-Sook Hoe et al., 2007). It has also been shown that *TIMP3* expression is increased in AD brain tissue (Dunckley et al., 2006), which may play a role in increased Abeta production. In our experiment, we saw *TIMP3* expression reduced with a log2FC of -1.95 in the APP-ABCC1(WT) cell line compared to the APP-Puro cell line (N=6, n=3, p=2.54E-110, padj=7.56E-107). *TIMP3* expression was also significantly downregulated in the APP-ABCC1(Y1189C) cell line compared to the APP-Puro cell line, with a log2FC of -0.81 (N=6, n=3, p=4.86E-23, padj=1.16E-20). There was a statistically significant difference in the expression of *TIMP3* between the two ABCC1 overexpressing cell lines, with the APP-ABCC1(Y1189C) cell line having a log2FC of 1.15 when compared to the APP-ABCC1(WT) cell line (N=6, n=3, p=3.88E-38, padj=5.53E-35). Logically, if an alpha-secretase inhibitor is significantly decreased in expression, alpha-secretase activity would be increased, which would result in the reduction of secreted Abeta species because of the mutual exclusivity of the alpha- versus beta-secretase cleavage of APP previously discussed. It is also possible that the reduction of *CD38* and *TIMP3* works synergistically to reduce extracellular Abeta by decreasing beta- and gamma-, and increasing alpha-secretase activity.

Second Set of APP Metabolite Experiments.

The second set of APP metabolite experiments were performed with a greater number of samples in order to confirm our results in the first APP metabolite experiment, as well as to see if

any effect is observed due to the ABCC1(R1342G) mutation. Experiments were repeated with cryogenically preserved cells (for the APP-Puro, APP-ABCC1(WT), and ABCC1(Y1189C) experiment), as well as new transfected cells (APP-Puro and APP-ABCC1(WT) cell lines were created again when generating the ABCC1(R1342G) cell line), and APP metabolites were measured using the Meso Scale Discovery (MSD) platform (Meso Scale Diagnostics LLC, Rockville, MD, USA) which allows for the simultaneous, single-well measurement of Abeta1-40 and Abeta1-42, or sAPPalpha and sAPPbeta.

ABCC1(Y1189C) MSD Experiment.

For the ABCC1(Y1189C) MSD experiment, the mean extracellular concentration of Abeta1-40 was 1096.25 pg/mL for the APP-Puro cell line, but 691.11 pg/mL and 731.02 pg/mL for the APP-ABCC1(WT) and APP-ABCC1(Y1189C) cell lines, respectively. There was a significant difference between the means of the groups [ANOVA; $F(2,15)=90.05$, $p=4.40E-09$]. Post-hoc analysis utilizing the Tukey HSD test revealed that the APP-Puro cell line had a significantly higher mean extracellular concentration of Abeta1-40 compared to the APP-ABCC1(WT) cell line [TukeyHSD; $p<0.0E-06$] and the APP-ABCC1(Y1189C) cell line [TukeyHSD; $p<0.0E-06$]. No significant difference was found between the ABCC1 cell lines.

Extracellular Abeta1-42 concentrations were measured to be 82.64 pg/mL for the APP-Puro cell line, while the APP-ABCC1(WT) and APP-ABCC1(Y1189C) cell lines had extracellular Abeta1-42 concentration of 48.86 pg/mL and 53.83 pg/mL, respectively. There was a significant difference between the means of the three groups [ANOVA; $F(2,15)=91.23$, $p=4.02E-09$]. Post-hoc analysis using the Tukey HSD revealed that the mean extracellular concentration of Abeta1-42 was significantly higher from the APP-Puro cell line compared to the APP-ABCC1(WT) cell line [TukeyHSD; $p<0.0E-06$] and the APP-ABCC1(Y1189C) cell line [TukeyHSD; $p<0.0E-06$]. There was no significant difference between the mean extracellular concentrations of Abeta1-42 from the ABCC1 cell lines.

The mean extracellular concentrations of sAPPalpha were measured as 153.09 ng/mL, 146.53 ng/mL, and 145.50 ng/mL for the APP-Puro, APP-ABCC1(WT), and APP-

ABCC1(Y1189C) cell lines, respectively. There was no statistically significant difference between the means of the three groups [ANOVA; F(2,15)=0.45, p=0.646]. The mean extracellular concentration of sAPPbeta were measured as 151.99 ng/mL for the APP-Puro cell line, while the means of APP-ABCC1(WT) and APP-ABCC1(Y1189C) cell lines were 107.22 ng/mL and 103.55 ng/mL, respectively. There was a significant difference between the means of the three groups [ANOVA; F(2,15)=25.67, p=1.44E-05]. Post-hoc analysis utilizing the Tukey HSD test revealed that the mean extracellular concentrations of sAPPbeta were significantly different between the APP-Puro cell line and the APP-ABCC1(WT) cell line [TukeyHSD, p=7.50E-05], as well as between the APP-Puro and APP-ABCC1(Y1189C) cell lines [TukeyHSD; p=3.20E-05]. There was no significant difference in the mean extracellular concentrations of sAPPbeta between the ABCC1 cell lines. Box plots of this data can be found in Figure 8.

Because the MSD platform allows for the simultaneous measurement of sAPPalpha and sAPPbeta in a single well, we used the ratio of sAPPalpha over sAPPbeta (sAPPalpha/sAPPbeta) to monitor alpha- versus beta-secretase cleavage of APP molecules because it controls for many of the confounding factors that could influence our measurements, and instead offers a mole-to-mole comparison. The mean ratio of extracellular sAPPalpha over sAPPbeta (no units) was calculated as 1.01 for the APP-Puro cell line, 1.37 for the APP-ABCC1(WT) cell line, and 1.41 for the APP-ABCC1(Y1189C) cell line. There was a significant difference between the mean ratio of these three groups [ANOVA; F(2,15)=36.58, p=1.70E-06]. Post-hoc analysis utilizing the Tukey HSD test revealed that the difference between the mean ratios of the APP-Puro cell line and the APP-ABCC1(WT) cell lines was significant [TukeyHSD; p=1.40E-05], as well as between the APP-Puro and APP-ABCC1(Y1189C) cell lines [TukeyHSD; p=3.20E-06]. There was no significant difference between the mean ratios of the ABCC1 cell lines. The ANOVA results are summarized in Table 3, and boxplots of the data with accompanying p-values can be found in Figure 9.

Table 3

ANOVA Table from the Third APP Metabolite Experiment

APP Metabolite Experiment (MSD) APP-Pur, APP-ABCC1(WT), APP-ABCC1(Y1189C)						
Analyte				**ANOVA Tables**		
Abeta1-40		**DF**	**Sum Sq**	**Mean Sq**	**F value**	**Pr (>F)**
	Var	2	2392997	1196498	90.05	4.40E-09
	Res	15	199300	13287		
Abeta1-42		**DF**	**Sum Sq**	**Mean Sq**	**F value**	**Pr (>F)**
	Var	2	15364	7682	91.23	4.02E-09
	Res	15	1263	84		
sAPPalpha		**DF**	**Sum Sq**	**Mean Sq**	**F value**	**Pr (>F)**
	Var	2	203	101.7	0.45	6.46E-01
	Res	15	3393	226.2		
sAPPbeta		**DF**	**Sum Sq**	**Mean Sq**	**F value**	**Pr (>F)**
	Var	2	8727	4364	25.67	1.44E-05
	Res	15	2550	170		
sAPPa/sAPPb		**DF**	**Sum Sq**	**Mean Sq**	**F value**	**Pr (>F)**
	Var	2	0.5811	0.29057	36.58	1.70E-06
	Res	15	0.1191	0.00794		

ABCC1(R1342G) MSD Experiment.

For the ABCC1(R1342G) MSD experiment, the mean extracellular concentration of Abeta1-40 was 1355.57 pg/mL for the APP-Puro cell line, 878.22 pg/mL for the APP-ABCC1(WT) cell line, and 951.87 pg/mL for the APP-ABCC1(R1342G) cell line. The differences between the means of the three groups was significantly different [ANOVA; F(2,15)=41.41, p=7.81E-07]. Post-hoc analysis utilizing the Tukey HSD test revealed that the mean extracellular concentrations of Abeta1-40 were significantly different between the APP-Puro cell line and the APP-ABCC1(WT) cell line [TukeyHSD; p=1.20E-06], as well as between the APP-Puro and the APP-ABCC1(R1342G) cell line [TukeyHSD; p=9.50E-06]. There was no statistically significant difference between the mean extracellular Abeta1-40 concentrations of the ABCC1 cell lines.

Mean Abeta1-42 extracellular concentrations were measured as 99.77 pg/mL for the APP-Puro cell line, 64.10 pg/mL for the ABCC1(WT) cell line, and 68.14 pg/mL for the ABCC1(R1342G) cell line. The mean extracellular Abeta1-42 concentrations were significantly

different between the three groups [ANOVA; F(2,15)=58.76, p=8.01E-08]. Post-hoc analysis using the Tukey HSD test revealed that the mean extracellular Abeta concentrations were statistically significant between the APP-Puro and APP-ABCC1(WT) cell lines [TukeyHSD; p=2.0E-07] as well as between the APP-Puro and APP-ABCC1(R1342G) cell lines [TukeyHSD; p=8.0E-07]. The means were not statistically significant when comparing the ABCC1 cell lines to one another.

Mean extracellular concentrations of sAPPalpha were measured as 129.35 ng/mL for the APP-Puro cell line, and as 108.31 ng/mL and 127.32 ng/mL for the APP-ABCC1(WT) and APP-ABCC1(R1342G) cell lines, respectively. There was a significant difference in the mean extracellular concentrations of the three groups [ANOVA; F(2,15)=6.94, p=7.35E-03]. Post-hoc analysis using the Tukey HSD test revealed that the mean extracellular concentration were statistically significant between the APP-Puro and APP-ABCC1(WT) cell lines [TukeyHSD; p=0.011], as well as between the APP-ABCC1(WT) and APP-ABCC1(R1342G) cell lines [TukeyHSD; p=0.021]. There was no statistically significant difference between the mean extracellular concentration of sAPPalpha between the APP-Puro and APP-ABCC1(R1342G) cell lines.

sAPPbeta mean extracellular concentrations were measured as 157.03 ng/mL for the APP-Puro cell line, 120.05 ng/mL for the APP-ABCC1(WT) cell line, and 132.52 ng/mL for the APP-ABCC1(R1342G) cell line. The means between the three groups were statistically significant [ANOVA; F(2,15)=7.869, p=4.60E-03]. Post-hoc analysis using the Tukey HSD test revealed that the mean extracellular sAPPbeta concentration were significantly different between the APP-Puro and ABCC1(WT) cell lines [TukeyHSD; p=3.80E-03], and is trending towards significance between the APP-Puro and APP-ABCC1(R1342G) cell lines [TukeyHSD; p=0.051]. There was no statistically significant difference between the mean extracellular concentrations of sAPPbeta for the APP-ABCC1(WT) and APP-ABCC1(R1342G) cell lines. Box plots of this data can be visualized in Figure 10.

Again, the ratio of sAPPalpha over sAPPbeta was calculated to look for skewing of the secretase pathway. The mean ratio for the APP-Puro cell line (no units) was 0.83, while the ratio

was 0.91 and 0.96 for the APP-ABCC1(WT) and APP-ABCC1(R1342G) cell lines, respectively. There was a statistically significant difference in the mean ratios of the three groups [ANOVA; F(2,15)=11.09, p=1.11E-03]. Post-hoc analysis utilizing the Tukey HSD test revealed that the mean ratios were significantly different between the APP-Puro and APP-ABCC1(WT) cell lines [TukeyHSD; p=0.043], as well as between the APP-Puro and APP-ABCC1(R1342G) cell lines [TukeyHSD; p=7.90E-04]. There was no statistically significant difference in the mean ratios between the APP-ABCC1(WT) and APP-ABCC1(R1342G) cell lines. The ANOVA results are summarized in Table 4, and the boxplots and accompanying p-values can be found in Figure 11.

Table 4

ANOVA Table from the Fourth APP Metabolite Experiment

Fourth APP Metabolite Experiment APP-Pur, APP-ABCC1(WT), APP-ABCC1(R1342G)						
Analyte				**ANOVA Tables**		
Abeta1-40		**DF**	**Sum Sq**	**Mean Sq**	**F value**	**Pr (>F)**
	Var	2	3170077	1585039	41.41	7.81E-07
	Res	15	574203	38280		
Abeta1-42		**DF**	**Sum Sq**	**Mean Sq**	**F value**	**Pr (>F)**
	Var	2	18310	9155	58.76	8.01E-08
	Res	15	2337	156		
sAPPalpha		**DF**	**Sum Sq**	**Mean Sq**	**F value**	**Pr (>F)**
	Var	2	1616	808.2	6.94	7.35E-04
	Res	15	1747	116.5		
sAPPbeta		**DF**	**Sum Sq**	**Mean Sq**	**F value**	**Pr (>F)**
	Var	2	4248	2124.1	7..869	4.60E-03
	Res	15	4049	269.9		
sAPPa/sAPPb		**DF**	**Sum Sq**	**Mean Sq**	**F value**	**Pr (>F)**
	Var	2	0.05641	0.028203	11.09	1.11E-03
	Res	15	0.03816	0.002544		

Second transcriptomic analysis experiments.

Cells were again subject to RNA-seq. In both experiments, *TIMP3* was significantly downregulated, with a log2FC of -0.64 in cryopreserved APP-ABCC1(WT) cells (N=6, n=3, p=0.015) and -0.82 in newly transfected APP-ABCC1(WT) cells (N=6, n=3, p=5.7E-03),

compared to the APP-Puro cryopreserved or newly transfected cells, respectively. For the cryopreserved APP-ABCC1(Y1189C) cells compared to the APP-Puro cryopreserved cells, *TIMP3* had a statistically significant log2FC of -0.54 (N=6, n=3, p=0.040), again demonstrating that overexpression of *ABCC1* results in decreased expression of *TIMP3*. When comparing the APP-ABCC1(R1342G) cell line to the newly transfected APP-Puro cell line, we observed a log2FC for *TIMP3* of -0.44, which was trending towards statistical significance (N=6, n=3, p=0.054).

In the cryopreserved cells, *CD38* had an insignificant log2FC of -0.53 in APP-ABCC1(WT) cell line compared to the APP-Puro cell line (N=6, n=3, p=0.24) and -0.48 (N=6, n=3, p=0.069) when comparing the newly transfected APP-ABCC1(WT) and APP-Puro cell lines. When comparing the cryopreserved APP-ABCC1(Y1189C) and APP-Puro cell lines, *CD38* expression had a log2FC of -0.40, though it was not statistically significant (N=6, n=3, p=0.38). When comparing the newly transfected APP-ABCC1(R1342G) and APP-Puro cell lines, *CD38* expression was decreased with a log2FC of -0.32, though this again was not statistically significant (N=6, n=3, p=0.23). However, we do not believe that this is necessarily a reason to completely disregard the involvement of CD38 in the altered APP metabolism observed, as it is trending towards significance in the newly generated APP-ABCC1(WT) versus APP-Puro cell lines. Furthermore, this confirms that the reduction in extracellular Abeta species is likely not due to integration of the transposable vectors within genes that alter APP processing, but rather that the increase in ABCC1 protein expression is likely altering transcription of genes whose products are capable of altering APP metabolism. These data can be visualized in Figure 12 and Figure 13.

qRT-PCR of ReNcell VM RNA.

To determine if the transcriptional effects were cell line specific, we co-transfected the vectors (with SB100X) into ReNcell VM cells (MilliporeSigma), a human neural progenitor line, and extracted RNA from differentiated cells (14 days without growth factors). Transcripts were quantified using TaqMan (Applied Biosystems, Foster City, CA, USA) quantitative reverse

transcriptase PCR (qRT-PCR), with targeted transcripts normalized to *ACTB* expression, using the relative quantification (RQ) method (Livak & Schmittgen, 2001). *TIMP3* and *CD38* mean RQs were 11.10% lower (t=3.236, df=22, p=3.80E-03) and 76.0% lower (t=-12.76, df=22, p=1.21E-11), respectively, in the *ABCC1*-overexpressing cells versus the empty vector control (see Figure 14). These results agree with our previous results, that ABCC1 overexpression significantly alters the transcription levels of *TIMP3* and *CD38*, in a direction consistent with the reduced extracellular Abeta, and increased alpha- over beta-secretase cleaved APP molecules, and further demonstrates that altered transcriptional regulation of this gene is due to increased expression of ABCC1, rather than disruption of these genes due to transposable integration of the vectors.

DISCUSSION

We chose to use the BE(2)-m17 human neuroblastoma cells for the *in vitro* analysis of our *ABCC1* variants because these cells endogenously express all of the molecular machinery required for the production of Abeta1-40, Abeta1-42, sAPPalpha, and sAPPbeta from the metabolism of the APP molecule. This allows us to observe changes to the extracellular APP metabolites as the result of the constitutive overexpression of *ABCC1* reference and mutant genes. In order to ensure that the APP metabolites would be within the quantitative range of our assays, a constitutively-expressing, and genomic-integrating *APP* vector was first transfected into the cell line. The resulting cell line was then used for the transfection of either the empty-vector control line (APP-Puro), the reference *ABCC1* allele (APP-ABCC1(WT)), the Tyr1189Cys *ABCC1* allele (APP-ABCC1(Y1189C)), and the Arg1342Gly *ABCC1* allele (APP-ABCC1(R1342G). Due to the different times at which the *ABCC1* variants were discovered, the first round of experiments focused on the reference and the Try1189Cys *ABCC1* alleles, including the ELISAs and the first flow cytometry experiment, and the first RNA-seq experiment. The second round of APP metabolite experiments, which utilized the MSD platform and a second round of RNA-seq experiments, included the reference and both of the mutant *ABCC1* alleles, and each experiment was kept separate. This is because the experiments that included the APP-ABCC1(Y1189C) cell

line used cryopreserved cells from the first round of experiments, while the experiments that included the APP-ABCC1(R1342G) cell line utilized all newly transfected and selected cells.

Figure 4

Results from the First and Second APP Metabolite Experiments

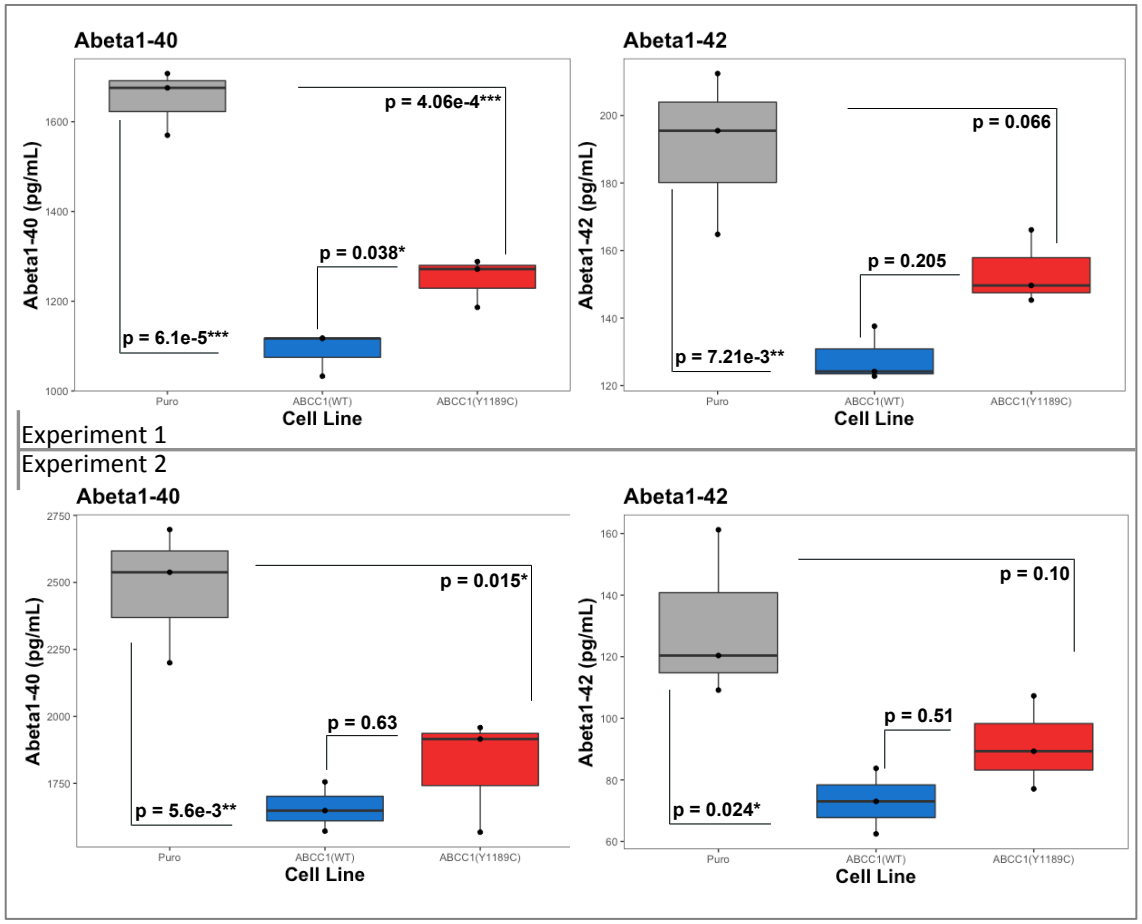

Note. Extracellular Abeta1-40 is significantly decreased in both of the *ABCC1*-overexpressing cell lines (labelled “ABCC1(WT)”, blue, and “ABCC1(Y1189C)”, red) compared to the empty-vector control cells (labelled “Puro”). Extracellular Abeta1-42 is significantly decreased in the reference *ABCC1*-overexpressing cells, in both experiments, while it is trending towards significance in the mutant *ABCC1*(p.Tyr1189Cys) cell line. P-values are indicated on the plots.

First APP Metabolite Experiments.

In the first round of APP metabolite experiments, we saw a significant decrease in the extracellular levels of Abeta1-40 and Abeta1-42 in both *ABCC1*-overexpressing cell lines with a significant difference between extracellular Abeta1-40 levels between the APP-ABCC1(WT) and APP-ABCC1(Y1189C) cell lines in the first experiment. This significant reduction in both Abeta species in both experiments between the APP-Puro control line and the APP-ABCC1(WT) cell line was surprising because the ABCC1 protein has been shown to be capable of exporting Abeta from the cytoplasm to the extracellular space (Krohn et al., 2011). Logically, if Abeta generated from the plasma membrane and released into the extracellular space was capable of entering the cytoplasm of the cells by any means, one would expect that the cells overexpressing an Abeta export molecule would have higher levels of Abeta in the extracellular space. However, in our experiment, we saw the exact opposite effect. Because of this strange result, we utilized a fluorescent-tagged Abeta1-42 molecule and flow cytometry to determine if our model is working as expected. If our model is working properly, and we treat our cells with Abeta, the *ABCC1*-overexpressing cells will have reduced intracellular Abeta compared to the control cells.

Figure 5

Ratio of Abeta to sAPPalpha from the First and Second APP Metabolite Experiments

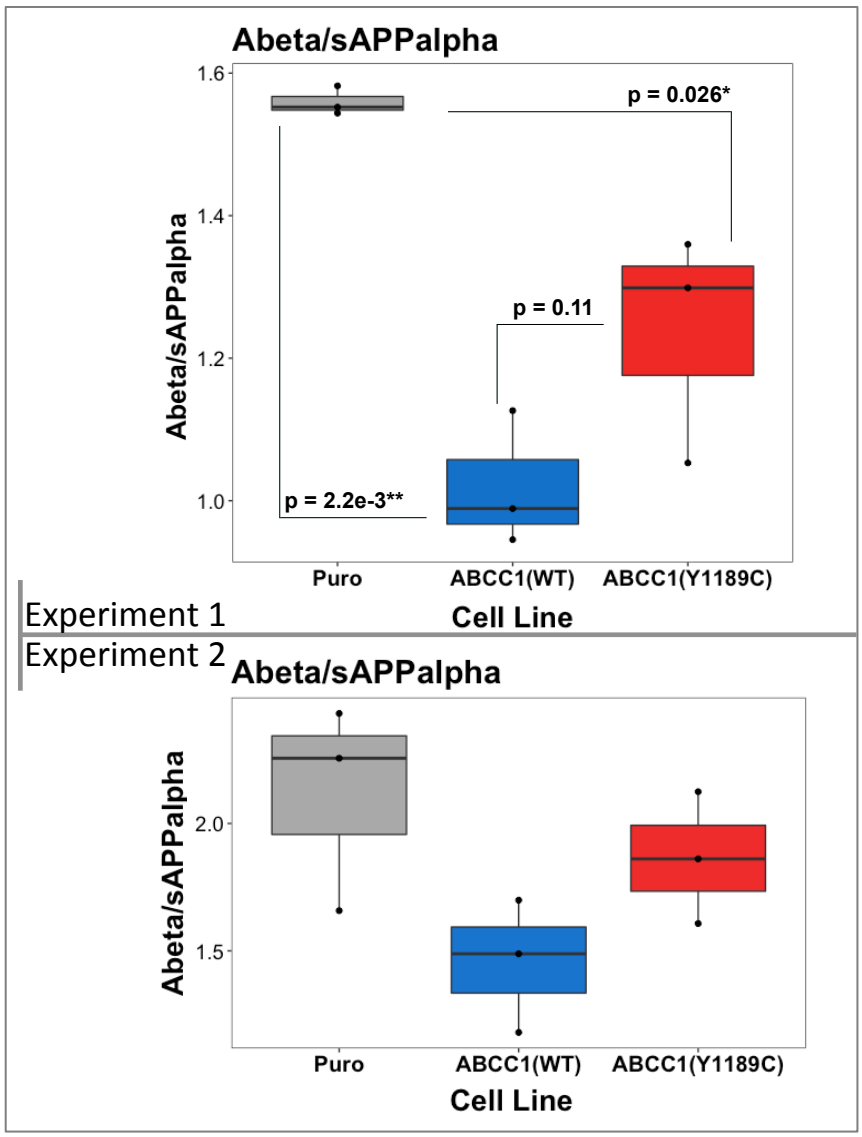

Note. The ratio of Abeta1-40 plus Abeta1-42 to sAPPalpha is significantly lower in both *ABCC1*-overexpressing cell lines (labelled “ABCC1(WT)”, blue, and “ABCC1(Y1189C)”, red) compared to the empty-vector control cell line (labelled “Puro”) in the first experiment, with no significant difference between the *ABCC1*-overexpressing cell lines. In the second APP metabolite experiment, no significant difference was found between the three groups, thus p-values are not indicated.

Flow Cytometry Experiment.

To demonstrate this, the APP-Puro, APP-ABCC1(WT), and the APP-ABCC1(Y1189C) cell lines were incubated with fluorescent Abeta1-42 for approximately 18 hours. Cells were then washed twice with PBS, dissociated, centrifuged, and then resuspended in ice-cold PBS supplemented with FBS to 1.0%. The experiment was gated with untreated cells, then experimental cells were analyzed using the flow cytometer to determine the percentage of fluorescent cells in each population in order to determine if the *ABCC1*-overexpressing cells are less fluorescent than the control cells, and thus determine if our model is working in accordance with previous literature. To further confirm that our model is working properly, we also incubated the cells with fluorescent Abeta and thiethylperazine, a small molecule that has previously been shown to increase ABCC1-mediated export of Abeta. If our model is appropriate for our study, *ABCC1*-overexpressing cells incubated with thiethylperazine should have the lowest percentage of population fluorescence of all groups in the experiment.

When the APP-Puro cells treated with just fluorescent Abeta were analyzed, 79.1% of the population displayed intracellular fluorescence, while the APP-ABCC1(WT) and APP-ABCC1(Y1189C) cell lines had a lower percentage of 68.4% and 70.6% fluorescent cells, respectively. When also treated with thiethylperazine, 61.5% of APP-Puro cells were fluorescent, while the APP-ABCC1(WT) cells were 41.5% fluorescent and the APP-ABCC1(Y1189C) cells were 38.4% fluorescent. This demonstrates that our model is working as expected, based upon previous literature. Therefore, the significant decrease in extracellular Abeta concentrations in the APP metabolite experiments is not due to a faulty model.

This flow cytometry experiment was later repeated to ensure that the results obtained were not due to mishandling of the fluorescent Abeta peptide, especially because this peptide is known to aggregate with itself. For the sake of simplicity, the experiment was repeated with only the APP-Puro and APP-ABCC1(WT) cell lines, and cells were treated with a fluorescent Abeta1-42 peptide, but the fluorophore conjugated to the peptide, and the flow cytometer used to analyze the cells, were different. The cells were also treated with or without thiethylperazine. Again, if our model is working properly, APP-ABCC1(WT) cell line should have a lower percentage of

fluorescent cells than the APP-Puro cell line, and when treated with thiethylperazine, the APP-ABCC1(WT) cells should have an even greater decrease in population fluorescence than the APP-Puro cells treated with thiethylperazine when compared to the non-thiethylperazine treated cells. For the APP-Puro cells, 94.44% of cells were fluorescent, while the APP-ABCC1(WT) cells were 84.32% fluorescent. When also treated with thiethylperazine, the APP-Puro cells were 91.84% fluorescent, while the thiethylperazine-treated APP-ABCC1(WT) were just 70.60% fluorescent. This confirms the results of our first flow cytometry experiment, and allows us to be confident that our cellular model is working as expected based upon previous literature: that ABCC1 exports Abeta from the cytoplasm to the extracellular space, and that this export activity can be increased by thiethylperazine.

Figure 6

Flow Cytometry Utilizing Fluorescent Abeta1-42 and Thiethylperazine

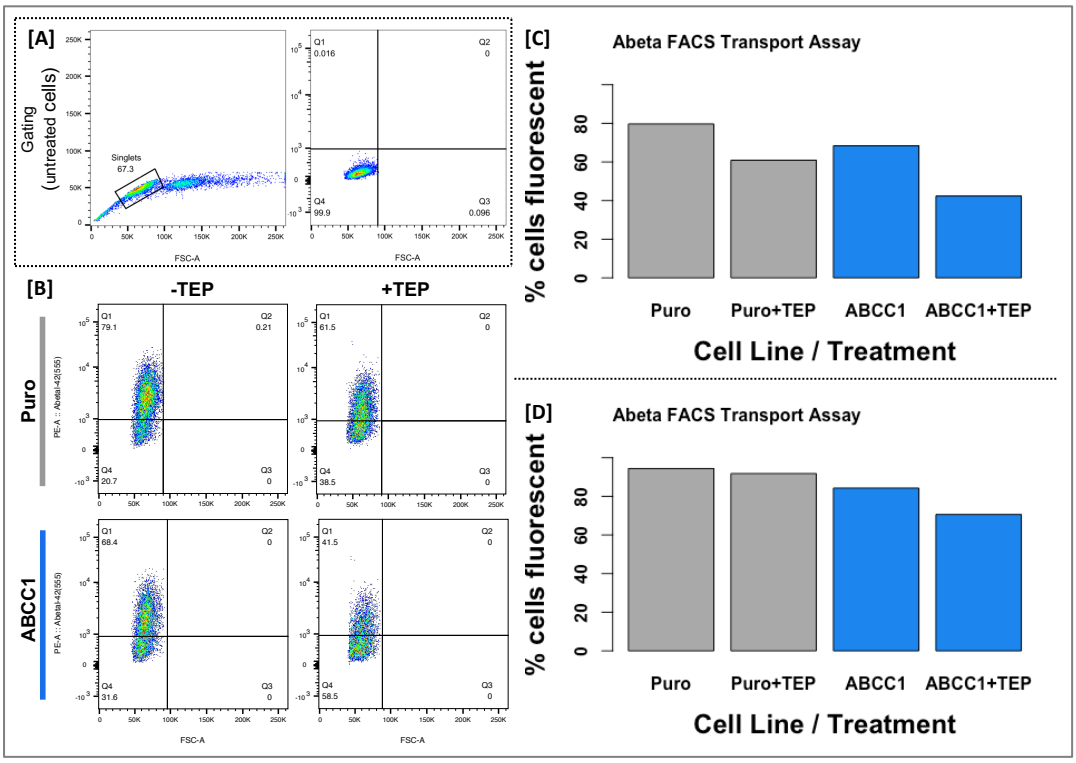

Note. The flow cytometry experiment was conducted by incubating the reference *ABCC1* cell line (labelled "ABCC1") and the empty-vector control cell line with fluorescent Abeta1-42, with or without thiethylperazine. The data confirm that ABCC1 exports Abeta from the cytoplasm to the extracellular space, and that this export is increased when treated with thiethylperazine.

First RNA-seq Experiment.

Because we know that our cellular model is working appropriately, but because we are observing reduced Abeta concentrations in the extracellular space of *ABCC1*-overexpressing cells, we hypothesized that the overexpression of *ABCC1* is altering the transcription of proteins capable of altering the metabolism of APP. To this end, we conducted RNA-seq of the cell lines to identify significantly differentially expressed genes whose altered transcription may account for the altered APP metabolism we observed. This analysis focuses on the difference between the

APP-Puro and the APP-ABCC1(WT) cell lines, as this is where the greatest difference in APP metabolite concentrations were observed.

Analysis revealed 2470 differentially expressed genes (DEGs) with adjusted p-values less than or equal to 0.001, of which 2192 were protein coding. We hypothesized that because of the drastic reduction in extracellular Abeta, if a single gene were responsible for the altered APP processing, that it would have a log base two fold-change (log2FC) with an absolute value greater than or equal to 1.5, which left 268 genes of interest (GOIs). Each gene was manually researched for their association to Alzheimer's disease and amyloid pathology. This left 55 GOIs, 10 of which have known roles in APP/Abeta metabolism or transport – but whose expression levels are altered in the opposite direction one would expect for the observed ELISA results – and two with expression levels that may account for the lower levels of extracellular Abeta. All GOIs are discussed in Appendix A with a focus on this experiment, and in the context of the proceeding two RNA-seq experiments discussed later.

The genes whose expression levels may account for the reduced extracellular Abeta levels are *CD38* and *TIMP3*. *CD38* encodes the Cluster of Differentiation 38, an enzyme that synthesizes and hydrolyzes cyclic adenosine 5'-diphosphate-ribose, a molecule that regulates intracellular calcium signaling (Chini et al., 2002). It has been shown that *Cd38* knockout AD mouse models have attenuated cognitive deficits, decreased cerebral amyloid burden, and that primary neurons cultured from those mice secrete significantly less Abeta species (Blacher et al., 2015). The authors found that knockout of *Cd38* alters beta- and gamma-secretase activity, effectively reducing both (Blacher et al., 2015). This aligns with the observations made in our experiment, that when CD38 expression is reduced (log2FC=-2.98, N=6, n=3, p=7.21e-09, padj=1.78e-07), extracellular Abeta levels are also reduced. Therefore, the reduction of *CD38* expression may contribute to the altered APP processing, though the mechanism by which ABCC1 alters *CD38* expression is not known.

TIMP3, our second candidate gene, encodes the Tissue Inhibitor of Metalloproteinases 3, a protein that can irreversibly inhibit APP-cleaving alpha-secretases like ADAM10 and ADAM17 (Hyang-Sook Hoe et al., 2007). It has also been shown that *TIMP3* expression is increased in AD

brain tissue (Dunckley et al., 2006), which may play a role in increased Abeta production. In our experiment, we saw *TIMP3* expression reduced with a log2FC of -1.95 in the ABCC1-overexpressing cell line compared to the empty vector control (N=6, n=3, p=2.54e-110, padj=7.56e-107). Logically, if an alpha-secretase inhibitor is significantly decrease in expression, alpha-secretase activity would be increased, which would result in the reduction of secreted Abeta species because of the mutual exclusivity of the alpha- versus beta-secretase cleavage of APP previously discussed. It is also possible that the reduction of *CD38* and *TIMP3* works synergistically to reduce extracellular Abeta by decreasing beta- and gamma-, and increasing alpha-secretase activity.

Figure 7

Normalized Counts for TIMP3 and CD38 from the First RNA-seq Experiment

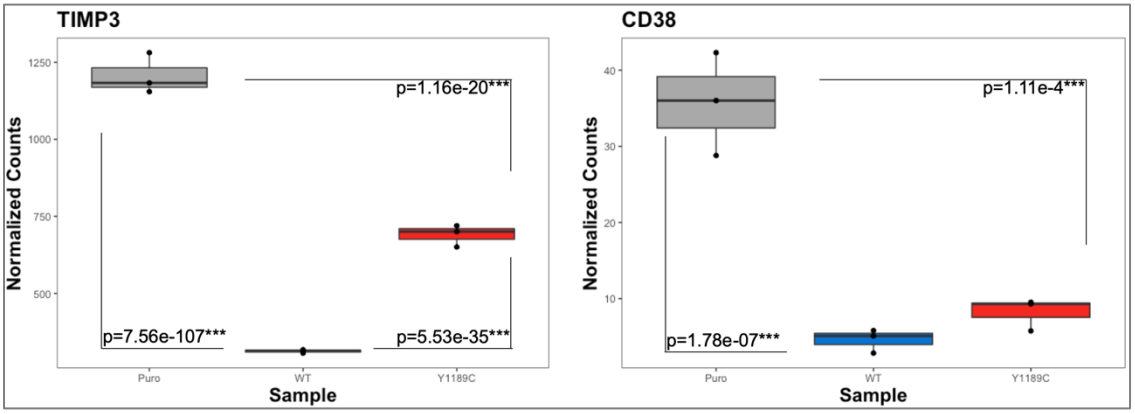

Note. *TIMP3* is differentially expressed between all three cell lines, and *CD38* is differentially expressed in both of the *ABCC1*-overexpressing cell lines compared to the empty vector control, with no significant difference between the reference (labelled “ABCC1(WT)”, blue) and mutant (labelled “ABCC1(Y1189C)”, red) *ABCC1* alleles. Only significant p-values are indicated on the plot.

Surprisingly, a number of genes were differentially expressed that have been shown to be capable of altering APP metabolism, though their expression was in the opposite direction

than would be expected if these genes were responsible for the altered APP processing we are observing. All of these genes will be discussed briefly.

GHRH encodes the Growth Hormone Releasing Hormone, a protein that is cleaved within the hypothalamus to produce the peptide somatoliberin, which stimulates the release of growth hormones from the pituitary gland (Dioufa et al., 2010). *GHRH* had a positive log2FC of 8.01 in our experiment when comparing the APP-ABCC1(WT) cell line to the APP-Puro cell line. A previous study has shown that administration of a GHRH antagonist, MIA-690, to the 5xFAD mouse reduced cerebral Abeta1-42 levels and Tau deposition (Jaszberenyi et al., 2012). Because the antagonist would effectively reduce or eliminate the activity of the GHRH protein in the 5xFAD mouse, we would expect to see a reduction in *GHRH* expression in our model if it were responsible for the reduction in extracellular Abeta that we observed.

PTGS1 encodes the Prostaglandin-Endoperoxide Synthase 1 protein, also known as Cyclooxygenase-1, or COX-1, a major regulator of angiogenesis (Hahn et al., 2005), as well as the main protein inhibited by nonsteroidal anti-inflammatory drugs (Vane & Botting, 1998). In our experiment, we saw a positive log2FC of 1.96 in the APP-ABCC1(WT) cell line compared to the APP-Puro cell line. A previous report has shown that expression of *PTGS1* in Chinese Hamster Ovary (CHO) cells increased the production of Abeta1-42 (Qin et al., 2003). However, in our experiment, we are observing increased expression of *PTGS1* in the APP-ABCC1(WT) cell line which has decreased extracellular Abeta1-42 concentrations. Therefore, increased *PTGS1* coinciding with decreased Abeta1-42 production is contrary to previous literature, and is likely not the reason for the decreased extracellular APP metabolites observed in our experiment.

The *SORCS2* gene encodes the Sortilin Related VPS10 Domain Containing Receptor 2, a protein that heterodimerizes to function as a receptor for growth factors that control axon growth and dendritic spine density (Glerup et al., 2014). In our experiment, we observed a negative log2FC of -1.53 in the APP-ABCC1(WT) cell line compared to the APP-Puro cell line. A previous study has shown that increasing *SORCS2* expression decreased Abeta production, while decreasing *SORCS2* expression increased gamma-secretase activity (Reitz et al., 2013), which would increase extracellular APP metabolite concentrations. In our model, *SORCS2* expression is

decreased, while extracellular concentrations of Abeta are also decreased. Therefore, previous literature indicates that the downregulation of *SORCS2* in the APP-ABCC1(WT) cell line is likely not the proper explanation for the decreased extracellular Abeta we observed.

SEZ6 encodes the Seizure Related 6 Homolog protein, which plays a role in neuronal membrane signaling and the development of proper synaptic excitation (Zhu et al., 2018). Mutations in this gene have been known to cause febrile seizures or dystonia (Mulley et al., 2011). The SEZ6 protein is known to be a substrate for BACE1, the major beta-secretase that cleaves APP to Abeta fragments (Pigoni et al., 2016). Presumably because of this, *SEZ6* overexpression results in reduced Abeta species (Paracchini et al., 2018), likely due to occupation of the catalytic domain of BACE1. In our experiment, *SEZ6* had a negative log2FC of -1.54 in our APP-ABCC1(WT) cell line compared to the APP-Puro cell line. Logically, this reduction in *SEZ6* expression would result in increased Abeta production, but Abeta production is decreased in our model. Therefore, the differential expression of *SEZ6* does not appear to be the reason for decreased extracellular Abeta production in the *ABCC1*-overexpressing cells.

The *MBP* gene encodes the Myelin Basic Protein, one of the major proteins that makes up the myelin sheath generated by oligodendrocytes in the brain, and Schwann cells in the spinal cord (Gow, Friedrich, & Lazzarini, 1992). One previous study has shown that the MBP protein can act as a chaperone for Abeta to limit its fibrillation (Hoos, Ahmed, Smith, & Van Nostrand, 2007), while another study has shown that the MBP protein has serine protease activity that is capable of degrading the Abeta peptide (M.-C. Liao, Ahmed, Smith, & Van Nostrand, 2009). In our experiment, we observed a negative log2FC of -2.34 in the APP-ABCC1(WT) cell line compared to the APP-Puro cell line. If the MBP protein were the reason for the decrease in extracellular Abeta species we observed in our experiment, we would have expected to see *MBP* expression increased, rather than decreased, as an increase in MBP protein could increase the degradation of Abeta, and thus reduce the extracellular concentration of Abeta that could be measured. Therefore, the decrease in *MBP* expression in the APP-ABCC1(WT) cell line is likely not the reason for the decrease in extracellular Abeta observed in our experiment.

KCNIP4 encodes the Potassium Voltage-Gated Channel Interacting Protein 4, which regulates the flow of potassium into cells in a manner dependent upon intracellular calcium concentrations (Tang et al., 2013). The longest isoform of the KCNIP4 protein has been shown to interact with PSEN2, a catalytic subunit of the gamma-secretase complex, which produces Abeta when it cleaves the APP molecule after a beta-secretase (Morohashi et al., 2002). A study has shown that decreasing the expression of *KCNIP4* results in increased production of both Abeta1-40 and Abeta1-42 (Massone et al., 2011), and another study showed that increasing expression of the shorter isoforms of *KCNIP4* does not alter APP processing (Morohashi et al., 2002). Taken together, a decrease in the expression of the longest isoform of *KCNIP4* should increase Abeta production, while a decrease in the shorter isoforms should not alter APP processing. In our experiment, the APP-ABCC1(WT) cells had a negative log2FC of -2.98 for the *KCNIP4* gene compared to the APP-Puro cell line, that coincided with a decrease in Abeta production. Therefore, it does not seem likely that the differential expression of the *KCNIP4* gene is responsible for the changes in APP metabolism that we observed in our experiment.

The *SORCS3* gene codes for the Sortilin Related VPS10 Domain Containing Receptor 3, a neuropeptide receptor that is highly expressed in the brain (Breiderhoff et al., 2013), and a gene that is associated with Alzheimer's disease (Reitz et al., 2013). One study has shown that the expression of *SORCS3* is reduced in the APP/PS1 AD mouse model after deposition of Abeta plaques within the brain (Hermey et al., 2019). Another study has shown that knockdown of *SORCS3* results in increased APP metabolism (Reitz et al., 2013). In our experiment, *SORCS3* expression was decreased with a negative log2FC of -3.24 in the APP-ABCC1(WT) cell line compared to the APP-Puro cell line. Since expression of *SORCS3* was decreased in the APP-ABCC1(WT) cells, we would expect to see increased APP metabolism, and thus increased Abeta production. Since we observed a decrease of both *SORCS3* expression and extracellular concentrations of Abeta, *SORCS3* is likely not the reason for altered APP metabolism in our experiment.

The *APLN* gene encodes the Apelin protein, which is cleaved into biologically active ligands for G protein-coupled apelin receptors that regulate different processes in different cell

types (Antushevich & Wójcik, 2018). A previous study has shown that exogenous administration of apelin-13, a peptide fragment resulting from the cleavage of the Apelin protein, reduced Abeta production by decreasing the beta-secretase activity of BACE1 and by increasing the activity of neprilysin, an Abeta-degrading enzyme (Luo et al., 2019). In our experiment, we observed that *APLN* had a negative log2FC of -6.21 in the APP-ABCC1(WT) cell line when compared to the APP-Puro cell line. Therefore, if *APLN* were the reason for decreased extracellular Abeta concentrations in the APP-ABCC1(WT) cell line, we would expect that *APLN* expression were increased compared to the APP-Puro cell line. Thus, differential expression of the *APLN* gene is likely not the cause of the decreased extracellular Abeta concentrations in our experiment.

INPP5D is the gene that codes for the Inositol Phosphate-5-Phosphatase D protein, expressed by hematopoietic cells, and is believed to be involved in the immune response in the brain in which microglia are capable of clearing misfolded proteins (Efthymiou & Goate, 2017). In our experiment, we observed that *INPP5D* had a negative log2FC of -6.99 in the APP-ABCC1(WT) cell line compared to the APP-Puro cell line. If the INPP5D protein were capable of signaling our cells to uptake and degrade Abeta, and if INPP5D were responsible for the decreased extracellular Abeta in the APP-ABCC1(WT) cell line, we would expect to see a significant increase in *INPP5D* expression, rather than the large decrease we observed. Therefore, it does not seem likely that the differential expression of *INPP5D* is responsible for altering the metabolism of APP in the manner we observed.

Finally, in terms of genes whose differential expression is in the opposite directed than expected to account for the decrease in extracellular Abeta species, is *MEGF10*. *MEGF10* encodes the Multiple EGF Like Domains Protein 10, a protein that has been shown to act as a phagocytosis receptor for the uptake of Abeta from the extracellular space (Singh et al., 2010). Had we observed a significant increase in *MEGF10* expression in our APP-ABCC1(WT) cell line compared to the APP-Puro cell line, this would be the most likely candidate for the decrease in extracellular Abeta. However, in our experiment, the expression of *MEGF10* had a dramatically negative log2FC of -11.55 in the APP-ABCC1(WT) cell line compared to the APP-Puro cell line. Therefore, we would expect that our APP-ABCC1(WT) cells uptake less Abeta than the APP-

Puro cells, and thus the APP-ABCC1(WT) cells should have higher extracellular levels of Abeta. However, this is the opposite of what was observed. Therefore, the differential expression of *MEGF10* is not likely the cause of the decreased concentration of extracellular Abeta in the APP-ABCC1(WT) cells.

All of the remaining GOIs identified in this RNA-seq experiment have no previously known direct connection to APP metabolism, but have been implicated in Alzheimer's disease via various methods. Because of this, these genes will not be discussed within the body of the text; however, a discussion of all GOIs can be found in Appendix A.

Second APP Metabolite Experiments.

After identifying a second, rare polymorphism in *ABCC1* (p.Arg1342Gly), we transfected a new batch of BE(2)-m17 human neuroblastoma cells to recreate the APP-Puro and ABCC1(WT) cell lines, as well as to generate the APP-ABCC1(R1342G) cell line to carry out the same APP metabolite experiment as before, but this time to assay the experiment using the MSD platform. The MSD platform allows for the simultaneous analysis of multiple analytes within a single well. For this experiment, one MSD plate allows us to measure the concentrations of both Abeta1-40 and Abeta1-42 in a single well, and the second MSD plate allows us to measure the concentrations of both sAPPalpha and sAPPbeta. Because we are also utilizing this new analysis method, we decided to also repeat the first set of APP metabolite experiment using the cryopreserved APP-Puro, APP-ABCC1(WT), and APP-ABCC1(Y1189C) cell lines. In these two sets of MSD-analyzed experiments, cryopreserved cells and newly transfected cells were kept as separate experiments because this allows us to confirm that the results we are seeing are due to the overexpression of *ABCC1*, rather than any of the other confounding factors that can be created when generating these cell lines (i.e. location-specific genomic integration of the vectors in genes that could alter APP processing or expression). Each of these experiments also analyze twice as many samples as the first two APP metabolite experiments which will increase the power of our statistical analyses. These two experiments will be discussed separately.

Figure 8

MSD Results from the Third APP Metabolite Experiment

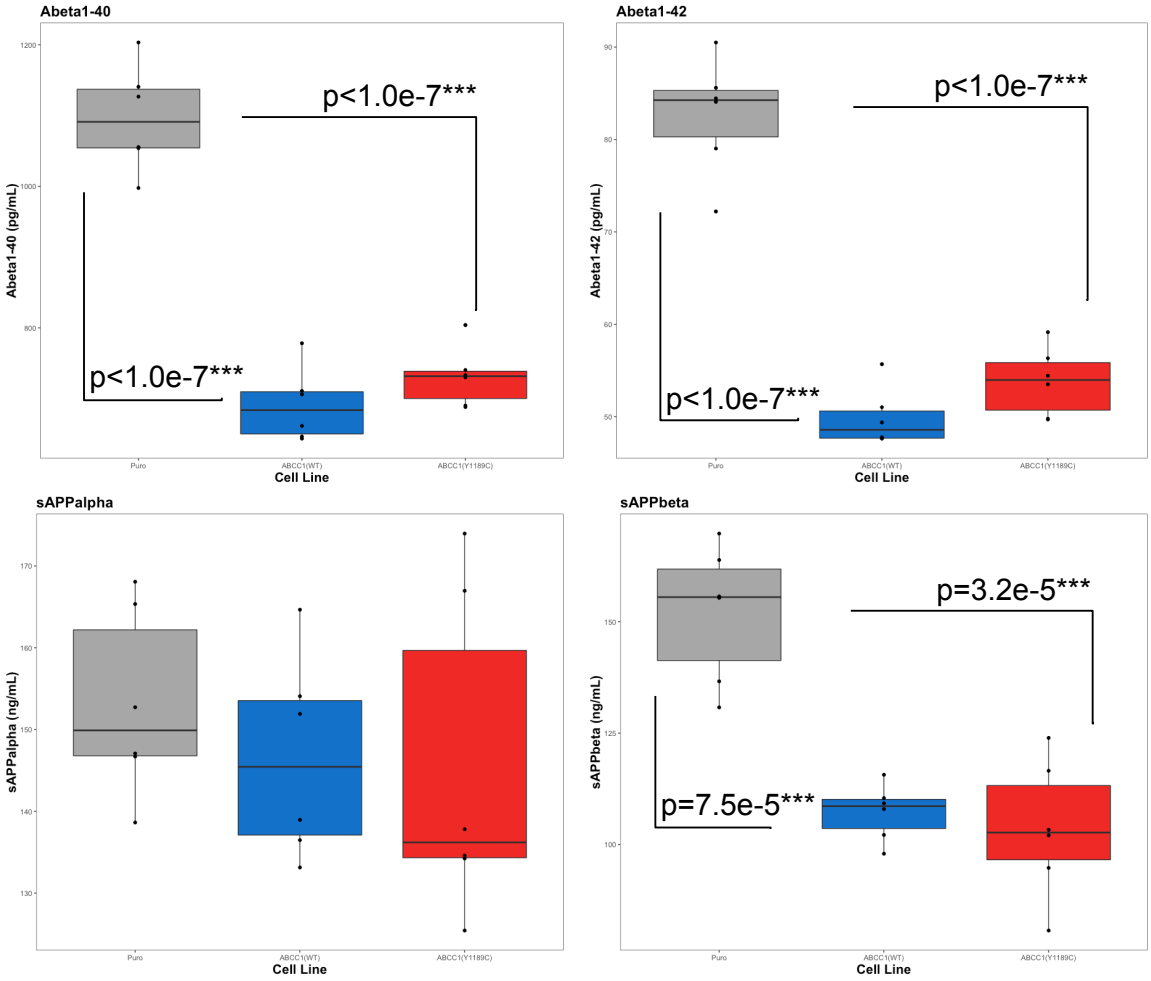

Note. Extracellular Abeta1-40, Abeta1-42, and sAPPalpha concentrations were significantly decreased in both *ABCC1*-overexpressing cell lines. There was no significant difference in the extracellular concentrations of any of the measured APP metabolites between the reference *ABCC1* and the mutant allele (labelled “ABCC1(WT)”, blue, and “ABCC1(Y1189C)”, red, respectively). Only significant p-values are displayed on the plot.

In the experiment utilizing the cryopreserved APP-Puro, APP-ABCC1(WT), and APP-ABCC1(Y1189C) cell lines, we again observed a significant decrease in the mean extracellular concentrations of Abeta1-40 and Abeta1-42 in both the APP-ABCC(WT) and APP-

ABCC1(Y1189C) cell lines compared to the APP-Puro control cell line. Though the mean concentrations of both of these analytes is slightly higher in the APP-ABCC1(Y1189C) cell line compared to the APP-ABCC1(WT) cell line, there is no statistically significant difference between the means of the two groups. In terms of sAPPalpha, there was no significant difference between the means of any of the groups; however, the mean extracellular concentrations of sAPPbeta were significantly lower in both *ABCC1*-overexpressing cell lines compared to the APP-Puro control. There was no significant difference between the mean extracellular concentrations of sAPPbeta between the APP-ABCC1(WT) and APP-ABCC1(Y1189C) cell lines.

Because the generation of sAPPalpha or sAPPbeta from a single APP molecule is mutually exclusive, we hypothesized that the best method to monitor the skewing of APP metabolism towards the alpha- or beta-secretase pathways is to calculate the ratio of sAPPalpha over sAPPbeta. By this method, and increase in this ratio, compared to the control cell line, would indicate that more APP molecules are being cleaved by an alpha-secretase (non-amyloidogenic pathway) than by a beta-secretase (amyloidogenic pathway), while a decrease in this ratio would indicate an increase in beta-secretase mediated cleavage of the APP molecule. Indeed, in both *ABCC1*-overexpressing cell lines, the mean ratio of extracellular sAPPalpha over sAPPbeta was significantly higher than the APP-Puro control line, but no significant difference was observed between the APP-ABCC1(WT) and APP-ABCC1(Y1189C) cell lines. This indicates that the increased expression of *ABCC1* skews APP processing towards the non-amyloidogenic alpha-secretase pathway. Furthermore, this result indicates that there is no significant difference in this skewing when the tyrosine 1189 of the ABCC1 protein is mutated to a cysteine. When coupled with the previous APP metabolite experiment, we are confident that overexpression of *ABCC1* results in decreased extracellular Abeta production, and that this seems to be due to either increased alpha-secretase activity, or decreased beta-secretase activity, with no significant difference observed due to the mutant protein.

Figure 9

Ratio of sAPPalpha to sAPPbeta from the Third APP Metabolite Experiment

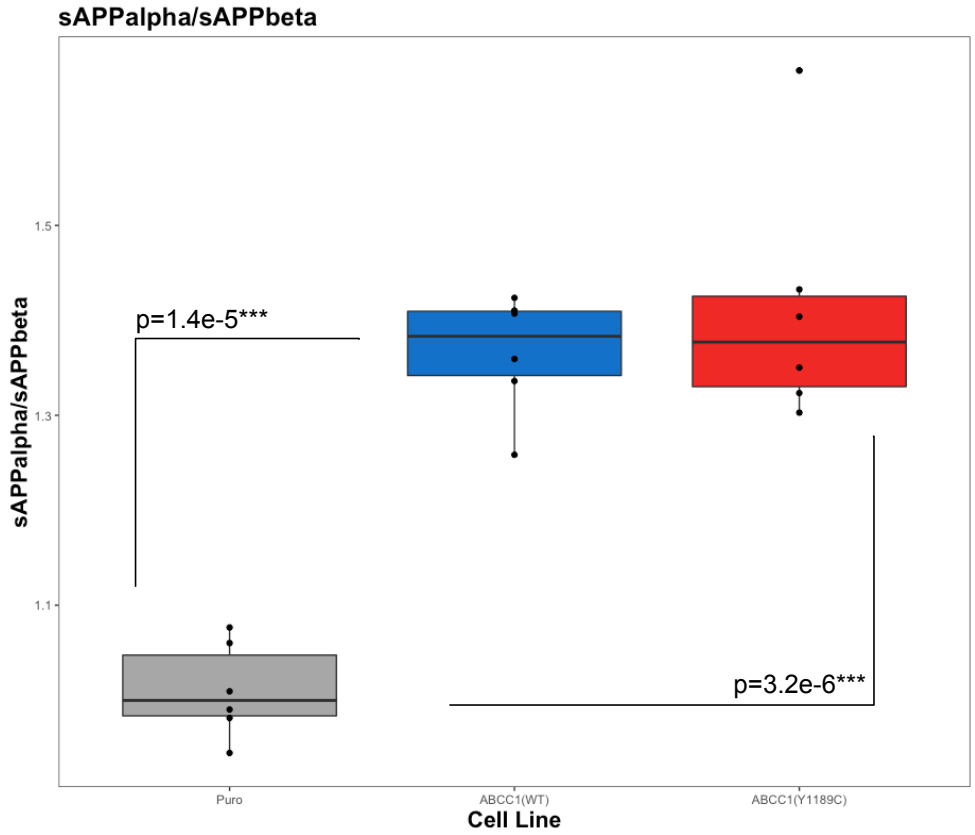

Note. The mean ratio of sAPPalpha to sAPPbeta is significantly higher in both of the *ABCC1*-overexpressing cell lines, indicating that ABCC1 skews APP processing away from the beta-secretase, amyloidogenic pathway, and towards the alpha-secretase pathway. There was no significant difference between the reference *ABCC1* allele and the mutant (labelled "ABCC1(WT)", blue, and "ABCC1(Y1189C"), red, respectively). Only significant p-values are shown on the plot.

For the newly transfected APP-Puro, APP-ABCC1(WT), and APP-ABCC1(R1342G) cell lines, we obtained similar results. In both *ABCC1* overexpressing cell lines, the extracellular concentrations of Abeta1-40 and Abeta1-42 were significantly lower when compared to the APP-Puro control cell line. There was no statistically significant difference between the extracellular concentrations of either of these metabolites between the APP-ABCC1(WT) and APP-

ABCC1(R1342G) cell lines. Interestingly, the extracellular concentrations of sAPPalpha were significantly lower in the APP-ABCC1(WT) cell line compared to the APP-Puro control line and the APP-ABCC1(R1342G) cell line, but there was no significant difference between the APP-Puro and the APP-ABCC1(R1342G) cell lines. For sAPPbeta, the extracellular concentration was significantly lower in the APP-ABCC1(WT) cell line compared to the APP-Puro control line, and was trending towards being significantly lower in the APP-ABCC1(R1342G) cell line compared to the control (N=12, n=6, p=0.051). There was no statistically significant difference between the APP-ABCC1(WT) and APP-ABCC1(R1342G) cell lines in terms of sAPPbeta.

Figure 10

MSD Results from the Fourth APP Metabolite Experiment

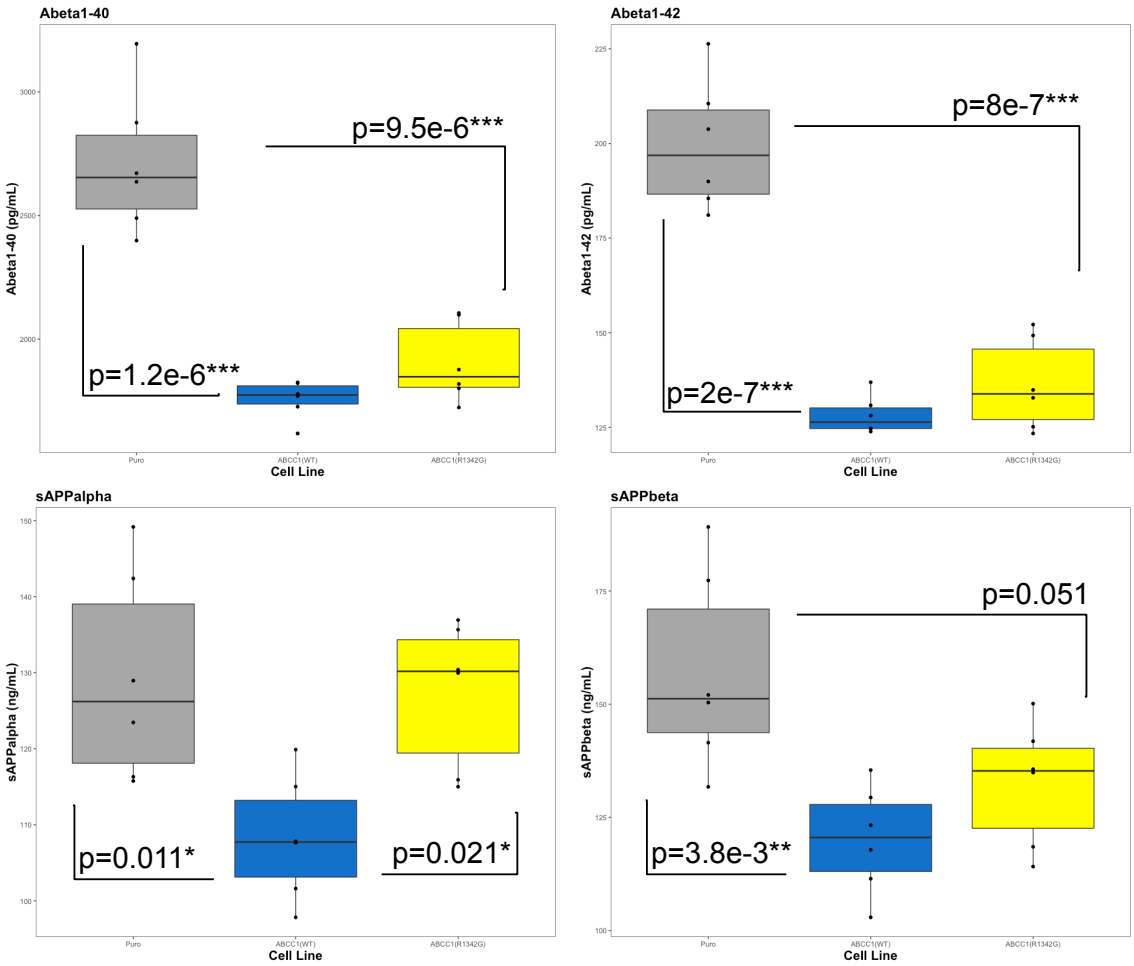

Note. Extracellular Abeta1-40 and Abeta1-42 concentrations were significantly lower in both the reference (labelled "ABCC1(WT)", blue) and mutant (labelled "ABCC1(R1342G)", yellow) *ABCC1*-overexpressing cell lines, compared to the empty vector control (labelled "Puro", gray). Extracellular sAPPalpha concentrations were significantly from the reference *ABCC1*-overexpressing cell line compared to the other two cell lines, while extracellular sAPPbeta concentrations were significantly lower in the reference *ABCC1*-overexpressing cell line, and were trending towards significance in the mutant *ABCC1*-overexpressing cell line compared to the empty vector control cell line.

Again, because of the mutual exclusivity of the generation of sAPPalpha or sAPPbeta from a single APP molecule, we analyzed the ratio of sAPPalpha over sAPPbeta, and again, the ratio was significantly higher in both *ABCC1*-overexpressing cell lines compared to the APP-Puro control cell line. Though the mean ratio was higher in the APP-ABCC1(R1342G) cell line compared to the APP-ABCC1(WT) cell line, there was no statistically significant difference between the two cell lines. This confirms our previous conclusion that overexpression of *ABCC1* skews the metabolism of APP away from the beta-secretase pathway and towards the alpha-secretase pathway. This also demonstrates that the results we are seeing are likely not due to location-specific integration of the vectors within the genome, as we see similar results in all four *ABCC1*-overexpressing vectors compared to both control lines. Therefore, increasing *ABCC1* expression or ABCC1 export activity may prove to be a viable method of reducing Abeta production within the brain.

Figure 11

Ratio of sAPPalpha to sAPPbeta from the Fourth APP Metabolite Experiment

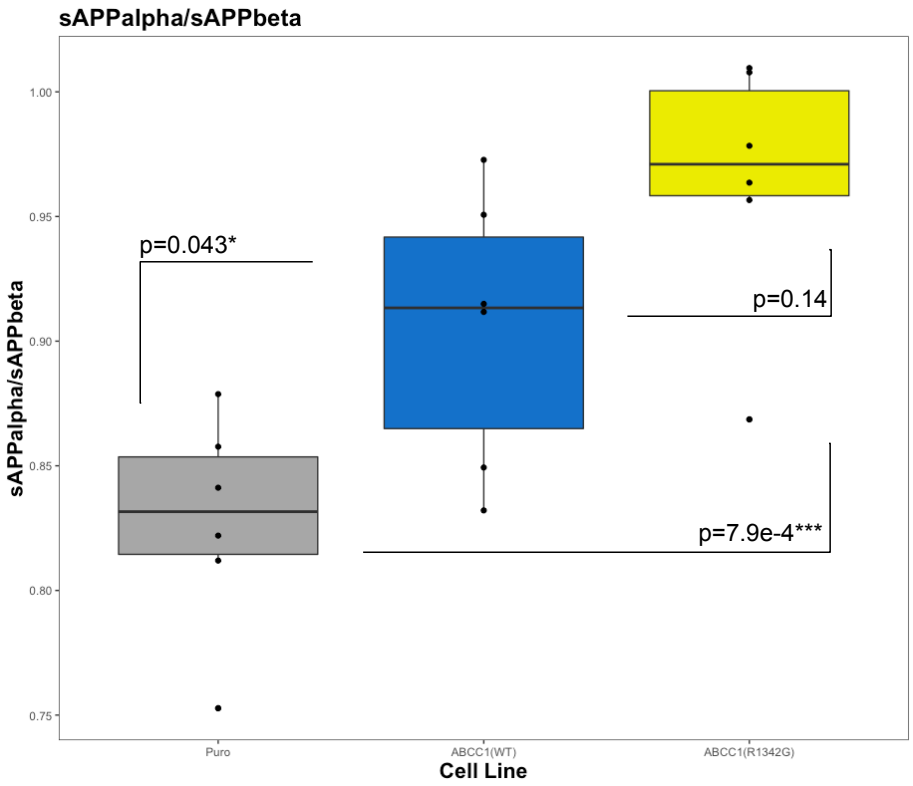

Note. The ratio of sAPPalpha to sAPPbeta is significantly higher in both *ABCC1*-overexpressing cell lines (labelled “ABCC1(WT)”, blue, and “ABCC1(R1342G)”, yellow) compared to the empty-vector control cell line (labelled “Puro”, gray). The p-value is not significant between the reference and the mutant *ABCC1*-overexpressing cell lines, and is shown on the plot to clarify this.

Second and Third RNA-seq Experiments.

In continuing to identify the mechanism by which overexpression of *ABCC1* alters APP processing, and to confirm the results of our first RNA-seq experiment, we again performed RNA-seq of all of the cell lines, and kept the experiments separated between the cryopreserved cells and the newly transfected cell lines. We performed these experiments under the hypothesis that both *TIMP3* and *CD38* expression would be significantly decreased in the *ABCC1*-overexpressing cell lines compared to the control cell line. For the RNA-seq experiment utilizing the

cryopreserved APP-Puro, APP-ABCC1(WT), and APP-ABCC1(Y1189C) cell lines, *TIMP3* expression was significantly decreased in both *ABCC1*-overexpressing cell lines compared to the APP-Puro control cell line. There was no significant difference between the APP-ABCC1(WT) and the APP-ABCC1(Y1189C) cell lines. In that same experiment, the mean expression of *CD38* was lower in both *ABCC1*-overexpressing cell lines compared to the APP-Puro control cell line, but there was no statistically significant difference between the means. We also looked at the expression levels of *ABCC1* and *APP*. As expected, expression of *ABCC1* from our vector was significantly higher in the *ABCC1*-overexpressing cell lines compared to the control cell line, with no significant difference between the APP-ABCC1(WT) and the APP-ABCC1(Y1189C) cell lines. Furthermore, there was no statistically significant difference in the expression of *APP* from our vector between any of the cell lines, which indicates that the results we are observing are not due to the knockdown or knockout of *APP*.

Figure 12

Results from the Second RNA-seq Experiment

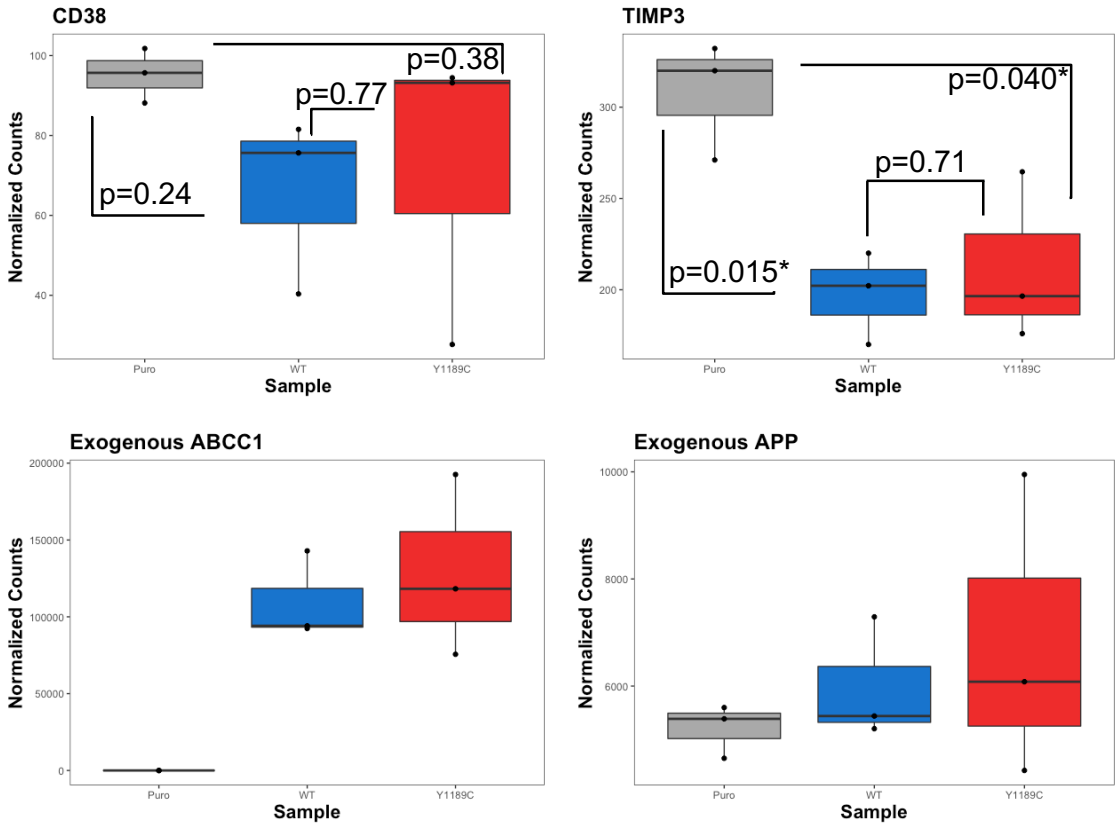

Note. Normalized counts for *CD38*, *TIMP3*, and both of the exogenous genes, *ABCC1* and *APP*, from the cryopreserved empty-vector control cell line (labelled “Puro”, gray), the reference *ABCC1*-overexpressing cell line (labelled “WT”, blue) and the mutant *ABCC1*-overexpressing cell line (labelled “Y1189C”, red). *TIMP3* expression is significantly reduced in both *ABCC1*-overexpressing cell lines compared to the empty vector control. As expected, exogenous *ABCC1* expression is not significantly different in the *ABCC1*-overexpressing cell lines, but is significantly higher than the empty-vector control (which is zero, as expected). Exogenous *APP* levels are not significantly different between any of the groups, indicating that the results observed in the APP metabolite experiments are not due to *APP* expression differences.

For the newly transfected cell lines, *TIMP3* expression was significantly lower in the APP-ABCC1(WT) cell line, and was trending towards significance in the APP-ABCC1(R1342G) cell

line (N=12, n=6, p=0.054), when compared to the APP-Puro control cell line. In terms of *CD38* expression levels, the APP-ABCC1(WT) cell line is trending towards being significantly lower than the APP-Puro cell line (N=12, n=6, p=0.069), but no significant difference exists between the other groups. Again, as expected, *ABCC1* expression from our vector was significantly higher in both of the *ABCC1*-overexpressing cell lines, and there was no significant difference between any of the groups when comparing the expression of *APP* from our vectors. This confirms that *TIMP3* expression is reduced when *ABCC1* expression is increased. This also indicates that *CD38* expression can be influenced by *ABCC1* expression, though its expression was no statistically significantly different in these experiments. However, because reduced *CD38* expression is trending towards significance in the newly transfected APP-ABCC1(WT) cell line, and that this effect was observed in the first RNA-seq experiment, we do not believe that the results of these experiments are necessarily a reason to exclude *CD38* as possibly having an effect on APP processing in our cell line models.

Figure 13

Results from the Third RNA-seq Experiment

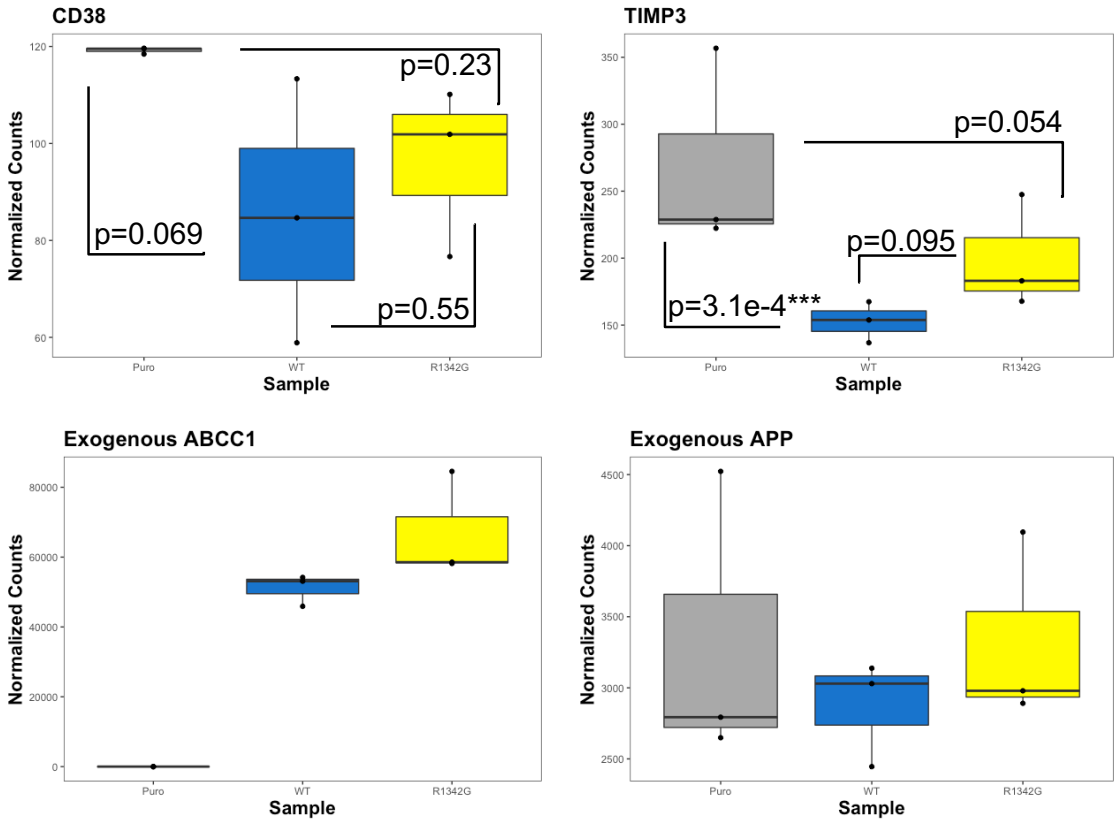

Note. Normalized counts for *CD38*, *TIMP3*, and both of the exogenous genes, *ABCC1* and *APP*, from the newly transfected empty-vector control cell line (labelled “Puro”, gray), the reference *ABCC1*-overexpressing cell line (labelled “WT”, blue) and the mutant *ABCC1*-overexpressing cell line (labelled “R1342G”, yellow). *TIMP3* expression is significantly reduced the reference *ABCC1*-overexpressing cell line, and is trending towards significance in the mutant *ABCC1*-overexpressing cell line, compared to the empty vector control. As expected, exogenous *ABCC1* expression is not significantly different in the *ABCC1*-overexpressing cell lines, but is significantly higher than the empty-vector control (which is zero, as expected). Exogenous *APP* levels are not significantly different between any of the groups, indicating that the results observed in the APP metabolite experiments are not due to *APP* expression differences.

ReNcell VM Model and qRT-PCR Assay.

While these APP metabolite experiments, coupled with the RNA-seq experiments, seem to show no significant differences between APP(WT) and either of the mutants, we are still observing a novel effect of *ABCC1* overexpression in our cell lines. That is, all of our experiments demonstrate that increased *ABCC1* expression reduces Abeta production, and skews APP processing towards the alpha-secretase pathway. The exact mechanism by which this occurs is still not fully understood, though it does seem that increasing *ABCC1* expression can lower the expression levels of both *TIMP3* and *CD38*, genes that encode for proteins capable of altering APP metabolism. To confirm this in another cell line, ReNcell VMs, a human neural progenitor cell line, was cotransfected with either our pSBbi-Puro or pSBbi-Puro-ABCC1(WT) vectors and the pCMV(CAT)T7-SB100 transposase vector. Cells were grown and given time to terminally differentiate, but not enough time to become fully matured neurons and astrocytes, before RNA extraction. RNA extracted was then used for a TaqMan assay to determine in *TIMP3* and *CD38* expression was decreased due to overexpression of *ABCC1*. Indeed, both *TIMP3* (N=24, n=12, p=3.80e-03) and *CD38* (N=24, n=12, p=1.21E-11) gene expression was significantly lower in the ReNcell VM-ABCC1(WT) cell line compared to the ReNcell VM-Puro cell line. This confirms, in a second human cell line, that overexpression of *ABCC1* reduced expression of both *TIMP3* and *CD38*. Therefore, the reduction of both of these genes, due to increased expression of *ABCC1*, may be the mechanism, or part of the mechanism, by which *ABCC1*-overexpression reduces Abeta production and skews APP processing towards the alpha-secretase pathway.

Figure 14

Taq-Man Results for TIMP3 and CD38 Relative Expression in ReNcell VM Cells

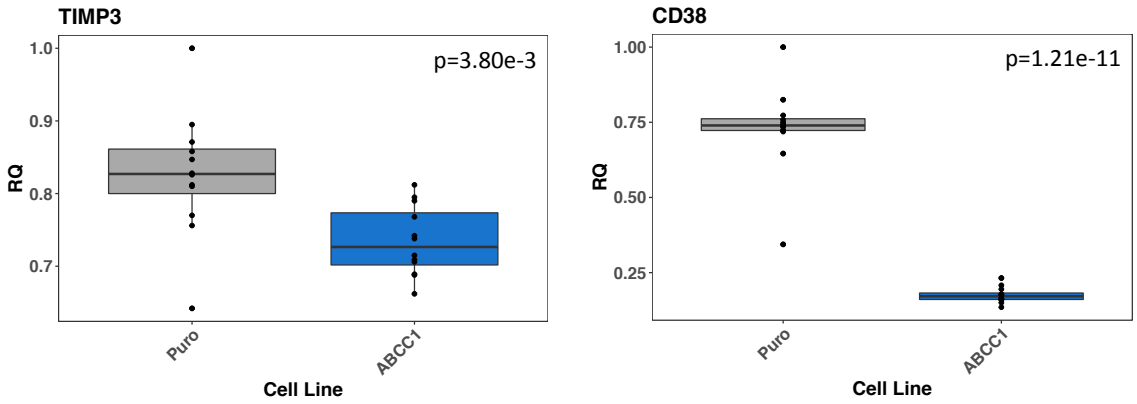

Note. Expression of *TIMP3* and *CD38* were significantly lower in the ReNcell VM cells overexpressing reference *ABCC1* (labelled "ABCC1", blue) compared to the empty-vector control cell line (labelled "Puro", gray). P-values are indicated on the plots, and are calculated using Student's two-tailed t-test.

This is important because previous literature has demonstrated that ABCC1 is capable of exporting Abeta from the cytoplasm of the endothelial cells of the blood brain barrier to the peripheral blood, and can therefore play a role in clearance of Abeta from the brain (Krohn et al., 2015, 2011); when coupled with our findings in this study, it appears that increasing *ABCC1* expression or activity could not only increase clearance of Abeta from the brain, but can also significantly reduce the amount of Abeta that is produced. If the amyloid cascade hypothesis holds true, which will likely be confirmed by human drug trials, then a reduction in Abeta production and an increase in Abeta clearance from the brain could prove to be a viable treatment or preventative intervention for Alzheimer's disease.

Many drug trials are underway that attempt to limit the production of Abeta via inhibition of the BACE1 protein, and many previous BACE1 antagonist trials have been halted early due to failure to provide any beneficial results, increased cognitive deficits, or organ damage (Das & Yan, 2019). This is likely due to unknown functions of BACE1 or off-target effects of the drug. There are also clinical trials underway that focus on the removal of Abeta from the brain by using

antibody therapeutics that can stimulate microglia-mediated clearance of the misfolded proteins (Tian Hui Kwan, Arfaie, Therriault, Rosa-Neto, & Gauthier, 2020). None of these trials have been effective in preventing or halting the progression of the disease.

If instead of antagonizing BACE1 to limit Abeta production or targeting Abeta with antibodies, a single drug that increases *ABCC1* expression, ABCC1 export activity, or both, may be capable of both increasing Abeta clearance from the brain, as well as limiting Abeta production. Many drug development pipelines have already been utilized to search for compounds that can inhibit ABCC1 transport activity or reduce *ABCC1* expression, as ABCC1 can confer chemoresistance to cancer cells by exporting them from the cytoplasm (S. M. Stefan, 2019). Logically, with hundreds of thousands of compounds tested, some have likely been identified that do the opposite of what was intended by the pipeline. That is, many compounds have likely already been identified that can increase *ABCC1* expression or transport activity, and these drugs should be studied in the context of Alzheimer's disease.

CHAPTER 4

EFFECTS OF ABCC1 MUTATION IN THE 5XFAD ALZHEIMER'S DISEASE MOUSE MODEL

Introduction

The initial results in our *in vitro* workup of the *ABCC1* (p.Tyr1189Cys) mutation led us to conclude that increased expression of *ABCC1* alters APP processing away from the beta-secretase, and towards the alpha-secretase pathway, but with less of an effect observed in the cells overexpressing the mutant protein. Because of this, we decided to generate an *in vivo* model of our variant in mice, using the CRISPR/cas9 system, to introduce the point mutation into the mouse homolog, *Abcc1*. This mouse model was then crossed with the 5xFAD Alzheimer's disease mouse model to look for cognitive or memory deficits, changes in APP metabolite profiles, and transcriptome alterations caused by the *Abcc1* mutation.

The full-length mouse Abcc1 protein is 1528 amino acids in length with 88% homology to the full-length human ABCC1 protein (Stride et al., 1996), which is 1531 amino acids in length (Cole, 2014). Because of this, the human ABCC1 Tyr1189Cys mutation is homologous to the mouse Abcc1 Tyr1186Cys mutation, and this was the heterozygous mutation generated in our mice. We decided to use the CRISPR/cas9 system to generate the point mutation because it allows for endogenous levels of *Abcc1* expression from the native locus in all tissues, rather than exogenously supplying a vector with either a ubiquitous or cell-specific promoter. This allows us to study the effects of this mutation in a manner that mirrors the human mutation and expression within the context of an AD mouse model.

The 5xFAD mouse model expresses two mutated human transgenes, *APP* and *PSEN1* (Oakley et al., 2006). The human *APP* gene expressed by the mice carry three FAD mutations which increase the amount of Abeta produced from cleavage of the APP molecule: the Swedish (Lys670Asn/Met671Leu), the Florida (Iso716Val), and the London (Val717Iso) mutations. The human *PSEN1* gene expressed by the mice carry two FAD mutations: Met146Leu and Leu286Val. Between these two human genes, a total of five FAD mutations are carried by the mice, thus the mouse is known as the 5xFAD Alzheimer's disease mouse model (Oakley et al., 2006).

The 5xFAD mouse has been extensively studied, as well as used as a model for the development of treatments and preventative measures for AD. The high expression of both of the human transgenes, as well as because of the mutations they carry, result in a robust model of amyloid plaque deposition and cognitive deficits in the mice as they age (Oakley et al., 2006). By the age of 1.5 months, amyloid accumulates in the neurons of the mice, and by the age of two months, extracellular plaques have begun to form and gliosis occurs (Oakley et al., 2006). Synaptic loss begins to occur at approximately four months, and is pronounced by nine months of age (Oakley et al., 2006). The spatial working memory of the mice in the Y-maze, as well as memory in the contextual fear conditioning tests, is impaired around five months of age (Kimura & Ohno, 2009; Oakley et al., 2006). Long term potentiation within the hippocampus deteriorates between the ages of four and six months (Crouzin et al., 2013; Kimura & Ohno, 2009). There are no Tau tangles observed in these mice (Oakley et al., 2006), as this requires the human transgene TAU, and often carrying a human mutation that leads to increased phosphorylation of the protein, which causes intraneuronal aggregation of the protein (Lee, Kenyon, & Trojanowski, 2005). Therefore, the 5xFAD mouse is ideal for studying the effects of our mutation on Abeta deposition and accumulation, as well as how our mutation affects the cognitive effects due to amyloid plaque burden.

Our approach to this study was to generate the *Abcc1* (p.Tyr1186Cys) mutation in the C57BL/6J mouse, then to cross this mouse with the 5xFAD mouse model to yield four different mouse strains to be used in the study: C57BL/6J that are homozygous for the wild-type *Abcc1* gene (denoted WT_NTG), C57BL/6J that are heterozygous for the Tyr1186Cys *Abcc1* mutation (denoted HET_NTG), 5xFAD mice that are homozygous for the wild-type *Abcc1* allele (denoted WT_5xFAD), and 5xFAD mice that are heterozygous for the Tyr1186Cys *Abcc1* mutation (denoted HET_5xFAD). These mice would then be subjected to the Y-maze test and the contextual fear acquisition test to quantitatively assess cognition and memory, and upon sacrifice, mouse brains would be used to quantify Abeta1-40 and Abeta1-42, as well as to look for transcriptomic changes via RNA-sequencing. All mice strains were generated and housed at the Jackson Laboratory Research Institute where the cognitive battery was also performed under

IACUC approval #16040. After sacrifice, mouse brain sections were sent to the Translational Genomics Research Institute for the APP metabolite and RNA-seq experiments.

Our experiments yielded some significantly different results, but none that were compelling enough to conclude that the Tyr1186Cys *Abcc1* mutation is significantly contributing to the AD phenotype. This could be for a few reasons. It is possible that the point mutation introduced a cryptic splice site within the mouse genome that results in a transcript that is degraded via the nonsense-mediated decay pathway. It is also possible that the mouse Abcc1 protein is less capable of exporting Abeta as the human protein, and therefore many more mice would be required to reach statistical significance in the APP metabolite experiment. It is also possible that the mice were not old enough for the real effects to be seen. That is, though the mice were generally around 14 months of age, approximately 12 months after extracellular plaques begin to form, allowing the mice to age more may have yielded different results. Regardless, none of the data we analyzed compelled us to continue aging the mice, or to breed more of them. However, mouse embryos from all four strains were cryopreserved to make future experimentation possible without having to regenerate the strains.

MATERIALS AND METHODS

Abcc1(Tyr1186Cys) Mutation Generation

Human ABCC1(Y1189C) is homologous to the mouse Abcc1(Y1186C), which was generated using the CRISPR/Cas9 technology. The guide RNA (gRNA) used to target the Cas9 complex to the proper location in the genome was 5'-ACCTGTTGGCCACAATGCTG-3', which was generated as a single guide RNA (sgRNA) incorporating the RNA sequences that allow for Cas9 to bind to and utilize the RNA molecule. The donor template used to for homology-directed repair was: 5'-

CAGTGTCATCCGTGCTTTTGAGGAGCAGGAGCGCTTCATTCACCAGAGTGACCTGAAAGTA

GATGAGAACCAGAAGGCCT**G**CTA**T**CC**CAGCATTGTGGCCAACAGGT**GGGTGTAGCGCTCA

GTAGAGTAG-3'. The bold **G** in the underlined codon is the substitution that generates the Abcc1(Y1187C) coding sequence, while the following bold and underlined **T** maintains the next

codon as coding for tyrosine, but mutates the PAM site to prevent Cas9-mediated double stranded breaks following integration of the donor template. The reverse complement of the gRNA is the run of 20 underlined and bolded nucleotides.

The sgRNA and Cas9 were complexed and injected into C57BL/6J mouse zygotes and embryos were transferred to pseudo pregnant female mice. Approximately 3 weeks after birth, tail biopsies were taken for genotyping, which involved crude lysate preparation, PCR of the locus, and Sanger sequencing of the amplicons to identify the founder mice that are heterozygous for the desired mutation.

5xFAD/Abcc1(Tyr1186Cys) Mouse Generation

Founder mice with the Abcc1(Y1186C) genotype were crossed with the heterozygous 5xFAD Alzheimer's disease mouse model to produce pups with four different genotypes (note: NTG stands for non-transgenic, meaning they do not carry the 5xFAD transgenes): 1. WT_NTG, 2. HET_NTG, 3. WT_5xFAD, and 4. HET_5xFAD. Mice were maintained on the C57BL/6J mouse background and genotyped prior to experimentation. These mice were used in the cognitive battery, as well as the APP metabolite and RNA-seq experiments.

Y-Maze Experiments

For the Y-maze experiments, mice were habituated beginning two days before the experiment by transporting them for at least one hour each day in the hallway outside of the testing room. Mice were then habituated to the testing room with cage covers removed at least one hour before testing in the same dimly lit lighting as is used for testing. Visual cues were placed in the appropriate areas outside of the Y-maze. Mice were randomized for testing and placed in the middle of the Y-maze to complete the test. Testing occurred for eight minutes in each case, and mouse movements were automatically recorded using the ANY-maze behavioral tracking software (Stoelting Co., Wood Dale, IL, USA).

Contextual Fear Acquisition Experiments

Experiments were automatically monitored using the motion detection algorithm, FreezeFrame (Actimetrics, Wilmette, IL, USA). Mice were habituated to transport and the testing room for three days before testing. For the fear acquisition, mice were habituated by placing them in the holding area outside of the test room for one hour, and then individually introduced into the training chamber. The training session lasted a total of 700 seconds. The mice in the training chamber received four 0.9 mA shocks lasting for one second starting at each of 199, 326, 419, and 554 seconds into the test. Trained mice were then transported to a secondary holding area, away from untrained mice, for at least one hour before being reintroduced to other mice. Once all mice have been trained and/or rested for one hour, all mice were reintroduced to their colony.

Contextual Fear Memory Experiments

The fear memory experiments were conducted 24 hours following fear acquisition. On testing day, mice are again transported to the holding area outside the training room and are allowed to habituate for one hour. Mice are again introduced into the training chamber where they remain for ten minutes with no electric shock. Mouse movements were automatically tracked using the FreezeFrame algorithm (Actimetrics). After testing, mice were left in solitary cages in a secondary holding space for one hour before reintroducing mice to each other and their colony.

Mouse Brain Preparation

Upon sacrifice, the hypothalamus is dissected from the brain and the remaining tissue is hemisected. The left hemisphere of the brain is fixed in paraformaldehyde, while the hippocampus, prefrontal cortex (PFC), motor cortex (MC), and mid/hind brain are dissected from the right hemisphere, and snap frozen. The PFC and MC were shipped on dry ice to our laboratory for analysis. Upon arrival, each piece of frozen PFC or MC was bisected and stored at -80 °C to allow for downstream APP metabolite analysis and RNA-seq from the same piece of tissue.

APP Metabolite Experiment

Mice provided for this experiment were WT_NTG to serve as the control group while WT_5xFAD mice and HET_5xFAD mice served as the experimental groups. One half of bisected PFC and MC from each mouse were each placed in a 1.5mL microcentrifuge tube with T-PER Tissue Protein Extraction Reagent (ThermoFisher Scientific), and homogenized using a Pellet Pestle (Kimble Chase Life Science, Vineland, NJ, USA). Samples were then centrifuged at 10,000xg for 5 minutes at 4 °C, and supernatant stored at -80 °C until assayed. APP metabolites were measured using the ECL method. Abeta1-40 and Abeta1-42 were measured simultaneously using the Abeta Peptide Panel 1 Multiplex Kit (Meso Scale Discovery), and sAPPalpha and sAPPbeta were measured simultaneously using the sAPPalpha/sAPPbeta Kit (Meso Scale Discovery). Raw data was analyzed using a four-parameter logistic regression. All data points are the means of technical quadruplicates. Statistical analyses performed were ANOVA and Tukey's Honest Significantly Different Test.

RNA-seq Experiment

One half of bisected PFC and MC from each mouse were subject to RNA extraction using the Quick-RNA Miniprep Plus Kit (Zymo Research) according to the manufacturer's instructions for solid tissue. Resulting RNA was aliquoted and flash frozen on dry ice, then stored at -80 °C. Library preparation occurred using the SMARTer Stranded Total RNA-Seq Kit v2 – Pico Input Mammalian (Takara Bio Inc.), and were sequenced on the NovaSeq 6000 (Illumina). FASTQs were generated with bcl2fastq v2.18 (Illumina). Reads were aligned with STAR v2.7.3a (Dobin & Gingeras, 2016) to generate BAM files, and differential expression analysis was accomplished using featureCounts from Subread package v2.0.0 (Y. Liao et al., 2014) and DeSeq2 v1.26.0 (Love, Huber, & Anders, 2014). Gene Set Enrichment Analysis (GSEA) was performed using the ReactomePA package (Yu & He, 2016) in R.

RESULTS

Y-Maze Experiments

For the Y-maze experiment, we are interested in the percent of spontaneous alternation between the arms of the Y-maze, as increased spontaneous arm alternation can be indicative of increased spatial memory and cognition, while a decrease in spontaneous alternation can indicate decreased spatial memory and cognition, when compared to the control (Kraeuter, Guest, & Sarnyai, 2019). For all mouse experiments, WT_NTG serves as the control.

For the WT_NTG mice, the mean percentage of spontaneous arm alternation was 53.08%. For the WT_5xFAD mice, the mean percentage for arm alternation was 54.15%. For the HET_NTG and the HET_5xFAD mice, the percentage of spontaneous arm alternation was 55.91% and 59.02%, respectively. Statistical analysis utilizing ANOVA revealed that there was no statistically significant difference between the means of any of the groups of mice [ANOVA; $F(3,187)=2.21$, $p=0.088$]. Data from this experiment can be visualized in Figure 15.

For the Y-maze test, we are also interested in the total number of arms entered, as a significant decrease compared to the control group could indicate a reduction in mobility or cognition, while an increase compared to the control group could indicate the opposite. For the WT_NTG mice, the mean total arms entered was 32.58 arms. For WT_5xFAD mice, the mean total arms entered was 33.38 arms. For the HET_NTG and the HET_5xFAD mice, the mean total arms entered was 29.21 and 30.02 total arms entered, respectively. ANOVA revealed that there was no statistical difference between the means of any of the groups [ANOVA; $F(3,187)=1.51$, $p=0.21$]. Data from this experiment can be visualized in Figure 16.

Finally, we are also interested in the percentage of alternate arm returns as mice with no cognitive deficits are less likely to return to an arm that was just previously entered. The mean percentage of alternate arm returns was 28.58% for the WT_NTG mice, 31.92% for the WT_5xFAD mice, 28.47% for the HET_NTG mice, and 25.21% for the HET_5xFAD mice. ANOVA revealed that there was a statistical difference between the groups [ANOVA; $F(3,187)=2.657$, $p=0.0497$. Post-hoc analysis utilizing the Tukey HSD test revealed that the significant difference in the means occurs when comparing the WT_5xFAD mice to the

HET_5xFAD mice [TukeyHSD; p=0.0287]. ANOVA results can be found in Table 5. Data from this experiment can be visualized in Figure 16.

Table 5

ANOVA Table from the Percent Alternate Arm Return of the Y-maze

	Percent Alternate Arm Alternation				
	df	**Sum Sq**	**Mean Sq**	**F-value**	**Pr (>F)**
Var	3	1130	376.5	2.657	0.0497
Res	187	26496	141.7		

Contextual Fear Acquisition Experiments

Because mice have a natural tendency to freeze when they are frightened (Rustay, Browman, & Curzon, 2008), for the contextual fear acquisition experiment, we are most interested in the percentage of time the mouse spends frozen following the final foot shock (foot shock number four). This is because the mice should quickly learn to fear the testing chamber, and that fear should elicit the natural freezing response, which is observable. A decrease in time spent frozen, compared to the control, could indicate decreased cognition and decreased ability to learn. Likewise, an increase in the time spent frozen following the fourth foot shock could be indicative of increased cognition and an increased ability to learn when compared to the control group (Rustay et al., 2008).

For the WT_NTG mice, the mean percentage of time spent frozen after the fourth foot shock was 56.50%. For the WT_5xFAD mice, the mean percentage of time frozen was 51.31%. The mean percentages of time frozen following the fourth foot shock for the HET_NTG mice and HET_5xFAD mice was 50.67% and 29.72%. Statistical analysis utilizing ANOVA revealed that there was a significant difference between the mean of the groups [ANOVA; F(3,27)=3.88, p=0.0199]. Post-hoc analysis utilizing the Tukey HSD test revealed that there was a significant difference between the WT_NTG control group and the HET_5xFAD group [TukeyHSD; p=0.016]. There was no statistically significant difference between the means of the other groups. The data from this experiment can be visualized in Figure 17.

Contextual Fear Memory Experiments

The contextual fear memory experiment is performed essentially in the same manner as the fear acquisition experiment, 24 hours after fear acquisition, but is done without foot shocks. This allows us to observe whether or not the mouse remembers the foot shocks from the previous day, and thus whether or not the mouse has learning deficits. Therefore, for this test, me are most interested in the total percentage of time that the mouse froze during their ten minutes within the testing apparatus.

For the control WT_NTG mice, the mean percentage of time spent frozen was 41.88%. For the WT_5xFAD mice, the mean time spend frozen was 41.77%. For the HET_NTG mice and the HET_5xFAD mice, the mean total percentage of time spent frozen was 47.77% and 27.83%, respectively. Statistical analysis utilizing ANOVA revealed that there was no statistically significant difference between the means of any of the groups [ANOVA; $F(3,39)=1.51$, $p=0.23$]. The data from this experiment can be visualized in Figure 18.

APP Metabolite Experiment

For Abeta1-40, the WT_NTG control mice had a mean concentration of 190.37 pg/mL while WT_5xFAD mice had a mean of 863.83 pg/mL and HET_5xFAD mice had a mean of 739.78 pg/mL of Abeta1-40. Statistical analysis utilizing ANOVA revealed that there was a significant difference between the means of the groups [ANOVA; $F(2,15)=12.36$, $p=6.74E-04$]. Post-hoc analysis utilizing the Tukey HSD test revealed that there was a statistically significant difference between the means of the control group and the WT_5xFAD mice [TukeyHSD; $p=8.30E-04$], as well as between the control group and the HET_5xFAD mice [TukeyHSD; $p=4.57E-03$]. There was no statistically significant difference between the means of the two transgenic groups, the WT_5xFAD mice and the HET_5xFAD mice.

For Abeta1-42, the WT_NTG control mice had a mean concentration of 24.14 pg/mL, while the WT_5xFAD mice and the HET_5xFAD mice had a mean concentration of 4186.06 pg/mL and 4504.88 pg/mL of Abeta1-42, respectively. Statistical analysis utilizing ANOVA revealed a statistically significant difference between the means of the three groups [ANOVA;

F(2,15)=23.86, p=2.19E-05]. Post-hoc analysis utilizing the Tukey HSD test revealed that there was a significant difference between the mean concentrations of Abeta1-42 between the control mice and the WT_5xFAD mice [TukeyHSD; p=1.07E-04], as well as between the control mice and the HET_5xFAD mice [TukeyHSD; p=4.86E-05]. There was no statistically significant difference between the mean concentrations of Abeta1-42 between the WT_5xFAD mice and the HET_5xFAD mice. The data from this experiment can be visualized in Figure 19.

RNA-seq Experiment

For the RNA-sequencing experiment, in terms of differential expression, we were most interested in the differences caused by the Abcc1(Y1186C) mutation either in the non-transgenic mice (HET_NTG compared to WT_NTG) or in the transgenic mice (HET_5xFAD compared to the WT_5xFAD). This is because transcriptomic differences between the non-transgenic mice versus the 5xFAD mice are known and expected, and the purpose of our experiment is to understand how the Abcc1(Y1186C) mutation alters the transcriptome.

When comparing the transcriptomes of the HET_NTG mice to the WT_NTG mice, only one gene is significantly downregulated, *Krt6a*, with a log2FC of -27.76 (N=12, n=6, p=6.20E-11, padj=2.10E-06). When comparing the HET_5xFAD mice to the WT_5xFAD mice, only three genes are significantly differentially expressed: *Krt6a*, *Xist*, and *A930017K11Rik*. The log2FC for *Krt6a* was -20.83 (N=12, n=6, p=5.75E-07, padj=0.0135). The log2FC for *Xist* was -9.21 (N=12, n=6, p=7.97E-07, padj=0.0135), though this is logically due to an imbalance between the number of males and females in this comparison. The log2FC for *A930017K11Rik* was 1.78 (N=12, n=6, p=4.13E-06, padj=0.0467).

Gene set enrichment analyses revealed no differences between the WT_NTG mice versus the HET_NTG mice, nor between the WT_5xFAD mice versus the HET_5xFAD mice, but did have significant differences found between the WT_NTG and WT_5xFAD, as well as between the HET_NTG and HET_5xFAD. The data from these experiments can be visualized in Figure 20 and Figure 21.

DISCUSSION

Generation of the 5xFAD mice carrying the mouse homolog of our human *ABCC1* mutation (human: ABCC1(Y1189C), mouse: Abcc1(Y1186C)) occurred concurrently with the *in vitro* work, and thus is not the logical progression from the conclusions of the *in vitro* work. However, because a mouse model is much more effective for studying the consequences of our mutation in the context of Alzheimer's disease, the results of that work will be discussed here.

All mice were housed at, and cognitive experiments were carried out at, the Jackson Laboratory Research Institute under IACUC approval #16040. Brain tissue was shipped on dry ice to the Translational Genomics Research Institute for Abeta concentration measurements and RNA-sequencing.

Four different genotypes of mice were used in the study. Mice that are homozygous wild-type for the *ABCC1* gene, and that do not carry the 5xFAD transgenes are referred to as WT_NTG. Mice that are homozygous wild-type for the *Abcc1* gene, but do carry the 5xFAD transgenes are referred to as WT_5xFAD. Mice that are heterozygous for the mouse homolog of our human mutation, but do not carry the 5xFAD transgenes are referred t as HET_NTG. Finally, mice that are both heterozygous for the mouse homolog of our human mutation and also carry the 5xFAD transgenes are referred to as HET_5xFAD. All genotypes were used in each experiment, but not necessarily all mice.

Y-maze Experiment

For the Y-maze test, the mean percentage of spontaneous alternation is used to assess the behavior of the mice because it is normal for a mouse to explore new areas of their enclosure, rather than to revisit arms of the maze that were just explored. Because of this, a significant decrease in spontaneous arm alternation during the trial could indicate a decline in cognition and typical behavior when compared to the control mice. In our study, there was no significant difference between the mean percentage of spontaneous arm alternation between any of the groups. This implies that neither the 5xFAD transgenes, which cause the buildup of amyloid

plaques within the mouse brain, nor the Abcc1(Y1186C) mutation, have a significant effect on the behavior of the mice within this test.

Figure 15

Spontaneous Alternation Averages Across Genotypes in the Y-maze

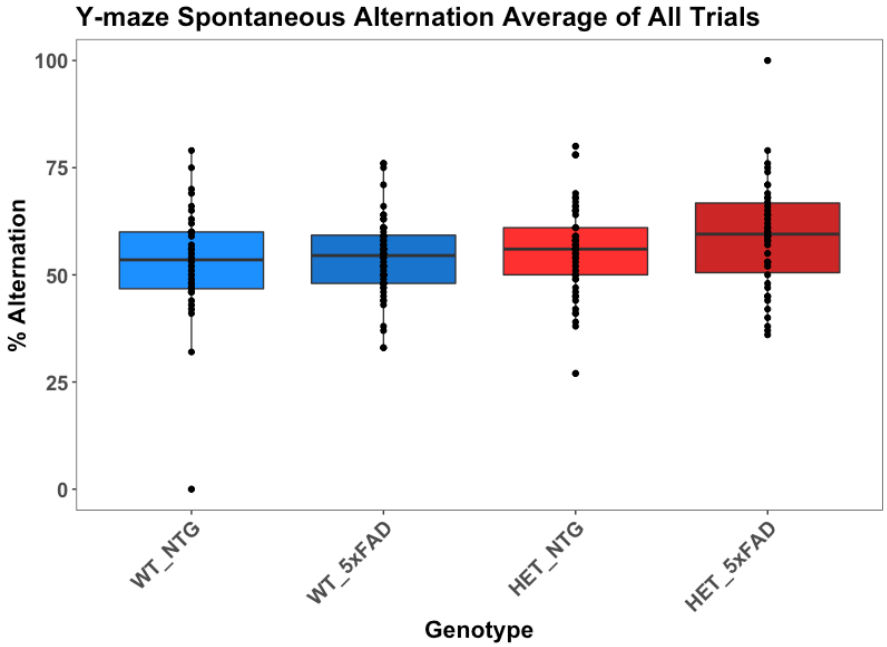

Note. There was no significant difference between the means of the spontaneous alternation averages in the Y-maze between any of the mouse genotypes.

The Y-maze also allows us to look at the mean number of total arm entries during the fixed time duration of the test, which generally would be decreased if the mice have locomotive issues or cognitive decline. If the experimental mice are unable to walk as well as the control mice, due to neurodegeneration or some other effect of the genetic alterations, these mice would logically walk less, and thus explore less of the Y-maze, and enter less arms. A significant decrease in the number of arms entered could also be due to cognitive deficits, as a mouse with improper brain function is less likely to explore their habitat in the same manner as a cognitively normal mouse. In this experiment, there was no significant difference between any of the groups of mice in terms of the mean number of total arm entries. Again, this implies that neither the

5xFAD transgenes, nor the *ABCC1* mutation, are having a measurable effect on cognition or locomotion in this particular test.

Figure 16

Total Arm Entries and Percent Alternate Arm Return Across Genotypes in the Y-maze

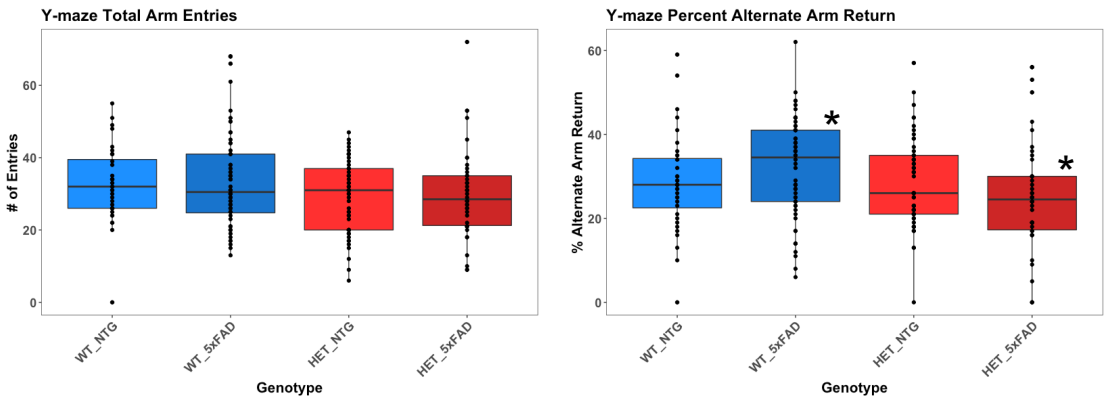

Note. There was no significant difference in the mean total arm entries between any of the genotypes. There was a significant difference in the mean percentage of alternate arm returns between the WT_5xFAD mice and the HET_5xFAD mice.

* p=0.029

With the Y-maze, we are also interested in the percentage of alternate arm returns; that is, the percentage of times that the mice went from one arm of the maze to another arm, then returned to the last previously entered arm. This is another means of looking for cognitive effects of the 5xFAD transgenes and the *Abcc1* mutation because a cognitively typical mouse is less likely to return to an arm of the maze that was just previously entered. Therefore, an increase in alternate arm return could indicate a cognitive or memory deficit, as either the mouse is not exhibiting typical behavior (cognitive deficit), or the mouse does not remember where it last was within the maze (memory deficits). In our experiment, there was a significant difference between the WT_5xFAD and the HET_5xFAD mice, where the HET_5xFAD mice had a lower percentage of alternate arm returns compared to the WT_5xFAD mice. This is the only analysis of the Y-maze test in which there is a significant difference between the two groups. Interestingly, the

5xFAD mice carrying the *Abcc1* mutation had a lower percentage of alternate arm return than those who are homozygous for the *Abcc1*(WT) allele. This implies that the *Abcc1* mutation may be having a protective effect against the effects of the 5xFAD transgenes, which may be improving their memory in this particular task. This is the opposite of what we had hypothesized, as we expected that the *Abcc1* mutation would cause more cognitive decline in the AD mouse model, and thus would increase the percentage of alternate arm return compared to the control. This is the first instance where a difference is observed between the *Abcc1* mutant and the *Abcc1* wild-type 5xFAD mice, and the difference contradicts our hypothesis, and thus implies, that the *Abcc1* mutation observed in our family is likely not significantly contributing to the onset of AD, which aligns with the results observed in our *in vitro* analysis of the human variant.

Contextual Fear Experiment

In the fear conditioning experiment, the first day of the experiment is the fear acquisition day in which the mice learn to fear the test chamber because of four small foot shocks received at defined intervals during the testing period. This fear can be quantified by measuring the percentage of time that the mice remain frozen following the fourth foot shock, as a mouse's natural reaction to fear is to freeze in place (Rustay et al., 2008). This allows us to monitor the cognition of the animals, as mice that do not freeze, and thus are not fearful of the foot shocks, likely have cognitive deficits. The second day of testing is to assess the mouse's memory of that fear when placed in the chamber. This is quantified as the total percentage of time that the mice stay frozen within the chamber without receiving foot shocks. This allows us to examine the memory of the mice, as the mice that remember that the testing chamber is what delivers foot shocks, should stay frozen for a larger percentage of time within the chamber than those mice who do not remember.

On the fear acquisition day, there was a significant difference between two of the groups in our experiment. The HET_5xFAD mice had a significantly lower percentage of freezing after the fourth foot shock compared to the WT_NTG mice [TukeyHSD; p=0.016]. At first glance, this may imply that the *Abcc1* mutation is causing this effect. However, since data was recorded for

only two WT_5xFAD mice in this experiment, it is more likely that this imbalance between the groups is what is driving the statistical significance to be only between the WT_NTG and the HET_5xFAD mice. That is, if more WT_5xFAD mice had been included, it is more likely that we would have seen this group's mean percentage of freezing drop towards the levels seen in the HET_5xFAD mice, which would mean that the decrease in the mean percentage of time spent frozen is likely due to the 5xFAD transgenes, rather than the *Abcc1* mutation. This hypothesis is supported by the fact that there is no significant difference between the WT_NTG and the HET_NTG mice, as one would expect if this *Abcc1* mutation were really altering cognition. However, it is also possible that our mutation is having an effect only in the mice carrying the 5xFAD transgenes because Abeta plaques will only accumulate in the mice carrying the 5xFAD transgenes. However, when coupled with the *in vitro* analysis and the fear acquisition experiments, it seems more likely that imbalance between the groups is the likeliest cause of this result. Therefore, the results of this experiment are inconclusive.

Figure 17

Percent Freezing Post Fourth Foot Shock from the Fear Acquisition Experiment

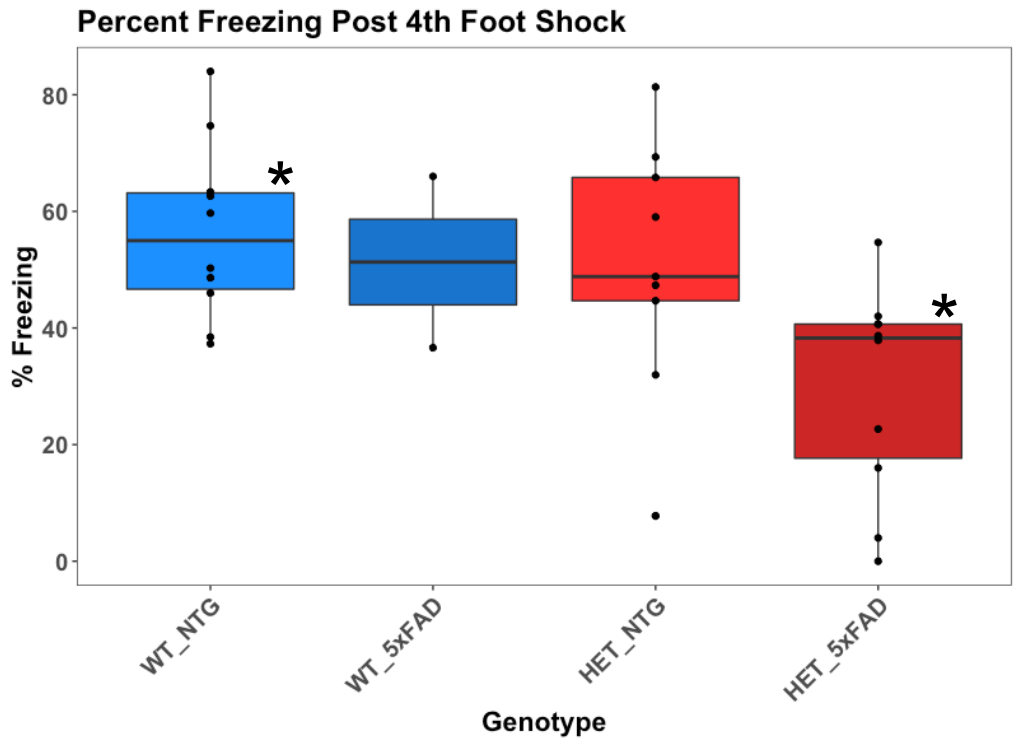

Note. There is one significant difference between the mean of the groups, WT_NTG and HET_5xFAD. WT_5xFAD mean percentage of freezing would likely be lower if more animals were tested.

* p=0.016

For the contextual fear memory experiment, the groups are much better balanced than with the fear acquisition experiment. Again, in this experiment, the mean percentage of time spent frozen within the chamber was lowest for the HET_5xFAD mice, but there was no statistically significant difference between any of the four groups. Therefore, the only conclusion that can be drawn from the data covering this experiment is that no effect is observed due to the *Abcc1* mutation. As with any experiment, significance might be achieved by testing more mice; however, when coupling this data with the previous data, it seems more likely that the *Abcc1* mutation is not having a significant effect, *in vivo*.

Figure 18

Mean Total Freezing Across Genotypes in the Fear Memory Experiment

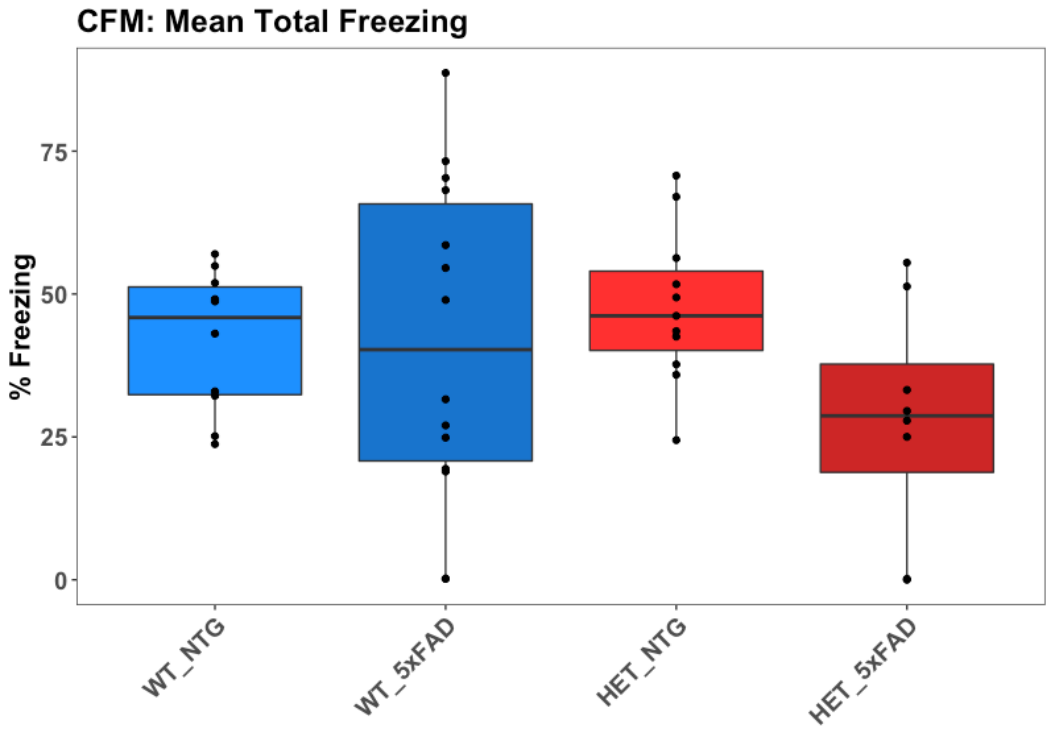

Note. No significant difference is observed between any of the genotypes, though the mean percentage of time spent frozen is lower in both 5xFAD mouse models, as expected.

APP Metabolite Experiment

After sacrifice, the prefrontal cortex and the motor cortex of some of the mice were shipped to us for homogenization and lysis to measure Abeta1-40 and Abeta1-42 using the MSD platform. For this experiment, we used the WT_NTG mice (referred to as NTG in the plot) as the main control group, and compared the Abeta levels of those mice to the WT_5xFAD and the HET_5xFAD mice. This allows us to ensure that the WT_5xFAD mice have significantly higher levels of both Abeta species, as this is expected due to the 5xFAD transgenes. We can then compare to the HET_5xFAD mice to the WT_5xFAD mice to see if the *Abcc1* mutation is having an effect on Abeta concentrations within the brain.

When measuring Abeta1-40, the concentrations were significantly higher in both the WT_5xFAD mice and the HET_5xFAD mice when compared to the WT_NTG mice. However, there was no significant difference in the mean concentrations of Abeta1-40 between the 5xFAD mice who are wild-type for the *Abcc1* gene and those carrying the Tyr1186Cys *Abcc1* mutation.

The same is true for Abeta1-42. The detectable levels of Abeta1-42 in the WT_NTG mice is basically null, while the concentrations in both the WT_5xFAD and the HET_5xFAD mice are very high. The levels of Abeta1-42 are much higher than the levels of Abeta1-40 because of the autosomal dominant AD mutations in the human *APP* transgene carried by the mice. These mutations are known to increase the amount of Abeta1-42 produced from the APP molecule, and this is why the mice have such dramatic amyloid plaque pathology, since Abeta1-42 is much more likely to aggregate than Abeta1-40 (Oakley et al., 2006). When comparing the mean concentrations of Abeta1-42 between the WT_5xFAD and the HET_5xFAD mice, there is no statistically significant difference between the two groups. Taken together with the Abeta1-40 results, the cognitive battery results, and the *in vitro* analysis, it does not appear that the *ABCC1* (p.Tyr1189Cys) mutation identified in our LOAD family is having any dramatic effect on AD pathology or cognitive decline due to progression of the disease.

Figure 19

MSD Results of the Mouse Brain APP Metabolite Experiment

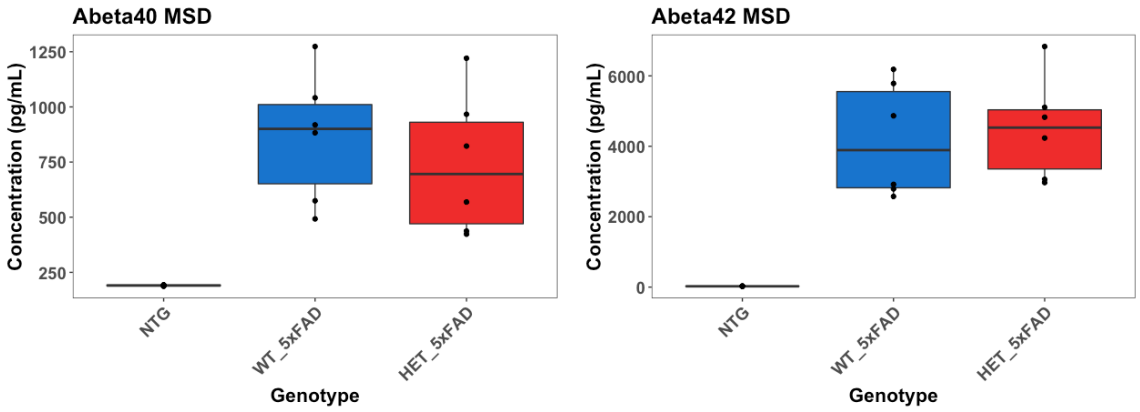

Note. There was no statistically significant difference in Abeta1-40 or Abeta1-42 concentrations between either of the 5xFAD mouse models.

RNA-seq Experiment

The results of the RNA-seq experiment was quite surprising because although we saw significant changes in expression of many interesting gene *in vitro*, we observed only three genes in total that were significantly differentially expressed in mice that carried the *Abcc1* mutant allele compared to their homozygous wild-type controls. We are interested in comparing only these two groups of pairs because we are only interested in the gene expression changes that result from the introduction of the *Abcc1* mutant allele in either wild-type or 5xFAD mice. When comparing the HET_NTG mice to the WT_NTG mice, the only gene found to be significantly differentially expressed was *Krt6a*, with a negative log2FC of -27.76. This is a fairly extreme log2FC for a gene's expression, especially when it is the only gene that reaches statistical significance. When comparing the HET_5xFAD mice to the WT_5xFAD mice, *Krt6a* is again significantly downregulated with a negative log2FC of -20.83. *Krt6a* encodes for Keratin, type II cytoskeletal 6A, a cytoskeleton scaffolding protein involved with wound healing (Wojcik, Bundman, & Roop, 2000), and is not a gene we would have expected to be differentially expressed from our *in vitro* analyses. Because the CRISPR/cas9 system was used in the generation of the mouse models, we hypothesize that *Krt6a* was subject to the off-target effects of the gRNA, and that either

hetero- or homozygous knockout of *Krt6a* occurred. This hypothesis is supported by the fact that the log2FC of *Krt6a* was so extreme in both comparisons.

Table 6

RNA-seq Results Comparing Abcc1 Genotypes in NTG and 5xFAD Mice

Non-transgenic: Abcc1(Tyr1186Cys) vs. Abcc1(WT)							
Ensemble Gene ID	**Gene**	**baseMean**	**log2FC**	**lfcSE**	**Stat**	**pvalue**	**padj**
ENSMUSG00000058354	*Krt6a*	7.351	-27.76	4.246	-6.539	6.20e-11	2.10e-06

5xFAD: Abcc1(Tyr1189Cys) vs Abcc1(WT)							
Ensemble Gene ID	**Gene**	**baseMean**	**log2FC**	**lfcSE**	**Stat**	**pvalue**	**padj**
ENSMUSG00000025727	*A930017K11Rik*	31.40	1.778	0.386	4.605	4.13e-06	0.0467
ENSMUSG00000058354	*Krt6a*	7.351	-20.83	4.166	-5.000	5.75e-07	0.0135
ENSMUSG00000086503	*Xist*	5280.9	-9.206	1.865	-4.936	7.97e-07	0.0135

The other two genes that were significantly differentially expressed when comparing the HET_5xFAD to the WT_5xFAD mice were *Xist* and *A930017K11Rik*. *Xist* encodes the inactive X specific transcripts, a gene that is encoded on the X chromosome and that functions in the X-inactivation of a single X chromosome during development in females (Bousard et al., 2019). Because this comparison utilized less HET_5xFAD females than WT_5xFAD females, we hypothesize that the significantly negative log2FC of -9.21 is simply due to the smaller number of females used in the RNA-seq experiment. *A930017K11Rik* encodes the RIKEN cDNA A930017K11Rik gene (The UniProt Consortium, 2019), which had a positive log2FC of 1.78 when comparing the HET_5xFAD to the WT_5xFAD mice. The human ortholog of this mouse gene is *PRR35*, which codes for the Proline Rich 35 protein (Bult et al., 2019). The function of this gene and its product is currently unknown in both mice and humans (Bult et al., 2019). Because of this, it is difficult to hypothesize as to why this gene is upregulated in the HET_5xFAD mice compared to the WT_5xFAD mice. However, because the only other two genes that are significantly differentially expressed in this comparison have very large log2FCs, and clear

reasons why they are significantly different, the increased expression of *A930017K11Rik* may be a sequencing artifact, or a gene that would not be significantly differentially expressed if more mice were used in the study.

Figure 20

Gene-Set Enrichment Analysis Comparing Abcc1(WT) 5xFAD and NTG Mice

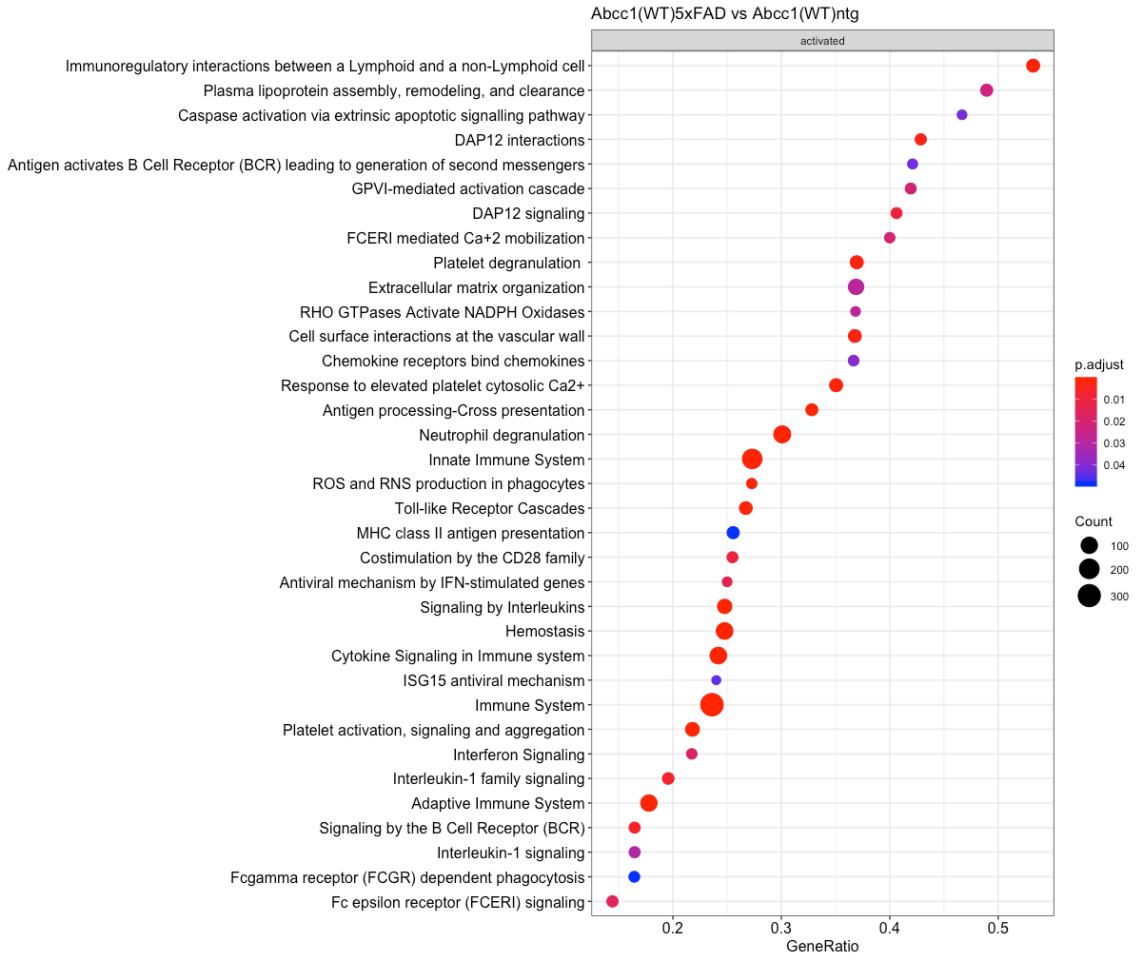

Note. This gene-set enrichment analysis compares only the WT_NTG and WT_5xFAD mouse models, and only shows significant gene sets. Adjusted p-values are indicated by color (red being lowest and blue being highest, but still <0.05). Total counts for that gene set are indicated by circle size (larger circle equals more counts).

For the gene set enrichment analyses (GSEAs), no gene sets were significantly enriched for when comparing the WT_NTG mice to the HET_NTG mice, or when comparing the WT_5xFAD mice to the HET_5xFAD mice, even when relaxing the p-value cut-off to 0.50. Therefore, the *Abcc1* mutation does not disrupt any major biological pathways in the brains of these mice. As expect, when comparing the WT_5xFAD mice to the WT_NTG mice, there were many gene sets that were significantly enriched, and almost all of these gene sets are involved in the immunological response. This makes sense as it has been well-established that the accumulation of amyloid plaques within the brain leads to inflammation, as well as that the innate immune cells of the brain, microglia, are involved in clearance of amyloid plaques from the brain. Using the same analysis methods to compare the HET_5xFAD mice to the HET_NTG mice, we see a smaller number of significantly enriched gene sets, but again, they are involved with the expected immunological response.

Figure 21

Gene-Set Enrichment Analysis Comparing Abcc1(Y1186C) 5xFAD and NTG Mice

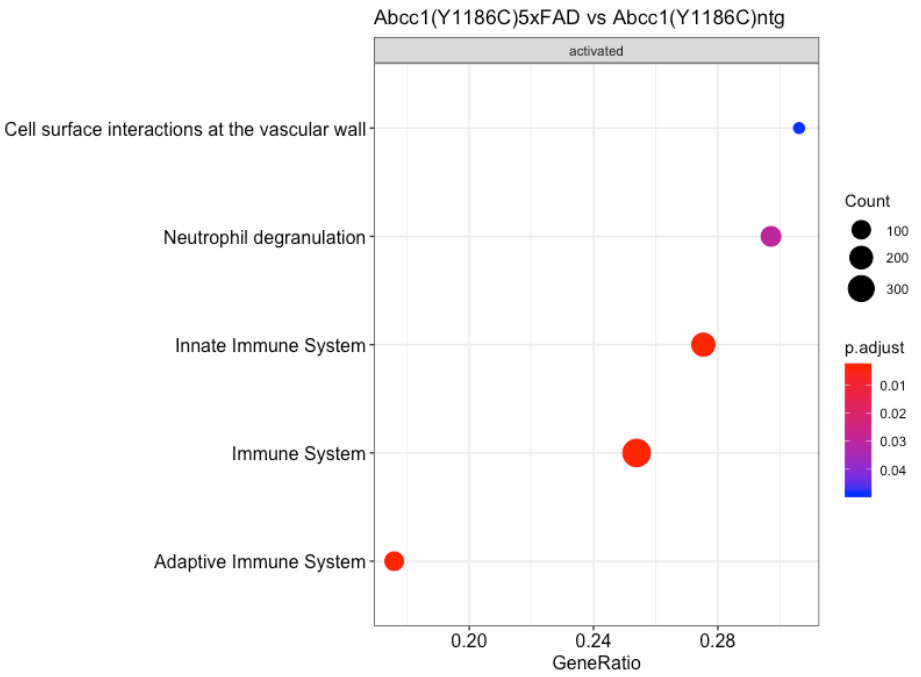

Note. This gene-set enrichment analysis compares only the HET_NTG and HET_5xFAD mouse models, and only shows significant gene sets. Adjusted p-values are indicated by color (red being lowest and blue being highest, but still <0.05). Total counts for that gene set are indicated by circle size (larger circle equals more counts).

All of the *in vivo* workup of the *ABCC1* mutation (p.Tyr1189Cys) identified in our LOAD family, which was introduced into the mouse homolog as the *Abcc1* (pTyr1186Cys) mutation, points to no significant difference in cognition, Abeta deposition, or genomic expression. Because of this, we conclude that the human Tyr1189Cys *ABCC1* mutation is not having a significant impact on the onset or progression of Alzheimer's disease in the LOAD family. However, the identification of this rare *ABCC1* allele is what led to the work identifying a novel consequence of *ABCC1* overexpression; that is, increase *ABCC1* expression reduces the production of Abeta1-40 and Abeta1-42 by skewing APP processing away from the beta-secretase, amyloidogenic

pathway, and towards the neuroprotective alpha-secretase pathway, which may make *ABCC1* a valid drug target for the prevention or treatment of Alzheimer's disease.

CHAPTER 5

DISCUSSION

Alzheimer's disease is the leading cause of dementia in the world and the sixth leading cause of death in the United States ("2020 Alzheimer's disease facts and figures," 2020). Although the disease has been studied since 1901 when it was first described by Alois Alzheimer, over a century's worth of research has yielded little in terms of preventing onset or slowing progression of the disease (Cipriani et al., 2011). While it is known that the pathological hallmarks of the disease are extracellular amyloid plaques, consisting of aggregated amyloid beta, and intraneuronal TAU tangles, consisting of aggregated, hyperphosphorylated TAU, not much is known about exactly why the metabolic processes take place that allow these proteins to aggregate in the first place, or why they are not degraded and properly cleared from the brain (Selkoe & Hardy, 2016). Furthermore, it is not clearly understood if the aggregation of these proteins is the cause or the consequence of the disease (Selkoe & Hardy, 2016).

The first FDA-approved drugs specifically for the treatment of AD were a class of drugs called acetylcholinesterase inhibitors, which are still widely used today. The first to hit the market in the United States was donepezil in 1996, followed by rivastigmine in 2000 and galantamine in 2001 (Sharma, 2019). All of these drugs have a similar mechanism of action whereby they inhibit the action of acetylcholinesterase in order to prevent the degradation of acetylcholine, a neurotransmitter involved in attention, memory, and cognition. By increasing acetylcholine levels, AD patients have temporarily attenuated cognitive decline, but the effects of these drugs are soon overcome by the progression of the disease (Sharma, 2019).

A second class of drugs, with only one FDA-approved member, has also been developed that strives to prevent neuroexcitotoxicity by inhibiting the *N*-methyl-D-aspartate (NMDA) receptor. This drug is called memantine, and has been approved for use since 2003 (Rogawski & Wenk, 2006). It is believed that the constant excitation of neurons within the brain is one of the causes of neuronal cell death, and by inhibiting this constant excitation, that AD progression can be slowed (Rogawski & Wenk, 2006). However, as with the acetylcholinesterase inhibitors, the effects of the drug are eventually overshadowed by the disease (Matsunaga, Kishi, & Iwata, 2015). Therefore,

there currently exists no AD treatment that can effectively prevent disease onset or slow or prevent disease progression.

Genetics offered hope to the Alzheimer's field by allowing for genome-wide association studies (GWAS) that promised to link common genetic variants to the onset of the disease, and thus identify metabolic pathways where pharmacological intervention could inhibit deleterious pathways or attenuate cognitive decline. While many AD genes have been identified via GWAS, there are alleles of two main genes that have been shown to significantly contribute to late-onset AD (LOAD) risk: *APOE* ε4 and *TREM2* (p.Arg47His) (Wolfe et al., 2019). Though carrying these alleles increases one's risk of AD, it by no means guarantees that individuals with these polymorphisms will develop the disease. Furthermore, none of the genetic variants identified by GWAS have led to the development of any new drugs for the treatment of AD.

The genetic studies that have provided a clear link between genetics and Alzheimer's disease were those that focused on familial Alzheimer's disease (FAD) which is also known as autosomal dominant Alzheimer's disease (ADAD), a form of early-onset AD (EOAD). These mutations occur in three genes – *APP*, *PSEN1*, and *PSEN2* – and each contributes to increased cleavage of the APP molecule to produce Abeta, the peptides that aggregate to form amyloid plaques (Lanoiselée et al., 2017). Patient's with these autosomal dominant mutations are almost guaranteed to develop AD before the age of 65. Patients with Down syndrome, also known as trisomy 21, in which patients carry a third chromosome 21, also often develop AD early in life, presumably because the *APP* gene is located on chromosome 21 (Hartley et al., 2015). It is believed that this extra dosage of *APP* expression leads to the excess generation of Abeta, and causes amyloid plaques to form. These insights have led to one of the leading theories as to how AD develops, known as the amyloid cascade hypothesis. This hypothesis states that due to excess beta-secretase cleavage of the APP molecule, or reduced clearance of Abeta peptides from the brain, results in the accumulation of extracellular amyloid plaques which leads to metabolic changes that cause intraneuronal hyperphosphorylated TAU to aggregate and cause neuronal cell death (Selkoe & Hardy, 2016).

These two groups described above, LOAD and EOAD, are the two main categories of AD, in which LOAD is defined as disease onset at or after the age of 65, and EOAD is defined as disease onset occurring before the age of 65 (Mendez, 2017). Within these major classifications are subgroups of AD. For LOAD patients, most are sporadic; however, rare familial cases of LOAD have been described, but not extensively studied (Bekris et al., 2010). Conversely, most EOAD cases tend to be familial, though sporadic cases of EOAD in patients not carrying any of the known ADAD mutations have also been described, but not studied extensively (Bekris et al., 2010). In this work, we strove to study the rare genetic variants in protein-coding genes in familial cases of LOAD and sporadic cases of EOAD in order to identify possible missing genetic components of the disease. This may allow us to identify novel drug targets to either prevent disease onset or halt disease progression.

To this end, we employed next-generation sequencing to identify rare, protein-coding variants in a familial case of LOAD and in sporadic cases of EOAD, in order to analyze these variants *in vitro*, and with the familial LOAD case, *in vivo*, in order to determine to what extent these variants may be altering disease pathology. In the LOAD family, we identified a rare *ABCC1* mutation (p.Tyr1189Cys) that is only carried by the affected individuals, as our variant of highest interest. In one of our sporadic EOAD cases, we also identified a rare *ABCC1* mutation (p.Arg1342Gly) that we hypothesized could impair ABCC1-mediated export of Abeta from the brain.

The first *in vitro* experiments, which utilized the BE(2)-m17 human neuroblastoma cell line expressing either the empty control vector, the human reference *ABCC1* allele, or the familial LOAD *ABCC1* mutation (p.Tyr1189Cys) yielded surprising results. We observed that *ABCC1*-overexpressing cells, regardless of which *ABCC1* allele was exogenously expressed, had significantly lower extracellular concentrations of both Abeta1-40 and Abeta1-42 when compared to the empty vector control cell line. This was surprising because the ABCC1 protein has been shown to export Abeta from the cytoplasm to the extracellular space (Krohn et al., 2011), and therefore, we would have expected extracellular Abeta concentrations to be higher in supernatant collected from *ABCC1*-overexpressing cells. We also observed significantly higher extracellular

concentrations of Abeta1-40 in the *ABCC1* (p.Tyr1189Cys) cell line compared to the human reference *ABCC1* cell line, and consistently higher, though never statistically significant levels of Abeta1-42, which encouraged us to generate a mouse model to better study the variant, and this will be discussed later.

In terms of the surprising result that extracellular concentration of Abeta are lower in the *ABCC1*-overexpressing cells, we had to determine if this was because of an unforeseen effect of the increased *ABCC1* expression, or if this was due to our model not working properly, such as the ABCC1 protein being inserted backwards into the plasma membrane. To test this, we incubated the cell lines with fluorescent Abeta1-42, with and without thiethylperazine, a small molecule previously shown to increase ABCC1-mediated export of Abeta, and utilized flow cytometry to calculate the percentage of the population of cells that are fluorescent. In both *ABCC1*-overexpressing cell lines, the fluorescent population percentage was lower than in the empty vector control line, and this difference was increased when supplemented with thiethylperezine. This experiment was confirmed with a second fluorescent Abeta1-42, tagged with an alternate fluorophore, and cells were counted on a different flow cytometer. This confirmed that ABCC1 was not being inserted backwards into the plasma membrane, that ABCC1 does export Abeta from the cytoplasm to the extracellular space, and that this export activity is increased by thiethylperazine.

Knowing that our model is working as expected, based upon previous literature, but that our APP metabolite experiments were yielding unexpected results, we employed RNA-sequencing to look at the transcriptomes of the cell lines in order to find a possible mechanism by which APP metabolism was being altered. The differential expression analysis revealed two genes whose downregulation may account for the reduction in extracellular Abeta species: *TIMP3* and *CD38*. *TIMP3* encodes the Tissue Inhibitor of Metalloproteinases 3, a protein that is capable of irreversibly inhibiting alpha-secretases such as ADAM10 and ADAM17 (H.-S. Hoe et al., 2007). The downregulation of this alpha-secretase inhibitor could be the reason why less beta-secretase mediated cleavage of the APP molecule is occurring. *CD38* encodes the Cluster of Differentiation

38, and previous studies have shown in mouse models that knockout of *CD38* reduces Abeta production by reducing beta- and gamma-secretase activity (Blacher et al., 2015).

We then identified the second rare *ABCC1* mutation (p.Arg1342Gly) in our EOAD patient, and generated entirely new cell lines, still utilizing the BE(2)-m17 human neuroblastoma cell line, in order to study this variant, as well as to ensure that the results we were seeing in our previous APP metabolite and RNA-seq experiments was not due to location-specific integration of our vectors. That is, because these vectors integrate almost randomly within the genome, it is possible that the previous cell lines had significantly downregulated *TIMP3* and *CD38* expression due to ablation of these genes within a subset of cells. We then used these new cells, as well as the cryopreserved cells from the first experiments, to repeat our APP metabolite experiments, this time using the Meso Scale Discovery platform, and our RNA-seq experiments.

The results of this APP metabolite experiment confirmed our previous conclusion that increased *ABCC1* expression results in reduced extracellular concentration of Abeta. This experiment also allowed us to conclude that more APP molecules are being cleaved by alpha- rather than beta-secretases by analyzing the ratio of the two metabolites. However, there was no statistically significant difference in the extracellular Abeta1-40, Abeta1-42, or ratio of sAPPalpha over sAPPbeta in either of the mutant *ABCC1*-overexpressing cell lines versus the human reference *ABCC1*-overexpressing cell lines. This allowed us to conclude that increased expression of *ABCC1* reduces the generation of Abeta by skewing APP metabolism away from the beta-secretase and towards the alpha-secretase pathway.

We also repeated the RNA-seq experiment using both the cryopreserved cells and the newly created cell lines, and found that *TIMP3* and *CD38* were always lower in *ABCC1*-overexpressing cells compared to the empty vector control, with *TIMP3* always statistically significant, and with *CD38* trending towards statistical significance in the newly generated cell lines. We confirmed these findings in a second cell line by transfecting ReNcell VM cells, a human neuroprogenitor cell line, with the empty vector or with the human reference *ABCC1* vector, extracting RNA, and performing qRT-PCR using the Taq-Man assay. In this second cell line, overexpression of *ABCC1* significantly reduced expression of both *TIMP3* and *CD38*.

The mechanism by which *ABCC1* overexpression reduces the expression of *TIMP3* and *CD38* was not fully investigated, though we hypothesize that one or some of ABCC1's canonical substrates may be responsible. That is, a reduction in intracellular glutathione, reduced glutathione, sphingosine-1-phosphate, leukotriene C4, or any other substrate of ABCC1 is resulting in these transcriptomic changes. It is also possible that increasing the extracellular concentrations of these molecules is what is causing a signaling cascade to suppress expression of *TIMP3* and *CD38*. Further investigation will be required to confirm or deny this hypothesis.

The *in vivo* work-up of our LOAD *ABCC1* mutation (p.Tyr1189Cys) utilized the CRISPR/cas9 system to introduce the point mutation into the mouse homolog *Abcc1* to change the codon at the homologous residue to reflect the human mutation (mouse, p.Tyr1186Cys). The cognitive battery, the APP metabolite assay, and the RNA-sequencing did not yield any result that would allow us to draw a distinction between the wild-type and the mutant *Abcc1* genes in the 5xFAD mouse model; therefore, we will not discuss this study any further here.

However, what is most important about this study in its entirety is the conclusion that increasing *ABCC1* expression results in reduced Abeta production and an increase in alpha- versus beta-secretase cleavage of the APP molecule. This is a novel insight about *ABCC1*. Previous literature has demonstrated that the ABCC1 protein is capable of exporting Abeta from the cytoplasm of endothelial cells lining the blood-brain barrier where it functions to clear Abeta from the brain and to move it to the peripheral blood (Krohn et al., 2011); however, no previous study has ever shown that increasing *ABCC1* expression alters APP processing away from the beta-secretase, amyloidogenic pathway, and towards the alpha-secretase, neuroprotective pathway.

As previously mentioned, two of the most prominent types of Alzheimer's disease clinical trials are those that are trying to reduce Abeta production via inhibition of BACE1, the main beta-secretase that cleaves the APP molecule, or by increasing clearance or degradation of Abeta from the brain via immune-stimulating anti-amyloid antibodies (Das & Yan, 2019; Huang, Chao, & Hu, 2020). However, many of these clinical trials have failed due to lack of efficacy, unforeseen neurological side effects, or damage to other organ systems.

BACE1 antagonists used in clinical trials for the treatment of AD that have failed included verubecestat, atabecestat, lanabecestat, elenbecestat, and umibecestat (Das & Yan, 2019; Huang et al., 2020). Verubecestat, also known as MK-8931, was developed and trialed by Merck (Kenilworth, NJ, USA), and showed promising results in early trials with significant CSF Abeta level reduction during treatment. However, a larger trial for the drug, called EPOCH, which enrolled patients with mild to moderate AD, was halted early due to safety concerns as those patients taking the drug had significantly higher rates of falls and injuries. The drug was reentered into a clinical trial, called APECS, for the prevention of AD onset by enrolling patients with mild cognitive impairment. This trial was also halted early as patients receiving the drug scored worse in terms of clinical dementia ratings, as well as reported more anxiety, sleep disturbances, and depression, compared to the placebo group (Das & Yan, 2019).

Atabecestat, also known as JNJ-54861911, was developed by Shionogi (Osaka, Japan) and licensed to Janssen Pharmaceuticals (Beerse, Belgium) who ran the clinical trials (Das & Yan, 2019). Like with verubecestat, early trials showed promise as CSF levels of the drug increased, and Abeta levels decreased, in a dose-dependent manner. However, later trials showed significantly increased liver enzyme levels in the blood, a marker of liver damage, in 36% of participants. In an additional trial, liver enzymes were again increased in many patients, and Janssen retired the drug from clinical trials (Das & Yan, 2019).

Lanabecestat, also known as AZD3293, was developed by AstraZeneca (Cambridge, United Kingdom) and tested in clinical trials in a joint effort with Eli Lilly and Company (Indianapolis, IN, USA) (Das & Yan, 2019). The drug also showed a decrease in CSF Abeta levels in a dose-dependent manner, and did not produce the negative effects associated with verubecestat or atabecestat, but was halted early following a futility analysis. That is, there was no significant positive effect in those taking the drug compared to placebo, and some patients taking the drug experienced psychiatric issues, minor weight loss, and discoloring of the hair (Das & Yan, 2019).

Elenbecestat, also known as E2609, was developed by Eisai (Tokyo, Japan), who cooperated with Biogen (Cambridge, MA, USA) for the clinical trials (Das & Yan, 2019). As with

the other BACE1 inhibitors, early trials demonstrated that the drug was safe and could lower CSF Abeta levels. It even showed no negative cognitive effects that were present in other BACE1 antagonist trials. However, as with the other BACE1 antagonists, the trial was ended early because no improvement to cognition was found, and those on the drug had more diarrhea, falls, and nightmares than those in the placebo group (Das & Yan, 2019).

Umibecestat, also known as CNP520, was developed by Novartis (Basel, Switzerland), and is being jointly developed with Amgen (Thousand Oaks, CA, USA) (Das & Yan, 2019). Again, as with the other BACE1 inhibitors, early trials showed the drug to be safe and effective at lowering CSF Abeta levels, but larger trials were halted early because patients taking the drug had worsening cognitive decline, decreased brain volume, and weight loss compared to the placebo group (Huang et al., 2020).

These five different drug trials, all employing small compounds that block BACE1 beta-secretase activity, resulted in no positive effect on cognition, a worsening of cognition, an increase in psychiatric events, and increase in falls and injuries, or significant liver damage in participants receiving the drug versus the placebo control group. This may be because of off-target effects of the drugs, or may be because of unknown biological effects of inhibiting the BACE1 enzyme. With all of these drugs failing in clinical trials, it seems most likely that BACE1, while a very logical drug target for the treatment or prevention of AD, is not the proper target for the reduction of Abeta production.

The other class of drugs at the forefront of AD prevention and treatment trials are those that target Abeta for clearance from the brain, or those that prevent Abeta from aggregating into insoluble amyloid plaques. These compounds include the antibodies aducanumab, solanezumab, gantenerumab, and lecenemab, as well as the small molecule ALZ-801 (Huang et al., 2020; Tolar, Abushakra, Hey, Porsteinsson, & Sabbagh, 2020; Vaz & Silvestre, 2020). The primary endpoints of these trials were decreases in cerebral Abeta, amyloid plaque deposition, or increased cognition.

Aducanumab, also known as BIIB037, was discovered by Neurimmune AG (Zurich, Switzerland) and developed by Biogen (Tolar et al., 2020; Vaz & Silvestre, 2020). This antibody

was designed to bind to insoluble amyloid plaques to trigger clearance of the molecules by microglial cells within the brain. An independent analysis during their largest drug trial determined that the antibody was unlikely to meet the desired endpoint, and the trial was cancelled in March of 2019 (Vaz & Silvestre, 2020). The results of that trial are still being debated, as some scientists believe the drug showed efficacy in certain cases, and should still be pursued, while other believe that any efficacy observed was minimal, and pursuit of this expensive drug should be ended (Vaz & Silvestre, 2020).

Solanezumab, also known as LY2062430, was developed by Eli Lilly and Company with drug safety trials beginning in 2006 (Tian Hui Kwan et al., 2020). This antibody was designed to bind to soluble Abeta to prevent aggregation into insoluble amyloid plaques. The largest clinical trial that employed this drug began in February of 2014, and it was announced in February of 2020 that the trial was failing, again because the primary endpoints of the trial were not being met. Eli Lilly and Company has officially ended the clinical trial and have ceased pursuing FDA approval (Tian Hui Kwan et al., 2020).

Gantenerumab, also known as RO4909832 or RG1450, was created by Chugai Pharmaceutical Company and developed by Hoffman-La Roche (Klein et al., 2021). This antibody was designed to bind to aggregated Abeta fibrils to promote degradation and clearance of the insoluble amyloid plaques or soluble fibrils (Tian Hui Kwan et al., 2020). The trials utilizing only this antibody have mostly been halted due to futility of the trial (Tian Hui Kwan et al., 2020). It is currently being studied in conjunction with a BACE1 inhibitor for the prevention or treatment of AD, in an attempt to both reduce Abeta production and to clear Abeta and amyloid plaques from the brain (Jacobsen et al., 2014).

Lecanemab, also known as BAN2401, was created by BioArctic Neuroscience and licensed to Eisai (Tolar et al., 2020). The antibody was designed to bind to Abeta protofibrils, which are soluble Abeta aggregates that have not yet grown into the insoluble amyloid plaques. Safety trials for the drug began in 2010, and Phase 3 efficacy trials are still underway for this antibody (Tolar et al., 2020).

Homotaurine is a small molecule that can bind to Abeta1-42 to prevent its oligomerization, but it has a relatively short half-life when ingested (Hey et al., 2018). ALZ-801 was designed as a prodrug for tramiprosate (homotaurine), which adds a biologically cleavable valine to the compound that, once removed, results in a homotaurine molecule. This increases the half-life of active compound which increases bioavailability and requires fewer daily doses to achieve potentially therapeutic cerebral levels of the drug. The prodrug was created by NeuroChem, now called BELLUS Health (Laval, Canada), and licensed to Alzheon (Framingham, MA, USA) for development. Clinical trials are still underway for this compound (Hey et al., 2018).

Previous to our study, another lab has shown that ABCC1 is capable of exporting Abeta from the cytoplasm of the endothelial cells lining the blood-brain barrier to the peripheral blood (Krohn et al., 2011), and that knockout of *ABCC1* increases cerebral Abeta levels in the APP/PS1 mouse (Krohn et al., 2015). The investigators in these studies have also targeted the ABCC1 protein with small molecules to increase ABCC1-mediated export of Abeta (Krohn et al., 2011). Currently, because of work from that lab, Immungenetics AG (Rostock, Germany) is running a Phase 2 clinical trial to assess the safety of thiethylperazine in older adults with Alzheimer's disease, as this compound was discovered to increase ABCC1-mediated export of Abeta from the brain (EudraCT number: 2014-000870-20). That is, they have targeted ABCC1 to remove Abeta from the brain, which is the main goal of the anti-amyloid antibody and small molecule therapies previously discussed.

In our study, we have shown that increased *ABCC1* expression results in decreased Abeta production by skewing APP processing away from the beta- and towards the alpha-secretase pathway, which is the goal of the BACE1 antagonist clinical trials, many of which have failed. Combining the work presented here with the previous ABCC1-related Alzheimer's studies, it is logical that targeting *ABCC1* for increased expression, or targeting ABCC1-medited export, may be a single-target method for both decreasing Abeta production and increasing Abeta export from the brain, which, separately, are the goals of the two main classes of current AD drug trials.

Luckily, *ABCC1* has been extensively studied and targeted in the field of cancer research where *ABCC1* is commonly known by its former name, *MRP1*, which encodes the former protein

name, Multidrug Resistance-associated Protein 1. This former name of *ABCC1* is derived from the protein's ability to confer chemoresistance to numerous chemotherapeutics because of its ability to export them from the cytoplasm to the extracellular space where they cannot have the desired effect (Cole, 2014). Because of this, many drug development pipelines have already been developed to screen thousands of compounds to find drugs that can either halt ABCC1-mediated export, or that can decrease expression of *ABCC1* (Cihalova, Ceckova, et al., 2015; Cihalova, Staud, et al., 2015; Csandl et al., 2016; Gana et al., 2019; Gao et al., 2020; Jiang et al., 2016; Kumar & Jaitak, 2019; Ranjbar et al., 2019; Sampson et al., 2019; Schafer et al., 2017; Schmitt et al., 2016; Silbermann et al., 2020, 2019; Sorf et al., 2019; K. Stefan et al., 2017; K. W. Tan et al., 2018; Whitt et al., 2016; Wong et al., 2018). As with all drug screens, it is highly likely that compounds have been discovered that result in the opposite effect that is desired. That is, while these pipelines were created to find compounds that inhibit ABCC1 or reduce expression of the gene, surely compounds that increase ABCC1-mediated export or increase *ABCC1* expression were identified. Such compounds should be studied within the context of Alzheimer's disease, as they may be the most effective way of both removing Abeta from the brain as well as reducing the amount of Abeta that is produced.

We hypothesize that compounds, other than thiethylperazine, that increase ABCC1-mediated export or increase *ABCC1* expression have already been identified and are "sitting on the shelf" because administration of these compounds would have the opposite effect of that which was desired by the cancer drug discovery pipeline. We call upon the principal investigators of these pipelines to publicly identify these compounds, or to collaborate with Alzheimer's disease researchers to study these drugs in the context of AD.

We would also like to identify the potential need to humanize the mouse *ABCC1* gene in the current AD mouse models when studying these compounds to make the studies more likely to translate to human subjects. The three main AD mouse models (5xFAD, 3xTg-AD, and APP/PS1) overexpress human forms of *APP* and *PSEN1*, which is what drives the progressive accumulation of AD-like pathology and resulting cognitive decline. It may be true that the mouse Abcc1 protein has different Abeta export capabilities compared to the human ABCC1. It is also possible that the

drugs that effectively target human ABCC1 are less effective at targeting the mouse Abcc1, or vice versa. Therefore, an AD mouse model homozygous for the humanized *ABCC1* gene would likely be the best model for testing these compound's abilities to increase *ABCC1* expression or ABCC1-mediated export of Abeta, and this is has been pursued by another laboratory (Krohn et al., 2019).

We hypothesize that targeting *ABCC1* for increased expression or increased ABCC1-mediated export would decrease Abeta production and increase clearance of Abeta from the brain, which could prove to be a viable option for the treatment or prevention of Alzheimer's disease due to the multimodal influence of ABCC1 on APP processing and Abeta clearance.

REFERENCES

2020 Alzheimer's disease facts and figures. (2020). *Alzheimer's & Dementia*, *16*(3), 391–460. https://doi.org/10.1002/alz.12068

Abduljaleel, Z., Al-Allaf, F. A., Khan, W., Athar, M., Shahzad, N., Taher, M. M., … El-Huneidi, W. (2014). Evidence of Trem2 variant associated with triple risk of alzheimer's disease. *PLoS ONE*, *9*(3). https://doi.org/10.1371/journal.pone.0092648

Antushevich, H., & Wójcik, M. (2018, August 1). Review: Apelin in disease. *Clinica Chimica Acta*. Elsevier B.V. https://doi.org/10.1016/j.cca.2018.05.012

Arcand, M. (2015, April 1). End-of-life issues in advanced dementia - Part 1: Goals of care, decision-making process, and family education. *Canadian Family Physician*. College of Family Physicians of Canada. Retrieved from www.cfp.ca

Bai, G., Chivatakarn, O., Bonanomi, D., Lettieri, K., Franco, L., Xia, C., … Pfaff, S. L. (2011). Presenilin-dependent receptor processing is required for axon guidance. *Cell*, *144*(1), 106–118. https://doi.org/10.1016/j.cell.2010.11.053

Bateman, R. J., Aisen, P. S., De Strooper, B., Fox, N. C., Lemere, C. A., Ringman, J. M., … Xiong, C. (2011). Autosomal-dominant Alzheimer's disease: A review and proposal for the prevention of Alzheimer's disease. *Alzheimer's Research and Therapy*. BioMed Central. https://doi.org/10.1186/alzrt59

Beecham, G. W., Hamilton, K., Naj, A. C., Martin, E. R., Huentelman, M., Myers, A. J., … Montine, T. J. (2014). Genome-Wide Association Meta-analysis of Neuropathologic Features of Alzheimer's Disease and Related Dementias. *PLoS Genetics*, *10*(9). https://doi.org/10.1371/journal.pgen.1004606

Bekris, L. M., Yu, C. E., Bird, T. D., & Tsuang, D. W. (2010, December). Review article: Genetics of Alzheimer disease. *Journal of Geriatric Psychiatry and Neurology*. NIH Public Access. https://doi.org/10.1177/0891988710383571

Bellenguez, C., Grenier-Boley, B., & Lambert, J. C. (2020, April 1). Genetics of Alzheimer's disease: where we are, and where we are going. *Current Opinion in Neurobiology*. Elsevier Ltd. https://doi.org/10.1016/j.conb.2019.11.024

Blacher, E., Dadali, T., Bespalko, A., Haupenthal, V. J., Grimm, M. O. W., Hartmann, T., … Levy, A. (2015). Alzheimer's disease pathology is attenuated in a CD38-deficient mouse model. *Annals of Neurology*, *78*(1), 88–103. https://doi.org/10.1002/ana.24425

Blomqvist, M. E. L., Andreasen, N., Bogdanovic, N., Blennow, K., Brookes, A. J., & Prince, J. A. (2004). Genetic variation in CTNNA3 encoding alpha-3 catenin and Alzheimer's disease. *Neuroscience Letters*, *358*(3), 220–222. https://doi.org/10.1016/j.neulet.2004.01.032

Bousard, A., Raposo, A. C., Żylicz, J. J., Picard, C., Pires, V. B., Qi, Y., … da Rocha, S. T. (2019). The role of Xist -mediated Polycomb recruitment in the initiation of X-chromosome inactivation . *EMBO Reports*, *20*(10). https://doi.org/10.15252/embr.201948019

Breiderhoff, T., Christiansen, G. B., Pallesen, L. T., Vaegter, C., Nykjaer, A., Holm, M. M., … Willnow, T. E. (2013). Sortilin-Related Receptor SORCS3 Is a Postsynaptic Modulator of Synaptic Depression and Fear Extinction. *PLoS ONE*, *8*(9). https://doi.org/10.1371/journal.pone.0075006

Bukhari, H., Glotzbach, A., Kolbe, K., Leonhardt, G., Loosse, C., & Müller, T. (2017, September 1). Small things matter: Implications of APP intracellular domain AICD nuclear signaling in the progression and pathogenesis of Alzheimer's disease. *Progress in Neurobiology*. Elsevier Ltd. https://doi.org/10.1016/j.pneurobio.2017.05.005

Bult, C. J., Blake, J. A., Smith, C. L., Kadin, J. A., Richardson, J. E., Anagnostopoulos, A., … Zhu, Y. (2019). Mouse Genome Database (MGD) 2019. *Nucleic Acids Research*, *47*(D1), D801–D806. https://doi.org/10.1093/nar/gky1056

Busby, V., Goossens, S., Nowotny, P., Hamilton, G., Smemo, S., Harold, D., … Lovestone, S. (2004). Alpha-T-catenin is expressed in human brain and interacts with the Wnt signaling pathway but is not responsible for linkage to chromosome 10 in Alzheimer's disease. *Neuromolecular Medicine*, *5*(2), 133–146. https://doi.org/10.1385/NMM:5:2:133

Cantarella, G., Di Benedetto, G., Puzzo, D., Privitera, L., Loreto, C., Saccone, S., … Bernardini, R. (2015). Neutralization of TNFSF10 ameliorates functional outcome in a murine model of Alzheimer's disease. *Brain*, *138*(1), 203–216. https://doi.org/10.1093/brain/awu318

Chang, X., Wang, J., Jiang, H., Shi, L., & Xie, J. (2019, May 27). Hyperpolarization-activated cyclic nucleotide-gated channels: An emerging role in neurodegenerative diseases. *Frontiers in Molecular Neuroscience*. Frontiers Media S.A. https://doi.org/10.3389/fnmol.2019.00141

Chini, E. N., Chini, C. C. S., Kato, I., Takasawa, S., & Okamoto, H. (2002). CD38 is the major enzyme responsible for synthesis of nicotinic acid - Adenine dinucleotide phosphate in mammalian tissues. *Biochemical Journal*, *362*(1), 125–130. https://doi.org/10.1042/0264-6021:3620125

Choi, H. Y., Liu, Y., Tennert, C., Sugiura, Y., Karakatsani, A., Kröger, S., … Herz, J. (2013). APP interacts with LRP4 and agrin to coordinate the development of the neuromuscular junction in mice. *ELife*, *2*(2). https://doi.org/10.7554/elife.00220

Cihalova, D., Ceckova, M., Kucera, R., Klimes, J., & Staud, F. (2015). Dinaciclib, a cyclin-dependent kinase inhibitor, is a substrate of human ABCB1 and ABCG2 and an inhibitor of human ABCC1 in vitro. *Biochemical Pharmacology*, *98*(3), 465–472. https://doi.org/10.1016/j.bcp.2015.08.099

Cihalova, D., Staud, F., & Ceckova, M. (2015). Interactions of cyclin-dependent kinase inhibitors AT-7519, flavopiridol and SNS-032 with ABCB1, ABCG2 and ABCC1 transporters and their potential to overcome multidrug resistance in vitro. *Cancer Chemotherapy and Pharmacology*, *76*(1), 105–116. https://doi.org/10.1007/s00280-015-2772-1

Cipriani, G., Dolciotti, C., Picchi, L., & Bonuccelli, U. (2011). Alzheimer and his disease: A brief history. *Neurological Sciences*, *32*(2), 275–279. https://doi.org/10.1007/s10072-010-0454-7

Cole, S. P. C. (2014, November 7). Multidrug resistance protein 1 (mrp1, abcc1), a "multitasking" atp-binding cassette (abc,) transporter. *Journal of Biological Chemistry*. American Society for Biochemistry and Molecular Biology Inc. https://doi.org/10.1074/jbc.R114.609248

Conseil, G., Deeley, R. G., & Cole, S. P. C. (2005). Role of two adjacent cytoplasmic tyrosine residues in MRP1 (ABCC1) transport activity and sensitivity to sulfonylureas. *Biochemical Pharmacology*, *69*(3), 451–461. https://doi.org/10.1016/j.bcp.2004.10.014

Crews, L., Adame, A., Patrick, C., DeLaney, A., Pham, E., Rockenstein, E., … Masliah, E. (2010). Increased BMP6 levels in the brains of Alzheimer's disease patients and APP transgenic mice are accompanied by impaired neurogenesis. *Journal of Neuroscience*, *30*(37), 12252–12262. https://doi.org/10.1523/JNEUROSCI.1305-10.2010

Crouzin, N., Baranger, K., Cavalier, M., Marchalant, Y., Cohen-Solal, C., Roman, F. S., … Vignes, M. (2013). Area-Specific Alterations of Synaptic Plasticity in the 5XFAD Mouse Model of Alzheimer's Disease: Dissociation between Somatosensory Cortex and Hippocampus. *PLoS ONE*, *8*(9). https://doi.org/10.1371/journal.pone.0074667

Csandl, M. A., Conseil, G., & Cole, S. P. C. (2016). Cysteinyl leukotriene receptor 1/2 antagonists nonselectively modulate organic anion transport by multidrug resistance proteins (MRP1-4)s. *Drug Metabolism and Disposition*, *44*(6), 857–866. https://doi.org/10.1124/dmd.116.069468

D'Amico, M., Di Filippo, C., Marfella, R., Abbatecola, A. M., Ferraraccio, F., Rossi, F., & Paolisso, G. (2010). Long-term inhibition of dipeptidyl peptidase-4 in Alzheimer's prone mice. *Experimental Gerontology*, *45*(3), 202–207. https://doi.org/10.1016/j.exger.2009.12.004

Dard, R. F., Dahan, L., & Rampon, C. (2019). Targeting hippocampal adult neurogenesis using transcription factors to reduce Alzheimer's disease-associated memory impairments. *Hippocampus*, *29*(7), 579–586. https://doi.org/10.1002/hipo.23052

Das, B., & Yan, R. (2019, March 6). A Close Look at BACE1 Inhibitors for Alzheimer's Disease Treatment. *CNS Drugs*. Springer International Publishing. https://doi.org/10.1007/s40263-019-00613-7

Deeley, R. G., Westlake, C., & Cole, S. P. C. (2006). Transmembrane transport of endo- and xenobiotics by mammalian ATP-binding cassette multidrug resistance proteins. *Physiological Reviews*. American Physiological Society. https://doi.org/10.1152/physrev.00035.2005

Dioufa, N., Schally, A. V., Chatzistamou, I., Moustou, E., Block, N. L., Owens, G. K., … Kiaris, H. (2010). Acceleration of wound healing by growth hormone-releasing hormone and its agonists. *Proceedings of the National Academy of Sciences of the United States of America*, *107*(43), 18611–18615. https://doi.org/10.1073/pnas.1013942107

Dobin, A., Davis, C. A., Schlesinger, F., Drenkow, J., Zaleski, C., Jha, S., … Gingeras, T. R. (2013). STAR: ultrafast universal RNA-seq aligner. *Bioinformatics*, *29*(1), 15–21. https://doi.org/10.1093/bioinformatics/bts635

Dobin, A., & Gingeras, T. R. (2016). Optimizing RNA-seq mapping with STAR. In *Methods in Molecular Biology* (Vol. 1415, pp. 245–262). Humana Press Inc. https://doi.org/10.1007/978-1-4939-3572-7_13

Dunckley, T., Beach, T. G., Ramsey, K. E., Grover, A., Mastroeni, D., Walker, D. G., … Stephan, D. A. (2006). Gene expression correlates of neurofibrillary tangles in Alzheimer's disease. *Neurobiology of Aging*, *27*(10), 1359–1371. https://doi.org/10.1016/j.neurobiolaging.2005.08.013

Edbauer, D., Willem, M., Lammich, S., Steiner, H., & Haass, C. (2002). Insulin-degrading enzyme rapidly removes the β-amyloid precursor protein intracellular domain (AICD). *Journal of Biological Chemistry*, *277*(16), 13389–13393. https://doi.org/10.1074/jbc.M111571200

Efthymiou, A. G., & Goate, A. M. (2017, May 26). Late onset Alzheimer's disease genetics implicates microglial pathways in disease risk. *Molecular Neurodegeneration*. BioMed Central Ltd. https://doi.org/10.1186/s13024-017-0184-x

Elkamhawy, A., Park, J. eun, Hassan, A. H. E., Pae, A. N., Lee, J., Park, B. G., … Roh, E. J. (2017). Design, synthesis, biological evaluation and molecular modelling of 2-(2-aryloxyphenyl)-1,4-dihydroisoquinolin-3(2H)-ones: A novel class of TSPO ligands modulating amyloid-β-induced mPTP opening. *European Journal of Pharmaceutical Sciences*, *104*, 366–381. https://doi.org/10.1016/j.ejps.2017.04.015

Ertekin-Taner, N., Ronald, J., Asahara, H., Younkin, L., Hella, M., Jain, S., … Younkin, S. (2003). Fine mapping of the a-T catenin gene to a quantitative trait locus on chromosome 10 in late-onset Alzheimer's disease pedigrees. *Hum Mol Genet.*, *12*(23), 3133–3143. https://doi.org/10.1093/hmg/ddg343

Ethell, D. W., & Buhler, L. A. (2003, September). Fas ligand-mediated apoptosis in degenerative disorders of the brain. *Journal of Clinical Immunology*. https://doi.org/10.1023/A:1025317516396

Evans, C. E., Miners, J. S., Piva, G., Willis, C. L., Heard, D. M., Kidd, E. J., … Kehoe, P. G. (2020). ACE2 activation protects against cognitive decline and reduces amyloid pathology in the Tg2576 mouse model of Alzheimer's disease. *Acta Neuropathologica*, *139*(3), 485–502. https://doi.org/10.1007/s00401-019-02098-6

Falkevall, A., Alikhani, N., Bhushan, S., Pavlov, P. F., Busch, K., Johnson, K. A., … Glaser, E. (2006). Degradation of the amyloid β-protein by the novel mitochondrial peptidasome, PreP. *Journal of Biological Chemistry*, *281*(39), 29096–29104. https://doi.org/10.1074/jbc.M602532200

Fourriere, L., Jimenez, A. J., Perez, F., & Boncompain, G. (2020, January 1). The role of microtubules in secretory protein transport. *Journal of Cell Science*. Company of Biologists Ltd. https://doi.org/10.1242/jcs.237016

Gana, C. C., Hanssen, K. M., Yu, D. M. T., Flemming, C. L., Wheatley, M. S., Conseil, G., … Fletcher, J. I. (2019). MRP1 modulators synergize with buthionine sulfoximine to exploit collateral sensitivity and selectively kill MRP1-expressing cancer cells. *Biochemical Pharmacology*, *168*, 237–248. https://doi.org/10.1016/j.bcp.2019.07.009

Gao, Q., Li, X. xiu, Xu, Y. ming, Zhang, J. zhao, Rong, S. di, Qin, Y. qing, & Fang, J. (2020). IRE1α-targeting downregulates ABC transporters and overcomes drug resistance of colon cancer cells. *Cancer Letters*, *476*, 67–74. https://doi.org/10.1016/j.canlet.2020.02.007

Glerup, S., Olsen, D., Vaegter, C. B., Gustafsen, C., Sjoegaard, S. S., Hermey, G., … Nykjaer, A. (2014). Article SorCS2 Regulates Dopaminergic Wiring and Is Processed into an Apoptotic Two-Chain Receptor in Peripheral Glia. *Neuron*, *82*, 1074–1087. https://doi.org/10.1016/j.neuron.2014.04.022

Good, P. F., Alapat, D., Hsu, A., Chu, C., Perl, D., Wen, X., … Kohtz, D. S. (2004). A role for semaphorin 3A signaling in the degeneration of hippocampal neurons during Alzheimer's disease. *Journal of Neurochemistry*, *91*(3), 716–736. https://doi.org/10.1111/j.1471-4159.2004.02766.x

Gosztyla, M. L., Brothers, H. M., & Robinson, S. R. (2018). Alzheimer's Amyloid-β is an Antimicrobial Peptide: A Review of the Evidence. *Journal of Alzheimer's Disease*. IOS Press. https://doi.org/10.3233/JAD-171133

Gow, A., Friedrich, V. L., & Lazzarini, R. A. (1992). Myelin basic protein gene contains separate enhancers for oligodendrocyte and Schwann cell expression. *Journal of Cell Biology*, *119*(3), 605–616. https://doi.org/10.1083/jcb.119.3.605

Grimm, M. O. W., Mett, J., Stahlmann, C. P., Grösgen, S., Haupenthal, V. J., Blümel, T., … Hartmann, T. (2015). APP intracellular domain derived from amyloidogenic β-and γ-secretase cleavage regulates neprilysin expression. *Frontiers in Aging Neuroscience*, *7*(APR), 77. https://doi.org/10.3389/fnagi.2015.00077

Hahn, C. N., Su, Z. J., Drogemuller, C. J., Tsykin, A., Waterman, S. R., Brautigan, P. J., … Gamble, J. R. (2005). Expression profiling reveals functionally important genes and coordinately regulated signaling pathway genes during in vitro angiogenesis. *Physiological Genomics*, *22*(1), 57–69. https://doi.org/10.1152/physiolgenomics.00278.2004

Han, M. R., Schellenberg, G. D., & Wang, L. S. (2010). Genome-wide association reveals genetic effects on human Aβ42and τ protein levels in cerebrospinal fluids: A case control study. *BMC Neurology*, *10*. https://doi.org/10.1186/1471-2377-10-90

Hartley, D., Blumenthal, T., Carrillo, M., DiPaolo, G., Esralew, L., Gardiner, K., … Wisniewski, T. (2015). Down syndrome and Alzheimer's disease: Common pathways, common goals. *Alzheimer's and Dementia*, *11*(6), 700–709. https://doi.org/10.1016/j.jalz.2014.10.007

Hermey, G., Hoffmeister-Ullerich, S. A., Merz, B., Groß, D., Kuhl, D., & Kins, S. (2019). Amyloidosis causes downregulation of SorLA, SorCS1 and SorCS3 expression in mice. *Biological Chemistry*, *400*(9), 1181–1189. https://doi.org/10.1515/hsz-2019-0146

Hey, J. A., Yu, J. Y., Versavel, M., Abushakra, S., Kocis, P., Power, A., … Tolar, M. (2018). Clinical Pharmacokinetics and Safety of ALZ-801, a Novel Prodrug of Tramiprosate in Development for the Treatment of Alzheimer's Disease. *Clinical Pharmacokinetics*, *57*(3), 315–333. https://doi.org/10.1007/s40262-017-0608-3

Hocker, M., Zhang, Z., Koh, T. J., & Wanga, T. C. (1996). *The Regulation of Histidine Decarboxylase Gene Expression*. *YALE JOURNAL OF BIOLOGY AND MEDICINE* (Vol. 69).

Hoe, H.-S., Cooper, M. J., Burns, M. P., Lewis, P. A., van der Brug, M., Chakraborty, G., … Rebeck, G. W. (2007). The Metalloprotease Inhibitor TIMP-3 Regulates Amyloid Precursor Protein and Apolipoprotein E Receptor Proteolysis. *Journal of Neuroscience*, *27*(40), 10895–10905. https://doi.org/10.1523/JNEUROSCI.3135-07.2007

Hoe, Hyang-Sook, Cooper, M. J., Burns, M. P., Lewis, P. A., van der Brug, M., Chakraborty, G., … Rebeck, G. W. (2007). The metalloprotease inhibitor TIMP-3 regulates amyloid precursor protein and apolipoprotein E receptor proteolysis. *The Journal of Neuroscience : The Official Journal of the Society for Neuroscience*, *27*(40), 10895–10905. https://doi.org/10.1523/JNEUROSCI.3135-07.2007

Hoos, M. D., Ahmed, M., Smith, S. O., & Van Nostrand, W. E. (2007). Inhibition of familial cerebral amyloid angiopathy mutant amyloid β-protein fibril assembly by myelin basic protein. *Journal of Biological Chemistry*, *282*(13), 9952–9961. https://doi.org/10.1074/jbc.M603494200

Horio, T., Murata, T., & Murata, T. (2014, October 7). The role of dynamic instability in microtubule organization. *Frontiers in Plant Science*. Frontiers Media S.A. https://doi.org/10.3389/fpls.2014.00511

Hoshino, T., Namba, T., Takehara, M., Nakaya, T., Sugimoto, Y., Araki, W., … Mizushima, T. (2009). Prostaglandin E2 stimulates the production of amyloid-β peptides through internalization of the EP4 receptor. *Journal of Biological Chemistry*, *284*(27), 18493–18502. https://doi.org/10.1074/jbc.M109.003269

Huang, L. K., Chao, S. P., & Hu, C. J. (2020, January 6). Clinical trials of new drugs for Alzheimer disease. *Journal of Biomedical Science*. BioMed Central Ltd. https://doi.org/10.1186/s12929-019-0609-7

Huang, R., & Poduslo, S. E. (2006, August). CYP19 haplotypes increase risk for Alzheimer's disease. *Journal of Medical Genetics*. https://doi.org/10.1136/jmg.2005.039461

Hughes, C. P., Berg, L., Danziger, W. L., Coben, L. A., & Martin, R. L. (1982). A new clinical scale for the staging of dementia. *British Journal of Psychiatry*, *140*(6), 566–572. https://doi.org/10.1192/bjp.140.6.566

Jacobsen, H., Ozmen, L., Caruso, A., Narquizian, R., Hilpert, H., Jacobsen, B., … Bohrmann, B. (2014). Combined treatment with a BACE inhibitor and anti-Aβ antibody gantenerumab enhances amyloid reduction in APPLondon mice. *Journal of Neuroscience*, *34*(35), 11621–11630. https://doi.org/10.1523/JNEUROSCI.1405-14.2014

Jaszberenyi, M., Rick, F. G., Szalontay, L., Block, N. L., Zarandi, M., Cai, R. Z., & Schally, A. V. (2012). Beneficial effects of novel antagonists of GHRH in different models of Alzheimersts's disease. *Aging*, *4*(11), 755–767. https://doi.org/10.18632/aging.100504

Jiang, T. T., Shi, L. Y., Wei, L. L., Li, X., Yang, S., Wang, C., … Li, J. C. (2017). Serum amyloid A, protein Z, and C4b-binding protein β chain as new potential biomarkers for pulmonary tuberculosis. *PLoS ONE*, *12*(3). https://doi.org/10.1371/journal.pone.0173304

Jiang, Y. Q., Xu, X. P., Guo, Q. M., Xu, X. C., Liu, Q. Y., An, S. H., … Tai, J. B. (2016). Reversal of cisplatin resistance in non-small cell lung cancer stem cells by Taxus chinensis var. *Genetics and Molecular Research*, *15*(3). https://doi.org/10.4238/gmr.15038336

Jimenez, S., Torres, M., Vizuete, M., Sanchez-Varo, R., Sanchez-Mejias, E., Trujillo-Estrada, L., … Vitorica, J. (2011). Age-dependent accumulation of soluble amyloid β (Aβ) oligomers reverses the neuroprotective effect of soluble amyloid precursor protein-α (sAPPα) by modulating phosphatidylinositol 3-kinase (PI3K)/Akt-GSK- 3β pathway in Alzheimer mouse model. *Journal of Biological Chemistry*, *286*(21), 18414–18425. https://doi.org/10.1074/jbc.M110.209718

Jun, G., Asai, H., Zeldich, E., Drapeau, E., Chen, C. Di, Chung, J., … Farrer, L. A. (2014). PLXNA4 is associated with Alzheimer disease and modulates tau phosphorylation. *Annals of Neurology*, *76*(3), 379–392. https://doi.org/10.1002/ana.24219

Kadavath, H., Hofele, R. V., Biernat, J., Kumar, S., Tepper, K., Urlaub, H., … Zweckstetter, M. (2015). Tau stabilizes microtubules by binding at the interface between tubulin heterodimers. *Proceedings of the National Academy of Sciences of the United States of America*, *112*(24), 7501–7506. https://doi.org/10.1073/pnas.1504081112

Karch, C. M., & Goate, A. M. (2015, January 1). Alzheimer's disease risk genes and mechanisms of disease pathogenesis. *Biological Psychiatry*. Elsevier USA. https://doi.org/10.1016/j.biopsych.2014.05.006

Karczewski, K. J., Francioli, L. C., Tiao, G., Cummings, B. B., Alföldi, J., Wang, Q., … MacArthur, D. G. (2020). The mutational constraint spectrum quantified from variation in 141,456 humans. *Nature*, *581*(7809), 434–443. https://doi.org/10.1038/s41586-020-2308-7

Kimura, R., & Ohno, M. (2009). Impairments in remote memory stabilization precede hippocampal synaptic and cognitive failures in 5XFAD Alzheimer mouse model. *Neurobiology of Disease*, *33*(2), 229–235. https://doi.org/10.1016/j.nbd.2008.10.006

Klein, G., Delmar, P., Kerchner, G. A., Hofmann, C., Abi-Saab, D., Davis, A., … Doody, R. (2021). Thirty-Six-Month Amyloid Positron Emission Tomography Results Show Continued Reduction in Amyloid Burden with Subcutaneous Gantenerumab. *Journal of Prevention of Alzheimer's Disease*, *8*(1), 3–6. https://doi.org/10.14283/jpad.2020.68

Kleineidam, L., Chouraki, V., Próchnicki, T., van der Lee, S. J., Madrid-Márquez, L., Wagner-Thelen, H., … Ramirez, A. (2020). PLCG2 protective variant p.P522R modulates tau pathology and disease progression in patients with mild cognitive impairment. *Acta Neuropathologica*. https://doi.org/10.1007/s00401-020-02138-6

Koca, E., Taşkapilioğlu, Ö., & Bakar, M. (2017, March 1). Caregiver burden in different stages of Alzheimer's disease. *Noropsikiyatri Arsivi*. Turkish Neuropsychiatric Society. https://doi.org/10.5152/npa.2017.11304

Kowalska, A. (2004). The beta-amyloid cascade hypothesis: a sequence of events leading to neurodegeneration in Alzheimer's disease. *Neurologia i Neurochirurgia Polska*. Neurol Neurochir Pol. Retrieved from https://pubmed.ncbi.nlm.nih.gov/15565529/

Kowarz, E., Löscher, D., & Marschalek, R. (2015). Optimized Sleeping Beauty transposons rapidly generate stable transgenic cell lines. *Biotechnology Journal*, *10*(4), 647–653. https://doi.org/10.1002/biot.201400821

Kraeuter, A. K., Guest, P. C., & Sarnyai, Z. (2019). The Y-Maze for Assessment of Spatial Working and Reference Memory in Mice. In *Methods in Molecular Biology* (Vol. 1916, pp. 105–111). Humana Press Inc. https://doi.org/10.1007/978-1-4939-8994-2_10

Krohn, M., Bracke, A., Avchalumov, Y., Schumacher, T., Hofrichter, J., Paarmann, K., … Pahnke, J. (2015). Accumulation of murine amyloid-β mimics early Alzheimer's disease. *Brain*, *138*(8), 2370–2382. https://doi.org/10.1093/brain/awv137

Krohn, M., Lange, C., Hofrichter, J., Scheffler, K., Stenzel, J., Steffen, J., … Pahnke, J. (2011). Cerebral amyloid-β proteostasis is regulated by the membrane transport protein ABCC1 in mice. *The Journal of Clinical Investigation*, *121*(10), 3924–3931. https://doi.org/10.1172/JCI57867

Krohn, M., Zoufal, V., Mairinger, S., Wanek, T., Paarmann, K., Brüning, T., … Pahnke, J. (2019). Generation and characterization of an ABCC1 humanized mouse model (HABCC1FLX/FLX) with knockout capability. *Molecular Pharmacology*, *96*(2), 138–147. https://doi.org/10.1124/mol.119.115824

Kumar, A., & Jaitak, V. (2019, August 15). Natural products as multidrug resistance modulators in cancer. *European Journal of Medicinal Chemistry*. Elsevier Masson SAS. https://doi.org/10.1016/j.ejmech.2019.05.027

Lanoiselée, H. M., Nicolas, G., Wallon, D., Rovelet-Lecrux, A., Lacour, M., Rousseau, S., … Campion, D. (2017). APP, PSEN1, and PSEN2 mutations in early-onset Alzheimer disease: A genetic screening study of familial and sporadic cases. *PLoS Medicine*, *14*(3). https://doi.org/10.1371/journal.pmed.1002270

Lashkari, K., Teague, G., Chen, H., Lin, Y. Q., Kumar, S., McLaughlin, M. M., & López, F. J. (2018). A monoclonal antibody targeting amyloid β (Aβ) restores complement factor I bioactivity: Potential implications in age-related macular degeneration and Alzheimer's disease. *PLoS ONE*, *13*(5). https://doi.org/10.1371/journal.pone.0195751

Lau, A., Bourkas, M., Lu, Y. Q. Q., Ostrowski, L. A., Weber-Adrian, D., Figueiredo, C., … Schmitt-Ulms, G. (2017). Functional Amyloids and their Possible Influence on Alzheimer Disease. *Discoveries*, *5*(4), e79. https://doi.org/10.15190/d.2017.9

Lee, V. M. Y., Kenyon, T. K., & Trojanowski, J. Q. (2005, January 3). Transgenic animal models of tauopathies. *Biochimica et Biophysica Acta - Molecular Basis of Disease*. Elsevier. https://doi.org/10.1016/j.bbadis.2004.06.014

Li, H., & Durbin, R. (2010). Fast and accurate long-read alignment with Burrows–Wheeler transform. *Bioinformatics*, *26*(5), 589–595. https://doi.org/10.1093/bioinformatics/btp698

Li, Y., Duffy, K. B., Ottinger, M. A., Ray, B., Bailey, J. A., Holloway, H. W., … Greig, N. H. (2010). GLP-1 receptor stimulation reduces amyloid-beta peptide accumulation and cytotoxicity in cellular and animal models of Alzheimer's disease. *Journal of Alzheimer's Disease : JAD*, *19*(4), 1205–1219. https://doi.org/10.3233/JAD-2010-1314

Li, Z., Shue, F., Zhao, N., Shinohara, M., & Bu, G. (2020, December 1). APOE2: protective mechanism and therapeutic implications for Alzheimer's disease. *Molecular Neurodegeneration*. BioMed Central Ltd. https://doi.org/10.1186/s13024-020-00413-4

Liao, M.-C., Ahmed, M., Smith, S. O., & Van Nostrand, W. E. (2009). Degradation of amyloid beta protein by purified myelin basic protein. *The Journal of Biological Chemistry*, *284*(42), 28917–28925. https://doi.org/10.1074/jbc.M109.050856

Liao, Y., Smyth, G. K., & Shi, W. (2014). FeatureCounts: An efficient general purpose program for assigning sequence reads to genomic features. *Bioinformatics*, *30*(7), 923–930. https://doi.org/10.1093/bioinformatics/btt656

Lincoln, S., Allen, M., Cox, C. L., Walker, L. P., Malphrus, K., Qiu, Y., … Ertekin-Taner, N. (2013). LRRTM3 interacts with APP and BACE1 and has variants associating with late-onset Alzheimer's disease (LOAD). *PloS One*, *8*(6), e64164. https://doi.org/10.1371/journal.pone.0064164

Linton, K. J., & Higgins, C. F. (2007, February 26). Structure and function of ABC transporters: The ATP switch provides flexible control. *Pflugers Archiv European Journal of Physiology*. Springer. https://doi.org/10.1007/s00424-006-0126-x

Liu, C. C., Kanekiyo, T., Xu, H., & Bu, G. (2013, February). Apolipoprotein e and Alzheimer disease: Risk, mechanisms and therapy. *Nature Reviews Neurology*. NIH Public Access. https://doi.org/10.1038/nrneurol.2012.263

Liu, H., & Naismith, J. H. (2008). An efficient one-step site-directed deletion, insertion, single and multiple-site plasmid mutagenesis protocol. *BMC Biotechnology*, *8*, 91. https://doi.org/10.1186/1472-6750-8-91

Liu, S., Liu, J., Miura, Y., Tanabe, C., Maeda, T., Terayama, Y., … Komano, H. (2014). Conversion of Aβ43 to Aβ40 by the successive action of angiotensin-converting enzyme 2 and angiotensin-converting enzyme. *Journal of Neuroscience Research*, *92*(9), 1178–1186. https://doi.org/10.1002/jnr.23404

Livak, K. J., & Schmittgen, T. D. (2001). Analysis of relative gene expression data using real-time quantitative PCR and the 2-ΔΔCT method. *Methods*, *25*(4), 402–408. https://doi.org/10.1006/meth.2001.1262

Love, M. I., Huber, W., & Anders, S. (2014). Moderated estimation of fold change and dispersion for RNA-seq data with DESeq2. *Genome Biology*, *15*(12), 550. https://doi.org/10.1186/s13059-014-0550-8

Luo, H., Xiang, Y., Qu, X., Liu, H., Liu, C., Li, G., … Qin, X. (2019). Apelin-13 suppresses neuroinflammation against cognitive deficit in a streptozotocin-induced rat model of Alzheimer's disease through activation of BDNF-TrkB signaling pathway. *Frontiers in Pharmacology*, *10*(MAR). https://doi.org/10.3389/fphar.2019.00395

Magdesian, M. H., Gralle, M., Guerreiro, L. H., Beltrão, P. J. I., Carvalho, M. M. V. F., Luís, L. E., … FerreiraSé, S. T. (2011). Secreted human amyloid precursor protein binds semaphorin 3a and prevents Semaphorin-Induced growth cone collapse. *PLoS ONE*, *6*(7). https://doi.org/10.1371/journal.pone.0022857

Mahley, R. W. (2016). Central nervous system lipoproteins: ApoE and regulation of cholesterol metabolism. *Arteriosclerosis, Thrombosis, and Vascular Biology*, *36*(7), 1305–1315. https://doi.org/10.1161/ATVBAHA.116.307023

Maler, J. M., Spitzer, P., Lewczuk, P., Kornhuber, J., Herrmann, M., & Wiltfang, J. (2006). Decreased circulating CD34+ stem cells in early Alzheimer's disease: Evidence for a deficient hematopoietic brain support? *Molecular Psychiatry*, *11*(12), 1113–1115. https://doi.org/10.1038/sj.mp.4001913

Massone, S., Vassallo, I., Castelnuovo, M., Fiorino, G., Gatta, E., Robello, M., … Pagano, A. (2011). RNA polymerase III drives alternative splicing of the potassium channel-interacting protein contributing to brain complexity and neurodegeneration. *Journal of Cell Biology*, *193*(5), 851–866. https://doi.org/10.1083/jcb.201011053

Matsunaga, S., Kishi, T., & Iwata, N. (2015). Memantine monotherapy for Alzheimer's Disease:A systematic review and meta-analysis. *PLoS ONE*, *10*(4). https://doi.org/10.1371/journal.pone.0123289

McKenna, A., Hanna, M., Banks, E., Sivachenko, A., Cibulskis, K., Kernytsky, A., … DePristo, M. A. (2010). The Genome Analysis Toolkit: a MapReduce framework for analyzing next-generation DNA sequencing data. *Genome Research*, *20*(9), 1297–1303. https://doi.org/10.1101/gr.107524.110

Mendez, M. F. (2017, May 1). Early-Onset Alzheimer Disease. *Neurologic Clinics*. W.B. Saunders. https://doi.org/10.1016/j.ncl.2017.01.005

Miyashita, A., Arai, H., Asada, T., Imagawa, M., Matsubara, E., Shoji, M., … Kuwano, R. (2007). Genetic association of CTNNA3 with late-onset Alzheimer's disease in females. *Human Molecular Genetics*, *16*(23), 2854–2869. https://doi.org/10.1093/hmg/ddm244

Moon, M., Song, H., Hong, H. J., Nam, D. W., Cha, M. Y., Oh, M. S., … Mook-Jung, I. (2013). Vitamin D-binding protein interacts with Aβ and suppresses Aβ-mediated pathology. *Cell Death and Differentiation*, *20*(4), 630–638. https://doi.org/10.1038/cdd.2012.161

Morohashi, Y., Hatano, N., Ohya, S., Takikawa, R., Watabiki, T., Takasugi, N., … Iwatsubo, T. (2002). Molecular cloning and characterization of CALP/KChIP4, a novel EF-hand protein interacting with presenilin 2 and voltage-gated potassium channel subunit Kv4. *The Journal of Biological Chemistry*, *277*(17), 14965–14975. https://doi.org/10.1074/jbc.M200897200

Mulley, J. C., Iona, X., Hodgson, B., Heron, S. E., Berkovic, S. F., Scheffer, I. E., & Dibbens, L. M. (2011). The role of seizure-related SEZ6 as a susceptibility gene in febrile seizures. *Neurology Research International*, *2011*. https://doi.org/10.1155/2011/917565

Munoz, M., Henderson, M., Haber, M., & Norris, M. (2007, October 27). Role of the MRP1/ABCC1 multidrug transporter protein in cancer. *IUBMB Life*. IUBMB Life. https://doi.org/10.1080/15216540701736285

Neu, S. C., Pa, J., Kukull, W., Beekly, D., Kuzma, A., Gangadharan, P., … Toga, A. W. (2017). Apolipoprotein E genotype and sex risk factors for Alzheimer disease: A meta-analysis. *JAMA Neurology*, *74*(10), 1178–1189. https://doi.org/10.1001/jamaneurol.2017.2188

Noda, M., Takii, K., Parajuli, B., Kawanokuchi, J., Sonobe, Y., Takeuchi, H., … Suzumura, A. (2014). FGF-2 released from degenerating neurons exerts microglial-induced neuroprotection via FGFR3-ERK signaling pathway. *Journal of Neuroinflammation*, *11*. https://doi.org/10.1186/1742-2094-11-76

O'Brien, R. J., & Wong, P. C. (2011). Amyloid precursor protein processing and alzheimer's disease. *Annual Review of Neuroscience*, *34*, 185–204. https://doi.org/10.1146/annurev-neuro-061010-113613

Oakley, H., Cole, S. L., Logan, S., Maus, E., Shao, P., Craft, J., … Vassar, R. (2006). Intraneuronal beta-amyloid aggregates, neurodegeneration, and neuron loss in transgenic mice with five familial Alzheimer's disease mutations: potential factors in amyloid plaque formation. *The Journal of Neuroscience : The Official Journal of the Society for Neuroscience*, *26*(40), 10129–10140. https://doi.org/10.1523/JNEUROSCI.1202-06.2006

Oh, S., Son, M., Choi, J., Lee, S., & Byun, K. (2018). sRAGE prolonged stem cell survival and suppressed RAGE-related inflammatory cell and T lymphocyte accumulations in an Alzheimer's disease model. *Biochemical and Biophysical Research Communications*, *495*(1), 807–813. https://doi.org/10.1016/j.bbrc.2017.11.035

Paracchini, L., Beltrame, L., Boeri, L., Fusco, F., Caffarra, P., Marchini, S., … Forloni, G. (2018). Exome sequencing in an Italian family with Alzheimer's disease points to a role for seizure-related gene 6 (SEZ6) rare variant R615H. *Alzheimer's Research and Therapy*, *10*(1). https://doi.org/10.1186/s13195-018-0435-2

Pigoni, M., Wanngren, J., Kuhn, P. H., Munro, K. M., Gunnersen, J. M., Takeshima, H., … Lichtenthaler, S. F. (2016). Seizure protein 6 and its homolog seizure 6-like protein are physiological substrates of BACE1 in neurons. *Molecular Neurodegeneration*, *11*(1), 1–18. https://doi.org/10.1186/s13024-016-0134-z

Plagman, A., Hoscheidt, S., McLimans, K. E., Klinedinst, B., Pappas, C., Anantharam, V., … Willette, A. A. (2019). Cholecystokinin and Alzheimer's disease: a biomarker of metabolic function, neural integrity, and cognitive performance. *Neurobiology of Aging*, *76*, 201–207. https://doi.org/10.1016/j.neurobiolaging.2019.01.002

Qin, W., Ho, L., Pompl, P. N., Peng, Y., Zhao, Z., Xiang, Z., … Pasinetti, G. M. (2003). Cyclooxygenase (COX)-2 and COX-1 Potentiate β-Amyloid Peptide Generation through Mechanisms That Involve γ-Secretase Activity. *Journal of Biological Chemistry*, *278*(51), 50970–50977. https://doi.org/10.1074/jbc.M307699200

Rahman, M. R., Islam, T., Zaman, T., Shahjaman, M., Karim, M. R., Huq, F., … Moni, M. A. (2020). Identification of molecular signatures and pathways to identify novel therapeutic targets in Alzheimer's disease: Insights from a systems biomedicine perspective. *Genomics*, *112*(2), 1290–1299. https://doi.org/10.1016/j.ygeno.2019.07.018

Rama, N., Goldschneider, D., Corset, V., Lambert, J., Pays, L., & Mehlen, P. (2012). Amyloid precursor protein regulates netrin-1-mediated commissural axon outgrowth. *Journal of Biological Chemistry*, *287*(35), 30014–30023. https://doi.org/10.1074/jbc.M111.324780

Ranjbar, S., Khonkarn, R., Moreno, A., Baubichon-Cortay, H., Miri, R., Khoshneviszadeh, M., … Firuzi, O. (2019). 5-Oxo-hexahydroquinoline derivatives as modulators of P-gp, MRP1 and BCRP transporters to overcome multidrug resistance in cancer cells. *Toxicology and Applied Pharmacology*, *362*, 136–149. https://doi.org/10.1016/j.taap.2018.10.025

Reitz, C., Tosto, G., Vardarajan, B., Rogaeva, E., Ghani, M., Rogers, R. S., … Mayeux, R. (2013). Independent and epistatic effects of variants in VPS10-d receptors on Alzheimer disease risk and processing of the amyloid precursor protein (APP). *Translational Psychiatry*, *3*. https://doi.org/10.1038/tp.2013.13

Rogawski, M. A., & Wenk, G. L. (2006). The Neuropharmacological Basis for the Use of Memantine in the Treatment of Alzheimer's Disease. *CNS Drug Reviews*, *9*(3), 275–308. https://doi.org/10.1111/j.1527-3458.2003.tb00254.x

Ruan, Y., Qiu, X., Lv, Y. D., Dong, D., Wu, X. J., Zhu, J., & Zheng, X. Y. (2019). Kainic acid Induces production and aggregation of amyloid β-protein and memory deficits by activating inflammasomes in NLRP3- and NF-κB-stimulated pathways. *Aging*, *11*(11), 3795–3810. https://doi.org/10.18632/aging.102017

Rustay, N., Browman, K., & Curzon, P. (2008). Cued and Contextual Fear Conditioning for Rodents (pp. 19–37). CRC Press/Taylor & Francis. https://doi.org/10.1201/noe1420052343.ch2

Saddiki, H., Fayosse, A., Cognat, E., Sabia, S., Engelborghs, S., Wallon, D., … Dumurgier, J. (2020). Age and the association between apolipoprotein E genotype and Alzheimer disease: a cerebrospinal fluid biomarker–based case–control study. *PLoS Medicine*, *17*(8), e1003289. https://doi.org/10.1371/JOURNAL.PMED.1003289

Sampson, A., Peterson, B. G., Tan, K. W., & Iram, S. H. (2019). Doxorubicin as a fluorescent reporter identifies novel MRP1 (ABCC1) inhibitors missed by calcein-based high content screening of anticancer agents. *Biomedicine and Pharmacotherapy*, *118*. https://doi.org/10.1016/j.biopha.2019.109289

Sarkar, C., Jones, J. W., Hegdekar, N., Thayer, J. A., Kumar, A., Faden, A. I., … Lipinski, M. M. (2020). PLA2G4A/cPLA2-mediated lysosomal membrane damage leads to inhibition of autophagy and neurodegeneration after brain trauma. *Autophagy*, *16*(3), 466–485. https://doi.org/10.1080/15548627.2019.1628538

Satoh, J. I., Kino, Y., Yanaizu, M., Tosaki, Y., Sakai, K., Ishida, T., & Saito, Y. (2017). Microglia express ABI3 in the brains of Alzheimer's disease and Nasu-Hakola disease. *Intractable and Rare Diseases Research*, *6*(4), 262–268. https://doi.org/10.5582/irdr.2017.01073

Schafer, A., Kohler, S. C., Lohe, M., Wiese, M., & Hiersemann, M. (2017). Synthesis of homoverrucosanoid-derived esters and evaluation as MDR modulators. *Journal of Organic Chemistry*, *82*(19), 10504–10522. https://doi.org/10.1021/acs.joc.7b02012

Scheyer, O., Rahman, A., Hristov, H., Berkowitz, C., Isaacson, R. S., Diaz Brinton, R., & Mosconi, L. (2018). Female Sex and Alzheimer's Risk: The Menopause Connection. *The Journal of Prevention of Alzheimer's Disease*, *5*(4), 225–230. https://doi.org/10.14283/jpad.2018.34

Schmitt, S. M., Stefan, K., & Wiese, M. (2016). Pyrrolopyrimidine Derivatives as Novel Inhibitors of Multidrug Resistance-Associated Protein 1 (MRP1, ABCC1). *Journal of Medicinal Chemistry*, *59*(7), 3018–3033. https://doi.org/10.1021/acs.jmedchem.5b01644

Selkoe, D. J., & Hardy, J. (2016). The amyloid hypothesis of Alzheimer's disease at 25 years. *EMBO Molecular Medicine*, *8*(6), 595–608. https://doi.org/10.15252/emmm.201606210

Sharma, K. (2019). Cholinesterase inhibitors as Alzheimer's therapeutics (Review). *Molecular Medicine Reports*. Spandidos Publications. https://doi.org/10.3892/mmr.2019.10374

Sierksma, A., Lu, A., Mancuso, R., Fattorelli, N., Thrupp, N., Salta, E., … Fiers, M. (2020). Novel Alzheimer risk genes determine the microglia response to amyloid-β but not to TAU pathology. *EMBO Molecular Medicine*, *12*(3). https://doi.org/10.15252/emmm.201910606

Silbermann, K., Li, J., Namasivayam, V., Baltes, F., Bendas, G., Stefan, S. M., & Wiese, M. (2020). Superior Pyrimidine Derivatives as Selective ABCG2 Inhibitors and Broad-Spectrum ABCB1, ABCC1, and ABCG2 Antagonists. *Journal of Medicinal Chemistry*, *63*(18), 10412–10432. https://doi.org/10.1021/acs.jmedchem.0c00961

Silbermann, K., Stefan, S. M., Elshawadfy, R., Namasivayam, V., & Wiese, M. (2019). Identification of Thienopyrimidine Scaffold as an Inhibitor of the ABC Transport Protein ABCC1 (MRP1) and Related Transporters Using a Combined Virtual Screening Approach. *Journal of Medicinal Chemistry*, *62*(9), 4383–4400. https://doi.org/10.1021/acs.jmedchem.8b01821

Sim, P. L., & Heese, K. (2010). Ligand-dependent activation of the chimeric tumor necrosis factor receptor-amyloid precursor protein (APP) reveals increased app processing and suppressed neuronal differentiation. *NeuroSignals*, *18*(1), 9–23. https://doi.org/10.1159/000242425

Šimić, G., Babić Leko, M., Wray, S., Harrington, C., Delalle, I., Jovanov-Milošević, N., … Hof, P. R. (2016, January 6). Tau protein hyperphosphorylation and aggregation in alzheimer's disease and other tauopathies, and possible neuroprotective strategies. *Biomolecules*. MDPI AG. https://doi.org/10.3390/biom6010006

Sims, R., Van Der Lee, S. J., Naj, A. C., Bellenguez, C., Badarinarayan, N., Jakobsdottir, J., … Schellenberg, G. D. (2017). Rare coding variants in PLCG2, ABI3, and TREM2 implicate microglial-mediated innate immunity in Alzheimer's disease. *Nature Genetics*, *49*(9), 1373–1384. https://doi.org/10.1038/ng.3916

Singh, T. D., Park, S.-Y., Bae, J., Yun, Y., Bae, Y.-C., Park, R.-W., & Kim, I.-S. (2010). MEGF10 functions as a receptor for the uptake of amyloid-β. *FEBS Letters*, *584*(18), 3936–3942. https://doi.org/10.1016/j.febslet.2010.08.050

Soleman, S., Filippov, M. A., Dityatev, A., & Fawcett, J. W. (2013, December 3). Targeting the neural extracellular matrix in neurological disorders. *Neuroscience*. https://doi.org/10.1016/j.neuroscience.2013.08.050

Sorf, A., Novotna, E., Hofman, J., Morell, A., Staud, F., Wsol, V., & Ceckova, M. (2019). Cyclin-dependent kinase inhibitors AZD5438 and R547 show potential for enhancing efficacy of daunorubicin-based anticancer therapy: Interaction with carbonyl-reducing enzymes and ABC transporters. *Biochemical Pharmacology*, *163*, 290–298. https://doi.org/10.1016/j.bcp.2019.02.035

Stefan, K., Schmitt, S. M., & Wiese, M. (2017). 9-Deazapurines as Broad-Spectrum Inhibitors of the ABC Transport Proteins P-Glycoprotein, Multidrug Resistance-Associated Protein 1, and Breast Cancer Resistance Protein. *Journal of Medicinal Chemistry*, *60*(21), 8758–8780. https://doi.org/10.1021/acs.jmedchem.7b00788

Stefan, S. M. (2019). Multi-target ABC transporter modulators: What next and where to go? *Future Medicinal Chemistry*. Future Medicine Ltd. https://doi.org/10.4155/fmc-2019-0185

Stride, B. D., Valdimarsson, G., Gerlach, J. H., Wilson, G. M., Cole, S. P., & Deeley, R. G. (1996). Structure and expression of the messenger RNA encoding the murine multidrug resistance protein, an ATP-binding cassette transporter. *Molecular Pharmacology*, *49*(6).

Sun, L., Guo, C., Wang, T., Li, X., Li, G., Luo, Y., & Xiao, S. (2014). LIMK1 is involved in the protective effects of bone morphogenetic protein 6 against amyloid-β-induced neurotoxicity in rat hippocampal neurons. *Journal of Alzheimer's Disease*, *42*(2), 543–554. https://doi.org/10.3233/JAD-140231

Szczepanik, A. M., Rampe, D., & Ringheim, G. E. (2001). Amyloid-beta peptide fragments p3 and p4 induce pro-inflammatory cytokine and chemokine production in vitro and in vivo. *Journal of Neurochemistry*, *77*(1), 304–317. https://doi.org/10.1046/j.1471-4159.2001.t01-1-00240.x

Talbot, C., Lendon, C., Craddock, N., Shears, S., Morris, J. C., & Goate, A. (1994, June 4). Protection against Alzheimer's disease with apoE ∈2. *The Lancet*. Lancet. https://doi.org/10.1016/S0140-6736(94)92557-7

Tan, K. W., Sampson, A., Osa-Andrews, B., & Iram, S. H. (2018). Calcitriol and calcipotriol modulate transport activity of ABC transporters and exhibit selective cytotoxicity in MRP1-overexpressing cells. *Drug Metabolism and Disposition*, *46*(12), 1856–1866. https://doi.org/10.1124/dmd.118.081612

Tan, V. T. Y., Mockett, B. G., Ohline, S. M., Parfitt, K. D., Wicky, H. E., Peppercorn, K., … Abraham, W. C. (2018). Lentivirus-mediated expression of human secreted amyloid precursor protein-alpha prevents development of memory and plasticity deficits in a mouse model of Alzheimer's disease. *Molecular Brain*, *11*(1). https://doi.org/10.1186/s13041-018-0348-9

Tang, Y. Q., Liang, P., Zhou, J., Lu, Y., Lei, L., Bian, X., & Wang, K. W. (2013). Auxiliary KChIP4a suppresses A-type K+ current through Endoplasmic Reticulum (ER) retention and promoting closed-state inactivation of Kv4 channels. *Journal of Biological Chemistry*, *288*(21), 14727–14741. https://doi.org/10.1074/jbc.M113.466052

Tapella, L., Cerruti, M., Biocotino, I., Stevano, A., Rocchio, F., Canonico, P. L., … Lim, D. (2018). TGF-β2 and TGF-β3 from cultured β-amyloid-treated or 3xTg-AD-derived astrocytes may mediate astrocyte–neuron communication. *European Journal of Neuroscience*, *47*(3), 211–221. https://doi.org/10.1111/ejn.13819

Tarafdar, A., & Pula, G. (2018, December 1). The role of NADPH oxidases and oxidative stress in neurodegenerative disorders. *International Journal of Molecular Sciences*. MDPI AG. https://doi.org/10.3390/ijms19123824

Taylor, C. J., Ireland, D. R., Ballagh, I., Bourne, K., Marechal, N. M., Turner, P. R., … Abraham, W. C. (2008). Endogenous secreted amyloid precursor protein-α regulates hippocampal NMDA receptor function, long-term potentiation and spatial memory. *Neurobiology of Disease*, *31*(2), 250–260. https://doi.org/10.1016/j.nbd.2008.04.011

Teng, T., Dong, L., Ridgley, D. M., Ghura, S., Tobin, M. K., Sun, G. Y., … Lee, J. C. (2019). Cytosolic Phospholipase A 2 Facilitates Oligomeric Amyloid-β Peptide Association with Microglia via Regulation of Membrane-Cytoskeleton Connectivity. *Molecular Neurobiology*, *56*(5), 3222–3234. https://doi.org/10.1007/s12035-018-1304-5

The UniProt Consortium. (2019). UniProt: a worldwide hub of protein knowledge. *Nucleic Acids Research*, *47*, D506–D515. https://doi.org/10.1093/nar/gky1049

Tian Hui Kwan, A., Arfaie, S., Therriault, J., Rosa-Neto, P., & Gauthier, S. (2020). Lessons Learnt from the Second Generation of Anti-Amyloid Monoclonal Antibodies Clinical Trials. *Dementia and Geriatric Cognitive Disorders*. https://doi.org/10.1159/000511506

Tolar, M., Abushakra, S., Hey, J. A., Porsteinsson, A., & Sabbagh, M. (2020, August 12). Aducanumab, gantenerumab, BAN2401, and ALZ-801 - The first wave of amyloid-targeting drugs for Alzheimer's disease with potential for near term approval. *Alzheimer's Research and Therapy*. BioMed Central Ltd. https://doi.org/10.1186/s13195-020-00663-w

Town, L., McGlinn, E., Fiorenza, S., Metzis, V., Butterfield, N. C., Richman, J. M., & Wicking, C. (2009). The metalloendopeptidase gene Pitrm1 is regulated by hedgehog signaling in the developing mouse limb and is expressed in muscle progenitors. *Developmental Dynamics*, *238*(12), 3175–3184. https://doi.org/10.1002/dvdy.22126

Vane, J. R., & Botting, R. M. (1998). Anti-inflammatory drugs and their mechanism of action. In *Inflammation Research* (Vol. 47). Birkhauser Verlag Basel. https://doi.org/10.1007/s000110050284

Vaz, M., & Silvestre, S. (2020, November 15). Alzheimer's disease: Recent treatment strategies. *European Journal of Pharmacology*. Elsevier B.V. https://doi.org/10.1016/j.ejphar.2020.173554

Wang, H., Gauthier, B. R., Hagenfeldt-Johansson, K. A., Iezzi, M., & Wollheim, C. B. (2002). Foxa2 (HNF3β) controls multiple genes implicated in metabolism-secretion coupling of glucose-induced insulin release. *Journal of Biological Chemistry*, *277*(20), 17564–17570. https://doi.org/10.1074/jbc.M111037200

Whitt, J. D., Keeton, A. B., Gary, B. D., Sklar, L. A., Sodani, K., Chen, Z. S., & Piazza, G. A. (2016). Sulindac sulfide selectively increases sensitivity of ABCC1 expressing tumor cells to doxorubicin and glutathione depletion. *Journal of Biomedical Research*, *30*(2), 120–133. https://doi.org/10.7555/JBR.30.20150108

Wojcik, S. M., Bundman, D. S., & Roop, D. R. (2000). Delayed Wound Healing in Keratin 6a Knockout Mice. *Molecular and Cellular Biology*, *20*(14), 5248–5255. https://doi.org/10.1128/mcb.20.14.5248-5255.2000

Wolfe, C. M., Fitz, N. F., Nam, K. N., Lefterov, I., & Koldamova, R. (2019, January 1). The role of APOE and TREM2 in Alzheimer's disease—Current understanding and perspectives. *International Journal of Molecular Sciences*. MDPI AG. https://doi.org/10.3390/ijms20010081

Wong, I. L. K., Zhu, X., Chan, K. F., Law, M. C., Lo, A. M. Y., Hu, X., … Chan, T. H. (2018). Discovery of Novel Flavonoid Dimers to Reverse Multidrug Resistance Protein 1 (MRP1, ABCC1) Mediated Drug Resistance in Cancers Using a High Throughput Platform with “click Chemistry.” *Journal of Medicinal Chemistry*, *61*(22), 9931–9951. https://doi.org/10.1021/acs.jmedchem.8b00834

Woo, R. S., Lee, J. H., Kim, H. S., Baek, C. H., Song, D. Y., Suh, Y. H., & Baik, T. K. (2012). Neuregulin-1 protects against neurotoxicities induced by Swedish amyloid precursor protein via the ErbB4 receptor. *Neuroscience*, *202*, 413–423. https://doi.org/10.1016/j.neuroscience.2011.11.026

Yu, G., & He, Q. Y. (2016). ReactomePA: An R/Bioconductor package for reactome pathway analysis and visualization. *Molecular BioSystems*, *12*(2), 477–479. https://doi.org/10.1039/c5mb00663e

Zaarur, N., Xu, X., Lestienne, P., Meriin, A. B., McComb, M., Costello, C. E., … Sherman, M. Y. (2015). RuvbL1 and RuvbL2 enhance aggresome formation and disaggregate amyloid fibrils. *The EMBO Journal*, *34*(18), 2363–2382. https://doi.org/10.15252/embj.201591245

Zheng, H., Cheng, B., Li, Y., Li, X., Chen, X., & Zhang, Y. (2018). TREM2 in Alzheimer’s Disease: Microglial Survival and Energy Metabolism. *Frontiers in Aging Neuroscience*, *10*. https://doi.org/10.3389/fnagi.2018.00395

Zhu, K., Xiang, X., Filser, S., Marinković, P., Dorostkar, M. M., Crux, S., … Herms, J. (2018). Beta-Site Amyloid Precursor Protein Cleaving Enzyme 1 Inhibition Impairs Synaptic Plasticity via Seizure Protein 6. *Biological Psychiatry*, *83*(5), 428–437. https://doi.org/10.1016/j.biopsych.2016.12.023

Zong, Y., Yu, P., Cheng, H., Wang, H., Wang, X., Liang, C., … Qin, C. (2015). MiR-29c regulates NAV3 protein expression in a transgenic mouse model of Alzheimer’s disease. *Brain Research*, *1624*, 95–102. https://doi.org/10.1016/j.brainres.2015.07.022

Zota, V., Nemirovsky, A., Baron, R., Fisher, Y., Selkoe, D. J., Altmann, D. M., … Monsonego, A. (2009). HLA-DR alleles in amyloid beta-peptide autoimmunity: a highly immunogenic role for the DRB1*1501 allele. *Journal of Immunology (Baltimore, Md. : 1950)*, *183*(5), 3522–3530. https://doi.org/10.4049/jimmunol.0900620

Zou, K., Gong, J. S., Yanagisawa, K., & Michikawa, M. (2002). A Novel Function of Monomeric Amyloid β-Protein Serving as an Antioxidant Molecule against Metal-Induced Oxidative Damage. *Journal of Neuroscience*, *22*(12), 4833–4841. https://doi.org/10.1523/jneurosci.22-12-04833.2002

APPENDIX A

GENES OF INTEREST TABLE FROM RNA SEQUENCING

Gene	Ensembl Gene ID	Ch.	Log2FC	Stat	p-val	p-adj	GOI?
GHRH	ENSG00000118702	20	8.00958478	6.5363983	6.30E-11	2.16E-09	No
	A GHRH antagonist, MIA-690, reduced Abeta1-42 and Tau deposition in 5xFAD mouse brains (Jaszberenyi et al., 2012); therefore, if GHRH were responsible for the reduced extracellular Abeta observed in our experiment, we would expect to see it down-, rather than up-regulated.						
GC	ENSG00000145321	4	6.02179664	4.38997943	1.13E-05	1.40E-04	No
	GC, aka DBP, can bind to Abeta to reduce oligomerization (Moon et al., 2013). Therefore, it may be possible, though unlikely, that increased GC is binding to Abeta and making it unrecognizeable by antibodies used in assays. However, GC upregulation is not significant in the second RNA-seq experiment, and is downregulated in the third experiment. Therefore, we do not believe that the differential expression of GC can account for reduced Abeta.						
CYP1A2	ENSG00000140505	15	5.43876407	4.12430361	3.72E-05	4.03E-04	No
	Only publication linking the two terms refers to the enzymatic profile of a drug that blocks Abeta-induced apoptosis (Elkamhawy et al., 2017). There is no known direct link to APP or Abeta metabolism.						
PLXNA4	ENSG00000221866	7	2.2827125	17.6165379	1.84E-69	1.31E-66	No
	Transfection of 3 isoforms of PLXNA4 did not alter APP processing, but the full-length isoform increased TAU phosphorylation (Jun et al., 2014). Literature does not demonstrate a direct connection between PLXNA4 expression and APP/Abeta metabolism.						
PTGS1	ENSG00000095303	9	1.96085251	4.05140616	5.09E-05	5.36E-04	No
	Expression of COX1, encoded by PTGS1, in CHO cells, resulted in increased Abeta1-42 (Qin et al., 2003); therefore, if PTGS1 expression were responsible for the decrease in extracellular Abeta observed, we would expect to see PTGS1 down-, rather than up-regulated.						
HCN1	ENSG00000164588	5	1.71441095	5.05079538	4.40E-07	7.73E-06	No
	Link to Abeta processing has to do with neuroexcitability, but authors also found that overexpression of HCN1 in Neuro2a cells decreased Abeta production (Chang et al., 2019). However, HCN1 was not significantly upregulated in the second experiment, and was downregulated in the third experiment. Expression of HCN1 cannot account for reduced Abeta in all experiments.						
FOXC1	ENSG00000054598	6	1.67804982	9.68683622	3.43E-22	3.32E-20	No

	Transcription factor found to be differentially expressed in AD (Rahman et al., 2020), not a catalytic enzyme. Furthermore, FOXC1 was insignficantly downregulated in the second experiment and insignificantly upregulated in the third experiment. Expression is not consistent to even account for changes in APP metabolizing enzymes.						
TGFB3	ENSG00000119699	14	1.63851504	9.48843155	2.35E-21	2.11E-19	No
	Oligomeric Abeta can induce TGFB3 production (Tapella et al., 2018), though the gene product is not linked to APP/Abeta metabolism. Furthermore, TGFB3 was insignificantly downregulated in the second experiment, and insignificantly upregulated in the third experiment. TGFB3 cannot logically account for altered APP processing observed.						
SORCS2	ENSG00000184985	4	-1.5340787	-9.9562092	2.37E-23	2.52E-21	No
	Increased SORCS2 decreased APP processing, and decreased SORCS2 increased gamma-secretase activity (Reitz et al., 2013). SORCS2 was significantly downregulated in all 3 RNA-seq experiments, which is the opposite of what we would expect if SORCS2 expression levels accounted for altered APP processing observed.						
SEZ6	ENSG00000063015	17	-1.5364914	-14.958268	1.38E-50	5.39E-48	No
	SEZ6 is a substrate for BACE1/2 (Pigoni et al., 2016). SEZ6 overexpression results in reduced Abeta species (Paracchini et al., 2018). SEZ6 expression was significantly downregulated in all 3 RNA-seq experiments, and thus it's expression is in the opposite direction expected to account for reduced extracellular Abeta species.						
NKX6-1	ENSG00000163623	4	-1.5453016	-4.6731491	2.97E-06	4.25E-05	No
	Association with amyloid is islet amyloid pancreatic polypeptide.						
NOX5	ENSG00000255346	15	-1.5880465	-15.399964	1.64E-53	7.00E-51	No
	Plays a role in oxidative stress in Alzheimer's disease (Tarafdar and Pula, 2018). No direct link to APP/Abeta metabolism.						
PTGER4	ENSG00000171522	5	-1.6250699	-4.0742588	4.62E-05	4.91E-04	No
	PTGER4 stimulation can result in PSEN1 endocytosis, and activation of the gamma-secretase (Hoshino et al., 2009), thus a decrease in PTGER4, as we observed, may result in reduced gamma-secretase activity. However, PTGER4 downregulation in the second and third RNA-seq experiments was statistically insignificant and carried very minimal log2FC of -0.189 and -0.021, respectively. Therefore, differential expression of PTGER4 does not likely account for decreased extracellular Abeta species seen in all experiments.						

MAFA	ENSG00000182759	8	-1.6918124	-4.564746	5.00E-06	6.81E-05	No
	Association with amyloid is islet amyloid pancreatic polypeptide.						
SEMA3A	ENSG00000075213	7	-1.6940126	-18.902189	1.09E-79	1.12E-76	No
	sAPPalpha can bind SEMA3A and inhibit it (Magdesian et al., 2011), and Sema3a may induce neuronal collapse in mice (Good et al., 2004), but Sema3a stimulation has been shown to increase Tau phosphorylation with no observed differences in APP processing (Jun et al., 2014). SEMA3A is significantly downregulated in all 3 RNA-seq experiments; however, we cannot find a link between SEMA3A and APP metabolism in the literature.						
FAS	ENSG00000026103	10	-1.775488	-8.4014521	4.41E-17	2.92E-15	No
	FAS is implicated in AD because of apoptosis (Ethell and Buhler, 2003). No direct link in literature between FAS and altered APP processing. FAS downregulation in the second and third RNA-seq experiments was insignificant.						
SSTR1	ENSG00000139874	14	-1.7856036	-11.357719	6.79E-30	1.11E-27	No
	SST (somatostatin) has been shown to bind to Abeta (Lau et al., 2017), and is the reason for the link between SSTR1 and Abeta; however, SSTR1 is a G-protein coupled receptor, with no known APP processing abilities, and its downregulation in the second and third RNA-seq experiments was insignificant. There is no reason to believe SSTR1 can be directly responsible for lowering extracellular Abeta.						
CYP19A1	ENSG00000137869	15	-1.8706075	-14.752983	2.94E-49	1.10E-46	No
	A SNP in CYP19A1 is associated with AD (Huang and Poduslo, 2006), but it has been shown that the SNP identified is not associated with altered APP processing (Han, Schellenberg and Wang, 2010). No direct link between CYP19A1 and APP metabolism found.						
NAV3	ENSG00000067798	12	-1.9473467	-5.548492	2.88E-08	6.35E-07	No
	Regulates axon guidance and has been shown to be downregulated in young APPswe/PS1deltaE9 mice (Zong et al., 2015). No direct link between APP processing, and downregulation was statistically insignificant in second and third RNA-seq experiments.						
TIMP3	ENSG00000100234	22	-1.9539687	-22.301951	3.5374E-110	7.56E-107	**YES**
	TIMP3 encodes the Tissue Inhibitor of Metalloproteinases 3, a protein that can irreversibly inhibit APP-cleaving alpha-secretases like ADAM10 and ADAM17 (Hoe et al., 2007). TIMP3 expression has also been shown to be reduced in AD brain tissue (Dunckley et al., 2006), which may play a role in increased cerebral Abeta. Logically, if TIMP3 expression is downregulated, more APP molecules are more						

likely to be cleaved by an alpha-secretase. This would result in decreased extracellular Abeta and an increase in alpha- versus beta-secretase cleavage of APP.

WNT4	ENSG00000162552	1	-1.9799445	-14.536432	7.12E-48	2.43E-45	No

No link to APP/Abeta metabolism.

NEUROD1	ENSG00000162992	2	-2.0840307	-7.3142458	2.59E-13	1.18E-11	No

Related to Alzheimer's disease because of its role in neurogenesis and differentiation (Dard, Dahan and Rampon, 2019), but linked to amyloid because of islet amyloid pancreatic polyprotein, as the gene is strongly associated with diabetes.

SNCAIP	ENSG00000064692	5	-2.2299991	-7.2718384	3.55E-13	1.58E-11	No

siRNA targeting SNCAIP reduced aggresome activity, and the aggresome is capable of storing and degrading aggregated proteins (Zaarur et al., 2015). No literature shows a direct link between SNCAIP and APP processing.

PLCG2	ENSG00000197943	16	-2.320263	-8.5616116	1.11E-17	7.67E-16	No

One study found PLCG2 is significantly upregulated when cells exposed to Abeta (Sierksma et al., 2020), and another found that a variant in PLCG2 protects against Tau phosphorylation, and expression seems to be responsive to Abeta (Kleineidam et al., 2020). No study has demonstrated that altered PLCG2 expression alters APP processing. Furthermore, downregulation of PLCG2 was not significant in the second or third experiments.

ACE2	ENSG00000130234	X	-2.3287002	-4.3401745	1.42E-05	1.72E-04	No

ACE2 activation reduces hippocampal soluble Abeta1-42 (Evans et al., 2020), which is in opposition to our results. However, ACE2 can convert Abeta1-43 to Abeta1-42, which can then be converted to Abeta1-40 by ACE (Liu et al., 2014). If, in our system, less Abeta1-43 is being converted to Abeta1-42, and is thus not detectable by our assay, downregulation of ACE2 may account for some of the reduction in extracellular Abeta observed. However, the downregulation of ACE2 was insignificant in the second RNA-seq experiment, and was insignificantly upregulated in the third experiment.

FGFR3	ENSG00000068078	4	-2.3335884	-10.261628	1.05E-24	1.20E-22	No

FGFR3 is released by neurons stimulated by oligomeric Abeta1-42 to recruit microglia to damaged tissue (Noda et al., 2014). No literature linking FGFR3 to APP/Abeta metabolism.

MBP	ENSG00000197971	18	-2.3392196	-3.9941838	6.49E-05	6.63E-04	No

	It has been shown that MBP can act as a chaperone protein for Abeta, limiting its fillibration (Hoos et al., 2007), and that MBP has serine proteinase activity that can degrade Abeta (Liao et al., 2009). Therefore, if MBP could account for reduced extracellular Abeta, we would expect to see it up-, not down-regulated, in the ABCC1-overexpressing cells.						
ABI3	ENSG00000108798	17	-2.5271572	-4.8113809	1.50E-06	2.31E-05	No
	Clusters of ABI3+ microglia are associated with amyloid plaques, which may suggest a role for ABI3+ in microglia motility (Satoh et al., 2017), and ABI3(S209F) has been found to be a risk factor for AD (Sims et al., 2017), but no literature links ABI3 directly to APP processing or metabolism.						
GRIK1	ENSG00000171189	21	-2.6364395	-4.9042159	9.38E-07	1.52E-05	No
	Stimulation of GRIK1 with kainic acid increased Abeta and oligomeric Abeta, likely because GRIK1 signaling increases phosphorylation and activation of NF-kappa B (Ruan et al., 2019), a transcription factor. Therefore, if the downregulation of GRIK1 observed in our experiment played a role in reducing extracellular Abeta, we would expect that the lack of GRIK1 signalling through NF-kappa B alters transcription of genes capable of altering APP metabolism, rather than GRIK1 directly playing a role.						
ERBB4	ENSG00000178568	2	-2.6467963	-16.468033	6.23E-61	3.66E-58	No
	ERBB4 is the neuroregulin (NRG1) receptor, and is cleaved by factor-alpha converting enzyme, then subsequently by PSEN-dependent gamma-secretase (Woo et al., 2012), the same gamma-secretase that cleaves the APP molecule. However, no literature directly links ERBB4 to altered APP/Abeta metabolism.						
CD38	ENSG00000004468	4	-2.9798536	-5.78603	7.21E-09	1.78E-07	**YES**
	CD38 encodes the Cluster of Differentiation 38, an enzyme that synthesizes and hydrolyzes cyclic adenosine 5'-diphosphate-ribose, a molecule that regulates intracellular calcium signaling (Chini et al., 2002). It has been shown that Cd38 knockout AD mouse models have improved cognitive deficits, decreased cerebral amyloid burden, and that primary neurons cultured from those mice secrete significantly less Abeta species (Blacher et al., 2015). The authors found that knockout of Cd38 alters beta- and gamma-secretase activity, effectively reducing both (Blacher et al., 2015). Therefore, downregulation of CD38 resulting in decreased extracellular Abeta is consistent with the literature.						
KCNIP4	ENSG00000185774	4	-2.9838801	-27.415115	1.81E-165	8.51E-162	No
	The longest isoform of KCNIP4 can interact with PSEN1 of the gamma-secretase, and decreasing expression of this longest isoform increases Abeta1-40 and Abeta1-42 production (Massone et al., 2011). In another study, KCNIP4, aka CALP, overexpression did not alter gamma-cleavage of APP (Morohashi et al., 2002).						

	Taken together, a decrease in KCNIP4 long isoform expression would increase extracellular Abeta, and a decrease in the short isoform should have no effect on APP processing. We see KCNIP4 expression decrease while extracellular Abeta species decrease. This is the opposite of what would be expected based on the literature.						
SORCS3	ENSG00000156395	10	-3.2424713	-5.4616931	4.72E-08	1.00E-06	No
	Expression reduced in frontal cortex after amyloid deposition in APP/PS1 mice (Hermey et al., 2019), and knockdown of SORCS3 increased APP processing (Reitz et al., 2013). Therefore, if SORCS3 could account for reduced extracellular Abeta, we would expect to see it up-, rather than down-regulated.						
MUSK	ENSG00000030304	9	-3.373102	-4.5068209	6.58E-06	8.67E-05	No
	Link between MUSK and APP is that they are LRP4 coreceptors at the neuromuscular junction (Choi et al., 2013), with no known link to APP processing.						
TNFRSF1B	ENSG00000028137	1	-3.6063976	-4.4895388	7.14E-06	9.34E-05	No
	A single study found that stimulation of their TNFRSF1B-APP-GFP chimeric receptor increased APP processing (Sim and Heese, 2010). The downregulation of TNFRSF1B is statistically insignificant in the second and third RNA-seq experiments. Downregulation of this receptor (with no known enzymatic function) cannot not directly account for altered APP processing.						
CTNNA3	ENSG00000183230	10	-3.8116282	-14.065955	6.15E-45	1.78E-42	No
	One study found SNPs in CTNNA3 were associated with increased cerebral Abeta levels (Ertekin-Taner et al., 2003), but two other studies found that the association is not significant (Blomqvist et al., 2004; Busby et al., 2004), and a fourth found the association only in females (Miyashita et al., 2007). However, no direct link between CTNNA3, a cell-to-cell adhesion molecule, and APP/Abeta metabolism has been found in the literature. Interestingly, knockdown of a gene nested within the CTNNA3 locus, LRRTM3, has been shown to decrease secreted Abeta species through its interaction with APP and BACE1 (Lincoln et al., 2013). That study found a relationship between mRNA levels of CTNNA3, LRRTM3, BACE1, and APP, but did not demonstrate that CTNNA3 alters APP metabolism. Furthermore, in the same study, when LRRTM3 is knocked down in SH-SY5Y cells, CTNNA3 mRNA levels increased (Lincoln et al., 2013); therefore, it seems that an increase in CTNNA3 would be associated with decreased secreted Abeta species, if any relationship exists at all.						
C4BPB	ENSG00000123843	1	-4.1219575	-8.0779878	6.58E-16	3.93E-14	No
	Link between C4BPB and amyloid is that C4BPB, amyloid A, and protein Z serum levels may serve as biomarkers for pulmonary tuberculosis (Jiang et al., 2017).						

CCK	ENSG00000187094	3	-4.3958699	-5.4313899	5.59E-08	1.17E-06	No
	One study found that CCK expression does not correlate with Abeta1-42 in AD patients (Plagman et al., 2019), and most studies linking CCK to amyloid pertain to islet amyloid pancreatic polypeptide.						
DCC	ENSG00000187323	18	-4.7379038	-7.2792154	3.36E-13	1.51E-11	No
	APP interacts with DCC and enhances Nestin signalling (Rama et al., 2012), and PSEN1 processes DCC to ensure fidelity of axon guidance (Bai et al., 2011), but no link between DCC and APP processing was found. Downregulation of DCC was statistically insignificant in second and third RNA-seq experiments.						
CD34	ENSG00000174059	1	-4.882655	-16.260743	1.87E-59	9.79E-57	No
	Decreased counts of circulating CD34+ cells correlates with Abeta1-42 levels in AD patients (Maler et al., 2006), but no link between CD34 and APP/Abeta processing.						
GLI3	ENSG00000106571	7	-4.8874424	-8.4404417	3.16E-17	2.10E-15	No
	GLI3 is a transcription factor that can repress Pitrm1 (Town et al., 2009), a metalloprotease capable of degrading Abeta when it accumulates in mitochondria (Falkevall et al., 2006). If GLI3 suppression were increasing PITRM1 expression, resulting in decreased Abeta species, PITRM1 would be on this list. There is no reason to believe that suppression of the transcription factor, itself, would decrease extracellular Abeta.						
HLA-DRB1	ENSG00000196126	6	-4.9849761	-11.456865	2.17E-30	3.59E-28	No
	HLA-DRB1 is part of the major histocompatibility complex, and specific isoforms have shown high immunoreactivity to Abeta species (Zota et al., 2009). A link between HLA-DR1 and amyloid, then, makes sense *in vivo*, not in a monoculture of neuroblastoma cells. Furthermore, if Abeta were binding to HLA-DRB1, thus removing it from the supernatant, and that was the reason for measuring reduced extracellular Abeta, we would expect HLA-DRB1 expression to be up-, rather than down-regulated.						
BMP6	ENSG00000153162	6	-5.4269376	-4.0259947	5.67E-05	5.90E-04	No
	It has been shown that Abeta increases BMP6 levels, in vitro (Crews et al., 2010), and BMP6 is neuroprotective against toxic effects of Abeta25-35 (Sun et al., 2014), but no link found between BMP6 and APP processing.						
PLA2G4A	ENSG00000116711	1	-5.6292257	-5.0104561	5.43E-07	9.30E-06	No
	PLA2G4A has been shown to contribute to Abeta-induced lysosomal membrane permeabilization (Sarkar et al., 2020), and cytosolic phospholipase A2 activation facilitates oligomeric Abeta endocytosis by microglia (Teng et al., 2019). If						

PLA2G4A expression were to account for the reduced extracellular Abeta level observed, we would expect to see it up-, rather than down-regulated.

TNFSF10	ENSG00000121858	3	-6.0304536	-4.0878419	4.35E-05	4.66E-04	No

Administration of antibodies that neutralize TNFSF10 reduces Abeta1-42 in the hippocampi of 3xTg AD mice (Cantarella et al., 2015); however, TNFSF10 is a cytokine, not an enzyme. Therefore, we would expect that downregulation of this gene would not directly account for altered APP processing, but reduced signaling by TNFSF10 may alter levels of other genes capable of altering APP processing.

OTX2	ENSG00000165588	14	-6.0337592	-4.1299129	3.63E-05	3.95E-04	No

OTX2 is a transcription factor involved in the maturation of perineuronal nets (Soleman et al., 2013). Reduced OTX2 may reduce expression of genes that can alter APP processing, but the transcription factor, itself, would not logically perform this task.

APLN	ENSG00000171388	X	-6.2095007	-19.586904	2.00E-85	2.47E-82	No

Administration of exogenous apelin-13, a peptide fragment resulting from cleavage of the APLN gene product, reduced Abeta production by decreasing BACE1 (beta-secretase) activity and increasing neprilysin (an Abeta degrading enzyme) activity (Luo et al., 2019). Therefore, if APLN expression could account for reduced extracellular Abeta observed in our experiment, we would expect APLN expression to be up-, rather than down-regulated.

HDC	ENSG00000140287	15	-6.5182389	-6.0764451	1.23E-09	3.40E-08	No

Converts histidine to histamine (Hocker et al., 1996). May be part of the signaling that results in differential expression of genes capable of altering APP metabolism, but a change in expression in either direction should not directly result in altered APP processing.

CFI	ENSG00000205403	4	-6.6038489	-4.8502187	1.23E-06	1.94E-05	No

CFI activity can be decreased by Abeta, which can activate the complement cascade (Lashkari et al., 2018), but no link found between CFI and APP/Abeta processing.

HNF1B	ENSG00000108753	17	-6.9354737	-5.5473661	2.90E-08	6.38E-07	No

Transcription factor that controls expression of many genes implicated in glucose-induced insulin resistance (Wang et al., 2002). Again, a transcription factor, itself, should not logically have a direct role in altering APP processing unless altering the expression levels of genes capable of this task.

INPP5D	ENSG00000168918	2	-6.9920428	-5.6192849	1.92E-08	4.38E-07	No
	INPP5D is believed to be involved in the immune response in the brain, regulating clearance of misfolded proteins by microglia (Efthymiou and Goate, 2017). If INPP5D had this function in our neuroblastoma monoculture, we would expect INPP5D to be up-, rather than down-regulated, if its expression accounted for the reduced extracellular Abeta observed.						
CD3D	ENSG00000167286	11	-7.0480262	-5.2660668	1.39E-07	2.71E-06	No
	Only article linking CD3D to amyloid discusses reduction of CD3D positive T-lymphocytes in sRAGE-MSC treated rats (Oh et al., 2018). CD3D is part of the T-cell receptor with no known link between CD3D and APP processing.						
KCNMB2	ENSG00000197584	3	-7.1102768	-18.687604	6.25E-78	6.11E-75	No
	KCNMB2 locus was associated with hippocampal sclerosis in a GWAS (Beecham et al., 2014), but no direct link in the literature between KCNMB2 and APP/Abeta metabolism.						
DPP4	ENSG00000197635	2	-8.5053795	-6.9526959	3.58E-12	1.41E-10	No
	Inhibition of DPP4 with sitagliptin can delay amyloid deposition by increasing GLP-1 levels in the brain (D'Amico et al., 2010), and GLP-1 receptor stimulation can lower Abeta secretion, in vitro (Li et al., 2010). However, if DPP4 downregulation in our study is resulting in increased GLP-1 levels, since GLP-1 is a hormone, not an enzyme, we would expect that GLP-1 signalling would alter the transcript levels of proteins involved with APP/Abeta processing, rather than directly activate/deactivate available enzymes with mRNA levels that are consistent between the two cell lines.						
MEGF10	ENSG00000145794	5	-11.550718	-17.774019	1.12E-70	8.52E-68	No
	The MEGF10 protein has been shown to function as a phagocytosis receptor for the uptake of Abeta (Singh et al., 2010). If MEGF10 were responsible for the decrease in extracellular Abeta, we would expect to see higher levels of MEGF10, which would likely result in increased phagocytosis of Abeta, and thus decreased extracellular levels of the peptides; however, the opposite of this was observed.						

APPENDIX B

WIRB APPROVAL LETTER FOR THE USE OF HUMAN SUBJECTS

wcg WIRB
The Trusted Partner in Ethical Review

Certificate of Action

Investigator Name: Vinodh Narayanan, MD	**Board Action Date:** 04/15/2020
Investigator Address: Suite 402, 3330 North 2nd Street Phoenix, AZ 85012, United States	**Approval Expires:** 05/14/2021 **Continuing Review Frequency:** Annually
Sponsor: Translational Genomics Research Institute (TGen) **Institution Tracking Number:**	**Sponsor Protocol Number:** dcraig12-003 **Amended Sponsor Protocol Number:** dcraig12-003
Study Number: 1132412	**IRB Tracking Number:** 20120789
Work Order Number: 1-1278095-1	**Panel:** 1 **Note: Panel 18 is a shared panel of CGIRB and WIRB. Panel 19 is a shared panel of Aspire and WIRB. Panel 21 is a shared panel of NEIRB and WIRB.**
Protocol Title: Genetic Studies of Patients and their Families with Diseases of Unknown Genetic Etiology	

THE FOLLOWING ITEMS ARE APPROVED:
Study and Investigator for an additional continuing review period. This approval expires on the date noted above.

Please note the following information:

THE IRB HAS APPROVED THE FOLLOWING LOCATIONS TO BE USED IN THE RESEARCH:
Arizona Pediatric Neurology & Neurogenetics Associates (APNNA), PLLC, Suite 402, 3330 North 2nd Street, Phoenix, Arizona 85012

ALL IRB APPROVED INVESTIGATORS MUST COMPLY WITH THE FOLLOWING:
As a requirement of IRB approval, the investigators conducting this research will:

- Comply with all requirements and determinations of the IRB.
- Protect the rights, safety, and welfare of subjects involved in the research.
- Personally conduct or supervise the research.
- Conduct the research in accordance with the relevant current protocol approved by the IRB.
- Ensure that there are adequate resources to carry out the research safely.
- Ensure that research staff are qualified to perform procedures and duties assigned to them during the research.
- Submit proposed modifications to the IRB prior to their implementation.
    - Not make modifications to the research without prior IRB review and approval unless necessary to eliminate apparent immediate hazards to subjects.
- For research subject to continuing review, submit continuing review reports when requested by the IRB.
- Submit a closure form to close research (end the IRB's oversight) when:
    - The protocol is permanently closed to enrollment
    - All subjects have completed all protocol related interventions and interactions
    - For research subject to federal oversight other than FDA:
        - No additional identifiable private information about the subjects is being obtained
        - Analysis of private identifiable information is completed
- For research subject to continuing review, if research approval expires, stop all research activities and immediately contact the IRB.
- Promptly report to the IRB the information items listed in the IRB's "Prompt Reporting Requirements" available on the IRB's Web site.
- Not accept or provide payments to professionals in exchange for referrals of potential subjects ("finder's fees.")

This is to certify that the information contained herein is true and correct as reflected in the records of this IRB. WE CERTIFY THAT THIS IRB IS IN FULL COMPLIANCE WITH GOOD CLINICAL PRACTICES AS DEFINED UNDER THE U.S. FOOD AND DRUG ADMINISTRATION (FDA) REGULATIONS, U.S. DEPARTMENT OF HEALTH AND HUMAN SERVICES (HHS) REGULATIONS, AND THE INTERNATIONAL CONFERENCE ON HARMONISATION (ICH) GUIDELINES.

- Not accept payments designed to accelerate recruitment that are tied to the rate or timing of enrollment ("bonus payments") without prior IRB approval.
- When required by the IRB ensure that consent, permission, and assent are obtained and documented in accordance with the relevant current protocol as approved by the IRB.
- Promptly notify the IRB of any change to information provided on your initial submission form.

Consistent with AAHRPP's requirements in connection with its accreditation of IRBs, the individual and/or organization shall promptly communicate or provide, the following information relevant to the protection of human subjects to the IRB in a timely manner:

- Upon request of the IRB, a copy of the written plan between sponsor or CRO and site that addresses whether expenses for medical care incurred by human subject research subjects who experience research related injury will be reimbursed, and if so, who is responsible in order to determine consistency with the language in the consent document.
- Any site monitoring report that directly and materially affects subject safety or their willingness to continue participation. Such reports will be provided to the IRB within 5 days.
- Reports from any data monitoring committee, data and safety monitoring board, or data and safety monitoring committee in accordance with the time frame specified in the research protocol.
- Any findings from a closed research when those findings materially affect the safety and medical care of past subjects. Findings will be reported for 2 years after the closure of the research.

For Investigator's Brochures, an approval action indicates that the IRB has the document on file for the research.

If the board approves a change of Principal Investigator - Once approved, the new Principal Investigator is authorized by the IRB to carry out the study as previously approved for the prior Principal Investigator (unless the Board provides alternate instructions to the new Principal Investigator). This includes continued use of the previously approved study materials. The IRB considers the approval of the new PI a continuation of the original approval, so the identifying information about the study remains the same.

If your research site is a HIPAA covered entity, the HIPAA Privacy Rule requires you to obtain written authorization from each research subject for any use or disclosure of protected health information for research. If your IRB-approved consent form does not include such HIPAA authorization language, the HIPAA Privacy Rule requires you to have each research subject sign a separate authorization agreement. "

For research subject to continuing review, you will receive Continuing Review Report forms from this IRB when the expiration date is approaching.

Thank you for using this WCG IRB to provide oversight for your research project.

DISTRIBUTION OF COPIES:
Contact, Company
Stephanie Buchholtz, MS, The Translational Genomics Research Institute (TGen)
Vinodh Narayanan, MD, Arizona Pediatric Neurology & Neurogenetics Associates (APNNA), PLLC
Kara Karaniuk, The Translational Genomics Research Institute (TGen)